RUSSIAN/U.S. WEAPONS LABORATORIES INTRODUCTORY TECHNICAL EXCHANGE IN COMPUTATIONAL AND COMPUTER SCIENCE

Lawrence Livermore National Laboratory
Livermore, California

October 19, 1992

RUSSIAN/U.S. WEAPONS LABORATORIES INTRODUCTORY TECHNICAL EXCHANGE IN COMPUTATIONAL AND COMPUTER SCIENCE

Monday, October 19, 1992 thru
Thursday, October 22, 1992

Building 451, White Room

SCHEDULE

Session A	Tuesday, October 20	8:30 a.m.
Session B	Tuesday, October 20	1:30 p.m.
Session C	Wednesday, October 21	8:30 a.m.
Session F	Wednesday, October 21	1:00 p.m.
Session E	Thursday, October 22	8:30 p.m.
Session D	Thursday, October 22	1:00 p.m.

SESSION A

Tuesday, October 20, 1992

8:30 a.m.

Algorithm Development I

Papers:

1. PAGOSA: A Massively-Parallel, Multi-Material Hydrodynamics Model for 3-D High-Speed Flow and High-Rate Material Deformation
   - Doug Kothe (LANL)

2. Modeling Flux Compression Generators with a 2-D Ale Code
   - Bob Tipton (LLNL)

3. Numerical Simulation of Heat Conductive Medium Spatial Shock-Wave Movements in Eulerian-Langrangian Coordinates
   - Boris Voronin (Arzamas)

4. Mathematical Modeling for Turbulent Flow in Multi-Component Media
   - Oleg Buryakov, Valentin Kuropatenko, et al. (Chelyabinsk)

5. Numerical Modeling of Multi-Dimensional Flows with Large Deformations
   - Vladimir Volkov, et al. (Chelyabinsk)

SESSION A

Algorithm Development I

PAGOSA: A Massively-Parallel, Multi-Material Hydrodynamics Model for Three-Dimensional High-Speed Flow and High-Rate Material Deformation

Doug Kothe

Technical Staff Member
Fluid Dynamics Group T-3
Theoretical Division
Los Alamos National Laboratory

An overview of the physical models, numerical methods and algorithms, and parallel implementation will be given for a new massively-parallel model known as PAGOSA. PAGOSA is an explicit, 3-D multi-material hydrodynamics code designed to model problems involving high-speed flow and high-rate deformation of solid materials. It has been developed over the past 3 years on the Connection Machine parallel supercomputer by a small team of computational physicists, numerical analysts, and computer scientists at the Los Alamos National Laboratory (LANL). Finite difference approximations to the continuum mechanical conversation equations are solved in PAGOSA in an Eulerian frame on a fixed, orthogonal hexahedral grid with a Lagrangian/remap algorithm. PAGOSA employs a second-order accurate predictor-corrector method for the Lagrangian phase and a third-order, van Leer-limited upwind scheme for the advection phase. A unique parallel implementation of Youngs' method for reconstructing interfaces from material volume fraction data enables a Lagrangian-like representation of material interfaces having arbitrarily complex topology. PAGOSA is written in the new data parallel Fortran 90 language, and was carefully designed and programmed to run at optimal efficiency on SIMD-like machines such as the Connection Machine CM-200 and CM-5 at LANL. Implementation and performance of PAGOSA on MIMD parallel computers such as the Intel and Ncube will also be discussed. PAGOSA has demonstrated quite impressive performance on complex hydrodynamic simulations, running 10-25 times faster than a very similar serial code at LANL that runs on one CRAY Y-MP processor. The properties and capabilities of PAGOSA will be illustrated with several representative calculations.

SESSION A

Algorithm Development I

MODELING FLUX COMPRESSION GENERATORS WITH A 2D ALE CODE

Robert Tipton
Lawrence Livermore National Laboratory
Livermore, CA

ABSTRACT

A 2D MHD ALE (Arbitrary Lagrangian Eulerian) code has been developed to aid in the design and understanding of magnetic flux compression generators. The hydro treatment is Lagrangian ahead of the armature-stator contact point and Eulerian behind. The code tracks the location of the high explosive detonation front and deposites the chemical energy behind it. Realistic equations of state are used for the detonation products, armature and stator. Strength of material effects for the armature and stator are included. The magnetic diffusion equations are solved implicitly and the magnetic forces are included in the hydrodynamic equations. The code has been used to model the performance of a coaxial flux compression generator designed at LANL as well as a continuously variable pitch, continuously variable conductor diameter helical generator designed at LLNL. Calculated results for each generator are presented and in the case of the coaxial generator, compared with data. The limitations of the code are discussed.

SESSION A

Algorithm Development I

A.N. Bykov, E.L. Voronin, A.G. Kozub, S.I. Skrypnik,
I.D. Sofronov, A.V. Urm.

Numerical Simulation of Heat Conduction Medium Spatial Shock - Wave Movements in Eulerian - Lagrangian coordinates.

Abstract

The report treats problems of numerical simulation of heat conduction medium spatial shock - wave movements in Eulerian - Lagrangian varyables.

Selecting variables, coordinate system types, and velocity vector decomposition bases, approximating multidimensional differential equations on non - orthogonal computational grids and other problems are considered.

The numerical technique based on concepts presented in the report is implemented in the technique and application program complex RAMZES designed for numerical solution of 2D and 3D problems.

Some computational results for 3D problems having exact solution as well as for a problem of practical interest are presented.

A.N.Bykov, B.L.Voronin, A.G.Kozub, S.I.Skrypnik,
I.D.Sofronov, A.V.Urm.

Numerical Simulation of Heat Conductive Medium Spatial Shock - Wave Movements in Eulerian - Lagrangian Coordinates.

1. The numerical simulation of many physical processes of application value need solving nonstationary gas dynamics problems with account of heat conductivity where movement is describec by the following differential equations system :

$$\begin{aligned} \frac{d\rho}{dt} &= -\rho\, div\, \bar{U} \\ \frac{d\bar{U}}{dt} &= -\frac{1}{\rho}\, grad\, P \\ \frac{d\varepsilon}{dt} &= -\frac{P}{\rho} div\, \bar{U} + \frac{1}{\rho} div(\chi\, grad\, T) \end{aligned} \qquad (1)$$

Here ρ is density, $\bar{U}$ is mass velocity, T is temperature, P is pressure, ε is specific internal energy, χ is heat conductivity factor.

The system of equations (1) is closed with heat conductive medium equations of state: $P = P(\rho,T)$, $\varepsilon = \varepsilon(\rho,T)$, $\chi = \chi(\rho,T)$.

The study of specific physical phenomena may yield problem formulations of various level of complexity and labour consumption: from one-dimensional to three-dimensional, so it is desirable for the developed numerical technique to allow effective problem solution at any of spatial formulations. In this connection important is selecting variables and coordinate system types used in the numerical technique.

The proposed technique uses two mutually orthogonal Eulerian coordinates and one Lagrangian. It allows most naturally compute problems with geometry in form of a set of laminated regions with possible heavy relative sliding, the contact region interfaces being traced with the Lagrangian variable.

The account of nature and orientation of processes at solving particular problems leads to necessity of employing curvilinear coordinates. With this purpose a special, orthogonal, curvilinear

coordinate system is developed including, as a specific case, cylindrical, spherical, and toroidal-type coordinate system [1]. These coordinates are defined by setting quite smooth curve called a support line in plane (R,Z) (Fig.1).

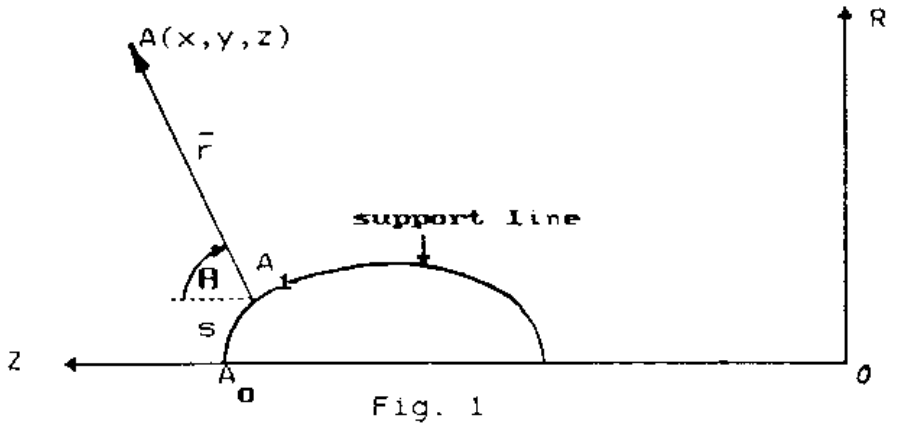

Fig. 1

If $R_0=R_0(s)$ $Z_0=Z_0(s)$ is a parametric support line equation, then the following variables are selected as coordinates :

r - a distance from the considered point (point A) to the support line;

s - a support line arc length to the trace of point A on it ($\cup A_0A_1$)

φ - the angle of (R,Z)-plane rotation around ØZ axis.

Relation between Cartesian coordinates (x,y,z) and curvilinear (r,s,φ) is expressed by the following correlations:

$$\begin{aligned} x &= [r\cdot\sin\theta(s) + R_0(s)]\cdot\cos\varphi \,, \\ y &= [r\cdot\sin\theta(s) + R_0(s)]\cdot\sin\varphi \,, \\ z &= r\cdot\cos\theta(s) + Z_0(s) \end{aligned} \qquad (2)$$

Conformably to a concrete problem the support line is usually selected similar to some contact boundary under condition that the form and position of the support line on the plane (R,Z) satisfy the coordinate system non-degeneracy conditions: $1 + K\cdot r > 0$, $r\cdot\sin\theta + R_0 > 0$, where $K=\frac{d\theta(s)}{ds}$ is support line curvature.

In the proposed technique (RAMZES) coordinates s,φ are Eulerian and coordinates r is replaced with Lagrangian $\bar{r}$ and the computational grid is generated by intersection of surfaces $\bar{r}$=const, s=const, φ=const. The RAMZES-technique finite difference algorithms are based on two mass velocity vector decomposition: U_0,V_0,W_0 is an orthogonal decomposition in the initial coordinate

system basis (r,s,φ) and U,V_0,W_0 is an oblique decomposition in the basis related with the problem computational grid $(\bar{r}_m,s_k,\varphi_l)$, thereby $U = U_0 - H_{12}\cdot V_0 - H_{13}\cdot W_0$ where H_{12} and H_{13} are parameters characterizing computational grid nonorthogonality [2]. Such an approach allows to considerably reduce negative effect of computational grid nonorthogonality on computational results quality while retaining capabilities of physical region set continuous computation as the constituent U is continuous at the contact discontinuity.

For some complex geometry problems one fails to compute in a single coordinate system, on a single computational grid. In this case the problem geometry is split into fragments each of which is computed in its own coordinate system, on its most suitable computational grid. Fragment intersection is provided through exchange boundary conditions of type [3], at that the boundary conditions transfer scheme works allowing to run parallel fragment computation.

2. Specificity of the problems being computed and existence of Lagrangian family $\bar{r}_m$ = const lead to nonorthogonal computational grids. The numerical solution quality is largely dependent on the manner of approximating the vector operator ***grad*** which is present in the initial equations (1). Considering as an example the heat conductivity equation

$$\frac{\partial T}{\partial t} = div\,(\chi\ grad\ T), \qquad (3)$$

one can see that the use, as it is usually the case, of local template (for example, 9-point in a 2D case) for highly nonorthogonal grids may lead to temperature definition needed to approximate gradient components by extrapolating using template temperature grid values. In this case one can observe deviation of numerical solution from exact one which could not be eliminated by space-time computational grid refinement. Approximation can be improved by extending the grid template necessary for obtaining the corresponding difference operator GRAD as it is done in some heat conductivity 2D equation computation techniques.

For the RAMZES technique a method has been developed and realized using nonlocal, time-variable template allowing to elimina-

te value extrapolation at approximating gradient components on grids of arbitrary nonorthogonality level. The essence of the technique is that derivatives with respect to the coordinates defining grad components are approximated directly (similar to one-dimensional case) with two-point difference, while the function values comprising this difference are defined by interpolation with respect to the grid function ones closest (in the sense of metric proximity) to that point. At deriving implicit difference schemes using this technique we arrive to a finite-difference equation system of the form

$$A\bar{u}^{n+1} = \bar{u}^{n+1} \qquad (4)$$

where A is a general form of weakly filled matrix. For such systems an economic solution technique has been developed. This technique consists in using directional splitting and reducing two-point difference of the equation system (4), at the expense of specific time approximation, to the equation system with the three-diagonal matrix

$$\bar{\bar{A}}\bar{\bar{u}}^{n+1} = \bar{\bar{C}}\bar{\bar{u}}^{n+1}, \qquad (5)$$

where $A=\bar{\bar{A}}+\bar{\bar{B}}$, $\bar{\bar{C}}=E-\bar{\bar{B}}$, $\bar{\bar{A}}$ is a three-diagonal matrix, $\bar{\bar{B}}$ is a weakly filled matrix of general form.

The practice of numerous 2D and 3D heat conductivity problem computations testifies that the scheme using a nonlocal template proves to be quite suitable (stable and monotone) allowing to obtain numerical solutions close to exact ones even on computational grids of high level of nonorthogonality , in contrast to schemes on local grid templates.

3. The directional splitting method (the method of fractional steps) appeared and developed to meet needs of multidimensional problem numerical solution when computers of relatively small efficiency are available. In the 1950s that method was used by Douglas, Peaceman, and Rachford to solve the 2D heat conductivity equation [4,5]. Later the method was extensively developed by various authors, in particular, N.N.Janenko in paper [6] uniformly treats numerous schemes using fractional steps as well as their application to solving a great variety of problems including multidimensional gas dynamics problems.

When the method was considered in more detail, it turned out that its use might be useful not only from economic point of view, but also to improve abendlessness and accuracy of multidimensional gas dynamics problem computations. In the method of directional splitting a multidimensional problem is split into a set of "one-dimensional" ones, the multidimensional computational grid appearing as a set of one-dimensional grids of "one-dimensional" problems. These one-dimensional grids are far from being always optimal for their "one-dimensional" problem.

The concept of multigrid method of directional splitting is that for the numerical solution of each problem of the whole set of "one-dimensional" problems to use its most optimal computational grid [7]. It means actually the use a quasi-regular grid with variable number of computational points along lines at the computation of each spatial direction, while the number of points along a fixed line may be time variable. As at such an approach the grid set of all directions does not yet comprise a single multidimensional computational grid, it is necessary to define a way of computation result exchange between directional grids. On the basis of the multigrid method the technique of multidimensional problem computation using Lagrangian direction quasi-regular computational grids and the technique for Eulerian direction contact boundary computations have been developed and programmed. Using them for 2D and 3D problem computations allowed to increase computation accuracy, to considerably improve their abendlessness and in some cases to compute complex gas dynamics flows retaining physical region boundary Lagrangian nature when it could not be done in frame of a regular approach.

For problem of highly irregular matter gas dynamic movements or of heterogeneous set of physical regions a method of concentrations is used allowing to compute such problems with regular computational grids.

4. On the basis of the developed technique a PAMPES program complex has been developed [8]. The programs of the complex are written in the FORTRAN programming language using preprocessor SWIFT [9]. The programs of the complex are run on highly efficient

computers ES-1066 and multiprocessor computer complex Elbrus-2. There is a complex version for personal computer PC-AT. Structure and architecture of the complex are quite universal. In particular, for the sake of convenience of a complex's user an initial data setting and program run control language have been developed similar, for example, to SIGMA complex [10]. The programs of the complex may be divided into the following parts from operational point of view: the translator of initial geometry and other initial data language and the notation interpreter; initial problem cut forming programs; time step computation programs; service-type programs.

Time step computation program structure fully reflects multilayer nature of problem splitting in geometry, processes and spatial directions characteristic, for example, of 2D program complex TIGR [11]. Time step computational programs follow the module principle and are supervised by a control module allowing to simply realize various computational modes using problem run control language: one-fragment and multifragment computations of 3D,2D and 1D problems. A separate module comprises computations of computational grid geometry characteristics that allowed to use either Cartesian or special curvilinear coordinate system when computing particular problems.

The technique and complex of RAMZES programs have been tested at a number of multidimensional heat conductivity and gas dynamics problems, in particular, at computing problems of heat wave collapse, of cube cooling, of adiabatic expansion of three-axial gas ellipsoid into vacuum having exact solution.

A problem of heat wave collapse[12].

In a spherical region the initial temperature distribution $T_0(r,\theta,\varphi)=(r\cdot\sin\theta\cdot\sin\varphi)^{4/5}$ is given, the exact solution of the initial value problem for the heat conductivity equation

$$\frac{\partial T}{\partial t}=\frac{1}{r^2}\frac{\partial}{\partial r}\left[T^{5/2}\cdot r^2\cdot\frac{\partial T}{\partial r}\right]+\frac{1}{r^2\cdot\sin\theta}\left[\frac{\partial}{\partial\theta}\left(T^{5/2}\cdot\sin\theta\cdot\frac{\partial T}{\partial\theta}\right)+\frac{\partial}{\partial\varphi}\left(T^{5/2}\cdot\frac{\partial T}{\partial\varphi}\right)\right]$$

is of the form $T(r,\theta,\varphi,t) = (1-3.6\cdot t)^{-2/5}\cdot T_0(r,\theta,\varphi)$.

This solution corresponds to the fact that initial profile at $t \longrightarrow 1/3.6$ continuously increases its slope and at $t=1/3.6$ any large temperature values are achieved at all the points.

The numerical solution was obtained in region $(0\le r\le 1, 0\le\theta,\varphi\le\frac{\pi}{2})$, on the outer boundary exact boundary conditions were set.

The computation was run at constant time step $\tau=0.001$ up to time $t=0.25$ in a spherical coordinate system. Spatial time grid was chosen uniform in each of the directions: $\Delta r=0.055$, $\Delta\theta=\Delta\varphi=5$.

The error of numerical solution with respect to the exact one was not greater than 3%, excluding regions of maximum temperature gradients ($\theta \approx 0$, $\varphi \approx 0$) where a little greater error was observed.

A problem of cube cooling [13].

In a unit cube $(0\le x,y,z\le 1)$ at initial time temperature $T=1$ was set. On the cube boundary at all later times temperature $T_{bound}=0$ was maintained. In course of time the cube cools according to the linear heat conductivity equation:

$$\frac{\partial T}{\partial t} = \frac{\partial^2 T}{\partial x^2} + \frac{\partial^2 T}{\partial y^2} + \frac{\partial^2 T}{\partial z^2}$$

The exact solution is of the form:

$$T(x,y,z,t)= \Psi(x,t)\cdot\Psi(y,t)\cdot\Psi(z,t)$$

where $$\Psi(x,t)= \frac{4}{\pi}\sum_{k=0}^{\infty}\frac{e^{-\pi^2\cdot(2k+1)\cdot t}}{2k+1}\cdot\sin\pi(2k+1)x\ .$$

The numerical solution was found in the Cartesian coordinate system on the uniform orthogonal grid $\nabla x=\nabla y=\nabla z=0.05$ and on nonuniform "parquet" type grid. The computations were run at time step $\tau=0.001$.

The error of numerical solution with respect to the exact one was not greater than 2.5% on the orthogonal grid and 3.5% on nonorthogonal one.

A problem of adiabatic expansion of three-axial gas ellipsoid

into vacuum [14].

Initial geometry of gas cloud is ellipsoid with half-axes equal to: $a_x=3$, $a_y=2$, $a_z=1$.

The equation of state is ideal gas $P=(\gamma-1)\cdot\rho e$, $\gamma=1.4$.

Initial density and pressure distribution depends on the same function, level lines of which are ellipsoids:

$$p = (1-\xi^2)^{\frac{\gamma}{\gamma-1}} \quad , \quad \rho = (1-\xi^2)^{\frac{1}{\gamma-1}} \quad , \quad \xi^2 = \frac{x^2}{a_x^2} + \frac{y^2}{a_y^2} + \frac{z^2}{a_z^2} \quad .$$

Boundary condition: $P_b(t)= 0$.

The movement scenario is the following: due to present pressure gradient from the cloud centre to its boundary the cloud begins to expand from its rest state with transition to stationary mode. At that the ellipsoid form is retained, but half axes ratio changes: the smallest half axis becomes the largest and vice versa. Exact values of cloud edge velocities along half axes at stationary state equal: $U_x=2.564$, $U_y=3.17$, $U_z=4.27$, and half axes ratios are $\frac{a_z}{a_x}= 1.66$, $\frac{a_y}{a_x}= 1.35$.

The problem numerical solution was found in a spherical coordinate system in the region $\{ 0 \le \theta \le \frac{\pi}{2} , 0 \le \varphi \le \frac{\pi}{2} \}$ up to time t=30 corresponding to stationary expanding. In Eulerian variables θ and φ the computation used 16 points and in Lagrangian ri: 10 points in the 1st variant and 20 points in the 2nd. Splitting in all the space variables is uniform.

The error of numerical solution with respect to half axes in both variants was similar and amounted to ≈1.35%, velocity error of the 2nd variant was ≈3%, being a half that of the 1st variant. As spherically symmetric cloud spreading computations have shown, it is explained mainly with improvement of initial density and pressure profile on the computational grid.

The programs of the RAMZES complex on multiprocessor computer complex Elbrus-2 are used to compute three-dimensional problems of gas dynamics, of detonation gas dynamics, of heat conductivity gas dynamics. Computations were run and results were obtained for quite a wide and representative 3D problem class as for their physical formulation. The technique and program implementation charac-

teristics allow efficient computations at two-dimensional spatial formulation without additional computational resources.

The RAMZES program complex and technique, in particular, proved to be an effective tools for studying shock-wave processes in point explosion problems applied in many spheres of science and technology. L.I.Sedov provided an exhaustive analysis of self-similar problem of powerful point explosion and obtained its closed form solution [15]. However, of most practical interest are nonuniform medium explosive process studies, in particular, studies of point explosions in atmosphere, density and pressure of which depend on altitude. Examples of similar processes may be provided by air explosions at various altitudes. Medium nonuniformity leads to two-dimensional (in case of single explosions) or three-dimensional (in case of multiple explosions) character of nonstationary gas dynamics flows. Computations using the RAMZES complex programs allowed to numerically study the evolution of the region of shock wave as well as to describe gas dynamics parameter distribution within the region both for a single and twin explosion in exponential atmosphere [16].

Nonviscous ideal gas is considered with adiabat exponent γ, heat conductivity and radiation are not taken into account. Density ρ and pressure P of gas (atmosphere) vary with altitude according to the law $\rho=\rho_0 \cdot e^{-\frac{z}{\Delta}}$, $P=P_0 \cdot e^{-\frac{z}{\Delta}}$. At initial time, at the same height h and distance ℓ from each other two point explosions take place of energy release ε each. The equation of state of considered gas is $P=(\gamma-1)\cdot\rho\varepsilon$, $\gamma=1.4$. Atmosphere parameter values at explosion height are $\rho_0=1$, $P_0=0$. Each explosion initial energy release is given within a sphere of radius $r_0=0.1$ (the distance is redefined in dimensionless form corresponding to the variable $\ell' = \frac{\ell}{\Delta}$) with density $\rho_\varepsilon = \frac{1}{\frac{4}{3}\cdot\pi\cdot r_0^3}$.

For numerical study of the above problem two-dimensional computations of single explosions ($\ell' \gg 1$ and $\ell'=0$) with energy release density ρ_ε and $2\rho_\varepsilon$, respectively, as well as three-dimensional computation of two explosions, corresponding to the case of $\ell'=2$, with initial energy release density ρ_ε each were ca-

de.

In case of single explosion of energy release ε the qualitative evolution of the process was as follows. Due to atmosphere nonuniformity, shock wave front movement velocity is not the same: at the higher portion it is greater than at the lower. Therefore in course of time the shock wave region becomes elongated in form, the volume of disturbance region being intensely increased due to upward shock wave front propagation, while explosion products are moving up. The shock wave moves upwards with increasing velocity, i.e. there is atmosphere break effect (Fig. 2). The double energy release computation results analysis shows qualitative coincidence of shock wave movement character, the similarity correlation being valid, in particular, the shock wave position at time t of energy release 2ε coincides with the shock wave position at time $\sqrt{2}t$ of energy release ε (Fig.3).

Shock wave front position along axes vs time

at energy release ε computation

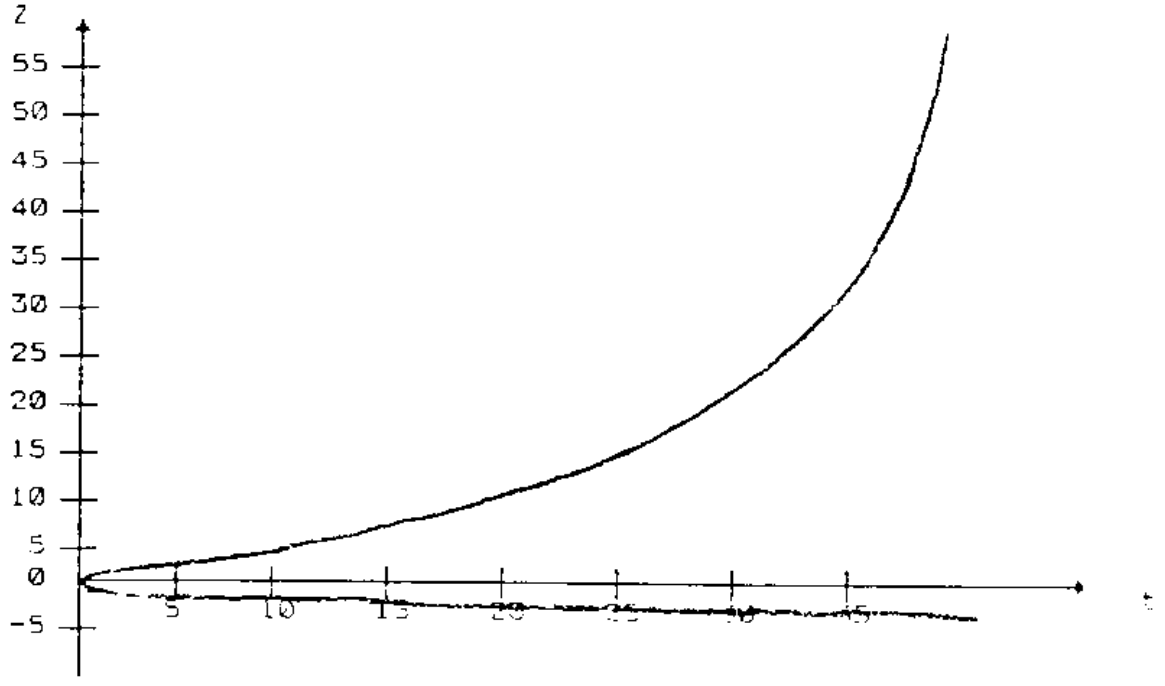

Fig. 2

At three-dimensional computation up to time $t_1 \approx 0.9$-1 explosions evolve as single ones independently, since time t_1 explosions begin interact (Fig.4). After explosion interaction the position of the diverging shock wave front is between the position of shock wave fronts of single explosions of energy release ε and 2ε (Fig.3).

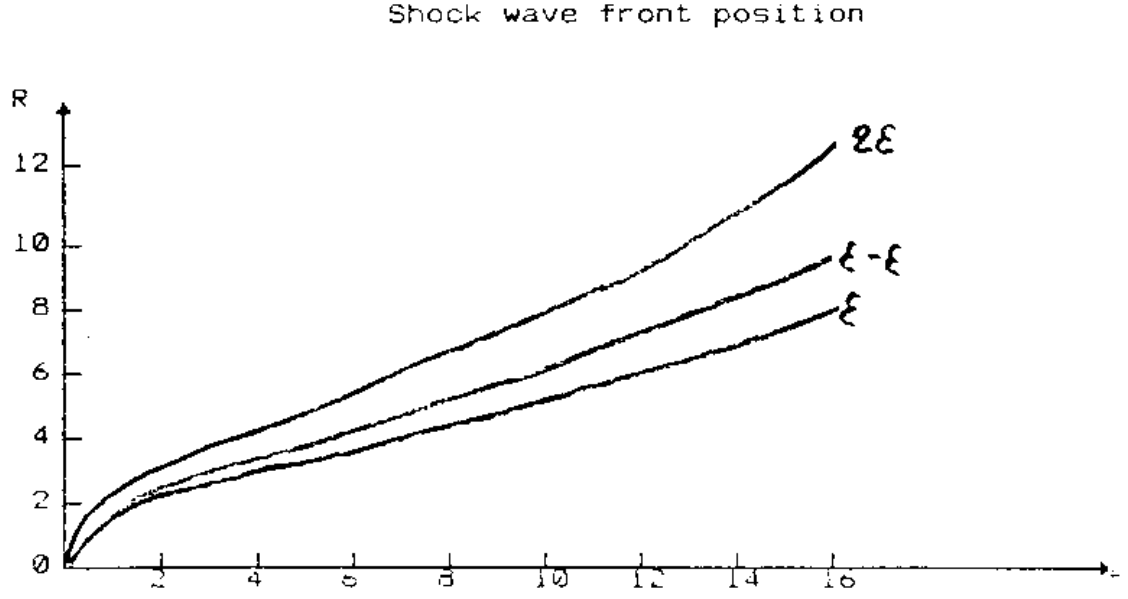

Fig.3

References

1.Voronin B.L.,Isavev V.N. On formulation of heat conductive gas movement equations in Eulerian-Lagrangian coordinates // Chislennyje Methody Mekhaniki Sploshnov Sredy. Novosibirsk, Computer Centre of the Siberia Department of the Academy of Science of the USSR. 1981. p.8-14.

2.Voronin B.L., Skrypnik S.I., Sofronov I.D. Eulerian-Lagrangian Technique of gas dynamics three-dimensional nonstationary problem solution with account of heat conductivity // Voprosy Atomnoy Nauki i Tekhniki. Series: Metodiki i Programmy Chislennogo Resheniya

Zadach Matematicheskoy Fisiki. -1988. -V.3. -p.3-8.

3. Zaguskin V.Z., Kondrashev V.E. On heat conductivity and gas dynamics computations using region run // Doklady Akademiyi Nauk SSSR, 1965, V.163, No.5, p.1107-1109.

4. Peaceman D.W., Rachford H.H., The numerical solution of parabolic and elliptic differential equations // J.Soc.Industr, Appl. Math., 1955, Vol.3, N 1, pp. 28-42.

5. Douglas J. On the numerical integration of $\frac{\partial^2 u}{\partial x^2}+\frac{\partial^2 u}{\partial y^2}=\frac{\partial u}{\partial t}$ by implicit methods // J.Soc.Industr, Appl. Math., 1955, Vol.3, N1, pp. 42-65.

6. Yanenko N.N. Fractional steps technique for computing mathematical physics multidimensional problems. Novosibirsk, Nauka Publishing House, 1967.

7. Voronin B.L. Multigrid dimensional splitting technique for multidimensional problem numerical solution // Voprosy Atomnoy Nauki i Tekhniki. Series: Matematicheskoye Modelirovaniye Fizicheskikh Protsessov. 1989. V.3, p.109-111.

8. Bykov A.N., Voronin B.L., Kozub A.G. et al. RAMZES program complex for heat conductivity 3D gas dynamics problems // Tekhnologiya Matematicheskogo Modelirovaniya. Novosibirsk, Computer Centre of the Siberia Department of the Academy of Science of the USSR 1989. p.37-41.

9. Danilov G.A., Mikivchuk A.M., Mikhailov A.T. FORTRAN mobile preprocessor SWIFT // Ibid. - p.47-52.

10. Batalova M.V., Bakhrakh S.M., Vinokurov V.A. et al. Complex "SIGMA" for 2D Gas Dynamics Problem Computations // Proc. of the All-Union Workshop on numerical methods of viscous fluid mechanics. Novosibirsk, Nauka Publishing House, 1969, p 288-289.

11. Gribov V.M., Neuvazhayev V.E., Frolov V.D. et al. Complex TIGR for mathematical physics 2D problems computations // Voprosy Atomnoy Nauki i Tekhniki. Series: Metodiki i Programmy Chislennogo Resheniya Zadach Matematicheskoy Fisiki. -1984. -V.3. -p.34-41.

12. Demchenko V.V., Markin V.D. On a certain family of multidimensional nonlinear heat conductivity equation exact solutions. Zhurnal Vychislitelnoj Matematiki i Matematicheskoy Fiziki. -1985. -V.25.-No.3, p 461-466.

13. Tikhonov A.N., Samarsky A.A. Mathematical Physics Equation, Moscow, Nauka Publishing House, 1977.

14. Nemchinov I.V., Three-axis gas ellipsoid expansion at a regular mode // Prikladnaya Matematika i Mekhanika. -1965. Issue 1, p 134-140.

15. Sedov L.I. Powerful shock wave propagation // Prikladnava Matematika i Mekhanika. -1946. V 10, Issue 2, p 8-14.

16 Voronin B.L., Zhmailo V.A., Kozub A.G. et al. Multidimensional computation of powerful explosions in exponential atmosphere // Voprosy Atomnoy Nauki i Tekhniki. Series: Matematicheskoye Modelirovaniye Fisicheskikh Protsessov. 1990. Issue 3, p.44-50.

SESSION A

Algorithm Development I

Mathematical Modeling of Turbulent Flow in Multi-Component Media
Oleg Buryakov, Valentin Kuropatenko, et al. (Chelyabinsk)

MATHEMATICAL MODELLING OF TURBULENT FLOW IN MULTICOMPONENT MEDIA

O. V. Buryakov, V. F. Kuropatenko, V. K. Mustafin, L. P. Brezgina, M. V. Dodonova and I. R. Makeeva (Chelyabinsk)

Introduction

The mathematical division of the All-Union Scientific Research Institute of Theoretical Physics has been developing, studying and implementing models of multicomponent and heterogeneous complicated media since the end of the 1970s.

The main efforts have been directed at developing a numerical method for calculating turbulent motion of complicated multilayered systems of various substances, including two-component mixtures. These layers may exist in the initial state of the system or arise during its movement owing to a loss of stability at the contact boundaries (CB) between the separate layers.

Thus, analytical and precise solutions of dynamics problems were found, and the properties of solutions for systems of equations describing the principal classes of known models of multicomponent and heterogeneous media were investigated in detail for simplified models (isothermal gases, polytropic gases, condensed media, uncompressed liquids).

Such a thorough investigation of the qualitative features of the solutions occurring in models of mixtures of substances after shock-wave (SW) interactions and under the influence of massive forces enabled a numerical method to be correctly chosen. This method highly accurately reproduces the principal features of SW processes in mixtures of substances (multiwave configurations, change of concentration profiles) and is suitable for describing processes with intensified relative movement of components.

The accuracy of the method is investigated using precise solutions constructed for a whole class of characteristic problems concerning the dynamics of multicomponent and heterogeneous media.

Terms describing the force and energy of component

interactions in a characteristic range of flow parameters are calibrated in actual applications of the basic problem.

As a practical example of the solution of this problem, an approach for modeling experiments on the mixing of liquids and gases will be demonstrated within the framework of the mechanics of heterogeneous media.

When discussing possible collaboration in this scientific endeavor, then, besides the general problems, such as

-the development of models of multicomponent and heterogeneous media by taking into account new physical processes;

-the investigation of the qualitative features of solutions of systems of equations for mathematical models of multicomponent and heterogeneous media;

-the construction of accurate solutions;

-the development of numerical methods;

-the creation of one-dimensional methods;

I would like to emphasize the special significance of studies concerning the creation of theoretical and experimental methods for investigating processes in mixtures of substances that hold great interest for applications and, primarily, for mixing and separation processes.

I will discuss in more detail the state of our efforts on this problem.

The main result of our work, the numerical method (we call it CMM, calculation of the movement of mixtures), is designed to calculate one-dimensional turbulent motion of a continuous medium in Lagrangian coordinates assuming adiabatic hydrodynamics.

Homogeneous substances, in particular, explosives, or mixtures of two different substances are acceptable as the layers in the calculated systems. The layers are separated from each other by CB or evacuated gaps. Two-component mixtures can arise during movement of the system owing to a loss of stability of the CB between individual layers and the separation of initially mixed substances to form a stable CB.

The movement of a homogeneous substance is described within

the framework of mechanics equations for a continuous medium by taking into account the porosity, strength, equilibrium phase transitions, and gravitational acceleration.

The movement of a two-component mixture is described within the framework of mechanics equations for multi-component and heterogeneous media by taking into account the velocity and temperature differences of the components, the variable internal structure of the medium, the porosity, strength, equilibrium phase transitions, and gravitational acceleration.

The thermodynamic properties of one-dimensional substances and the components in mixtures of substances are described by characteristic state equations. The state equations of a mixture of substances do not need to be known.

Phase transitions in a homogeneous substance and of component mixtures are calculated and considered at the level of the state equation.

The movement of a mixture of phases of a given substance or a given component of a mixture of substances is calculated assuming constant-velocity thermomechanical equilibrium.

1. Mathematical model of a heterogeneous and multicomponent medium

The conservation laws for a homogeneous substance have the following form:

$$\frac{\partial \rho}{\partial t} + \frac{\partial}{\partial r}(\rho u) + \frac{(\nu-1)\rho u}{r} = 0 \qquad (I.1)$$

$$\rho \frac{du}{dt} + \frac{\partial p}{\partial r} = \rho g \qquad (I.2)$$

$$\rho \frac{dE}{dt} + \frac{\partial}{\partial r}(pu) - \frac{(\nu-1)pu}{r} = \rho g u \qquad (I.3)$$

$$p = f_p(\rho, E, \Phi) \qquad (I.4),$$

where $$\delta = E + \frac{u^2}{2},$$

$$\frac{d}{dt} = \frac{\partial}{\partial t} + u\frac{\partial}{\partial z}$$

ρ is the density, u is the velocity, p is the pressure, e is the specific total energy, E is the specific internal energy, g is gravitational acceleration, Φ is the phase, ν is a symmetry index of the problem ($\nu = 1$, planar; $\nu = 2$, cylindrically symmetric; $\nu = 3$, spherically symmetric), z is the Euler coordinate, and t is the time.

The hypothesis about the mutually penetrating continua proposed by Rakhmatulin [1], which is valid for the following assumptions, provides a basis for describing flows in layers of two-component mixtures.

1. The particle size of the components in the heterogeneous medium is much greater than the molecular-kinetic dimensions, *i.e.*, the particles contain a large number of molecules.

2. The particle size is much less than the distances within which the macroscopic or averaged parameters of the heterogeneous medium or components substantially vary (outside the explosion surface).

Thus, a two-component heterogeneous medium is a combination of two continuous media, each of which is described by its own velocity, partial density, specific internal energy, pressure, temperature, etc. These continuous media interpenetrate each other and simultaneously occupy the same volume. The latter is also valid for multicomponent media, for example, mixtures of gases.

The conservation laws for a two-component mixture have the following form [2]

$$\frac{\partial \alpha_i \rho_i}{\partial t} + \frac{\partial}{\partial z}(\alpha_i \rho_i u_i) + \frac{(\nu-1)\alpha_i \rho_i u_i}{z} = 0 \qquad (I.5)$$

$$\alpha_i \rho_i \frac{du_i}{dt} + \frac{\partial \alpha_i p_i}{\partial z} = \alpha_i \rho_i g + \overline{R_i} \qquad (I.6)$$

$$\alpha_i \rho_i \frac{d\delta_i}{dt} + \frac{\partial}{\partial z}(\alpha_i u_i p_i) + \frac{(\nu-1)\alpha_i p_i u_i}{z} = \alpha_i \rho_i g u_i + \overline{\Phi_i} \qquad (I.7)$$

$$p_i = f_{p_i}(\rho_i, E_i, \Phi_i); \quad T_i = f_{T_i}(\rho_i, E_i, \Phi_i) \qquad (I.8),$$

where

$$\alpha_1 + \alpha_2 = 1, \qquad \eta_1 + \eta_2 = 1,$$

$$\frac{d_i}{dt} = \frac{\partial}{\partial t} + u_i \frac{\partial}{\partial z},$$

$$\mathcal{E}_i = E_i + \frac{u_i^2}{2}, \qquad (i = 1,2, \; i \neq j)$$

$$\bar{R}_1 + \bar{R}_2 = 0, \qquad \bar{\Phi}_1 + \bar{\Phi}_2 = 0.$$

ν is the symmetry index of the problem, ρ_i is the physical (true) density of the i component, α_i and η_i are the volume and mass concentrations of the i component, u_i is the velocity of the i component, p_i is the pressure of the i component, T_i is the temperature of the i component, Φ_i is the phase of the i component, g is gravitational acceleration, and $\bar{R}_i$ and $\bar{\Phi}_i$ are the intensities of pulse and energy exchange between components. The remaining notations have the same meaning as above.

The equations given above are common for a number of mathematical models of heterogeneous and multicomponent media. The specifics occur in the representation of the expressions for the functions $\bar{R}_i$ and $\bar{\Phi}_i$, which describe the force and energy of component interactions. However, the presence in them as additive terms of the volume forces R_i and volume energy sources Φ_i is common to all representations of $\bar{R}_i$ and $\bar{\Phi}_i$. These functions have the following form

$$R_i = \gamma_i \frac{u_j - u_i}{\tau_{ij}^u} \qquad (I.9)$$

$$\Phi_i = R_i u_i + k_i R_i (u_j - u_i) + \frac{p_j - p_i}{\tau_{ij}^p} + \gamma_i \frac{T_j - T_i}{\tau_{ij}^T} \qquad (I.10)$$

3. Results of numerical calculations

MAX is widely used for calculating various classes of problems. By way of example, one can name calculations of two-dimensional corrections in using a hydrodynamic method to determine the strength of underground nuclear explosions in joint Soviet-American tests at the Nevada and Novaya Zemlya test sites.

Several ways of calculating the convection flows and processes having strong deformations in the contact surfaces are illustrated in the following problems:

1. The formation and motion of cumulative streams;
2. Hydrodynamic instability.

One of the forward-looking directions in creating new technologies for explosions being used for a wide range of economic purposes, is the development and implementation of cumulative charges. A grooved metal-faced cartridge of an explosive substance comprises the base of the charge. Due to the complex processes of flinging and deforming, either a high-speed compact element or a cumulative flow is formed from the facing material. The facing is capable of performing various functions when it couples with an obstruction. The task of creating a highly effective cumulative charge is today still topical.

One type of construction for an industrial cumulative charge having a conical shape has been studied. As a result of numerical modeling, we have gained an overall picture of the characteristics of the compression processes and the deformation and motion of the cumulative stream. Figure 1 shows the stream's shape at two points in time. A comparison with the experiment is given.

The following examples are related to studies on hydrodynamic instability. The study of hydrodynamic instability is exceedingly important when solving many applied problems, in particular those that deal with energy cumulations. MAX performs direct numerical modeling of impulse (Richtmeyer-Meshkov instability) and gravitational instability (**[TN] -Taylor instability).

Gravitational instability.

The simplest modeling problem is being studied, in which a heavy substance is lying on a light one in the field of gravity. Figure 2 illustrates the process of developing a unimodal small perturbation and causing the separation boundary to interact with the upper and lower rigid walls.

[TN] Name illegible in original Russian text

Figure 3 shows the evolution of chaotic small perturbations at the separation boundary of two substances of varying density, where non-steady energy release is defined in each substance.

Figure 4 depicts the results of calculating a problem on the convergence of a spherical shell. Initially, the disturbed shock wave front moves out to the external boundary, and a non-steady energy release is defined in the shell. Here at different time intervals, all types of hydrodynamic instability exist. The figure illustrates the form of the shell and the gas at the last point in the calculation.

Impulse instability

In 1989 an international conference took place in Pleasanton (USA). The conference was devoted to the research on the turbulent intermixing of liquefiable mediums. The initiator and chairman of the meeting was Dr. B. Rupert from Lawrence National Laboratory. Before the conference he presented conference participants with two test problems to verity and compare numerical methods. A significant portion of the reports given [at the conference] were devoted to the calculations of these problems. In the problems one had to study the development of perturbations at the boundary of gases of varying densities that were acted upon by the impulse acceleration elicited by a stationary shock wave (SSW). The shock wave enters the contact boundary from the heavy gas into the light gas and vice versa. It was also necessary to examine the interaction in the zone of mutual penetration of gas caused by the shock waves reflecting off the boundaries. The initial perturbations in the contact boundary were defined in the form of one mode and the superposition of five modes.

Figure 5.8 represents the results of the calculation of these problems, as generated by MAX. A change in the form of the contact boundary and perturbation amplitude overtime is shown, as is a comparison of the results obtained by Dr. B. Rupert.

Figure 9 depicts the results of calculating the S.G. Zaitsev experiment [2]. The development of unimodal perturbations on the contact boundary of gases of various densities were studied, as they are effected by a "strong" shock wave (MAX = 3.5). Also depicted are the form of the contact boundary and the isometric line of the velocity vector at one time interval.

BIBLIOGRAPHY

1. C.W. Hirt, A.A. Amsdem, J.L. Cook. "An Arbitrary Lagrangian-Eulerian Computing Method for all Flow Speeds." *Journal of Computational Physics*, 14, 3, 1974.

2. A.N. Alyeshin, E.B. Lazarev, S.G. Zaitsev, V.B. Rozanov, et al. "A Study of Linear, Non-linear and Transitional Stages of Richtmeyer-Meshkov Instability Development." *DAN SSSR*, 1990, v. 310, no.5, pp. 1105-1108.

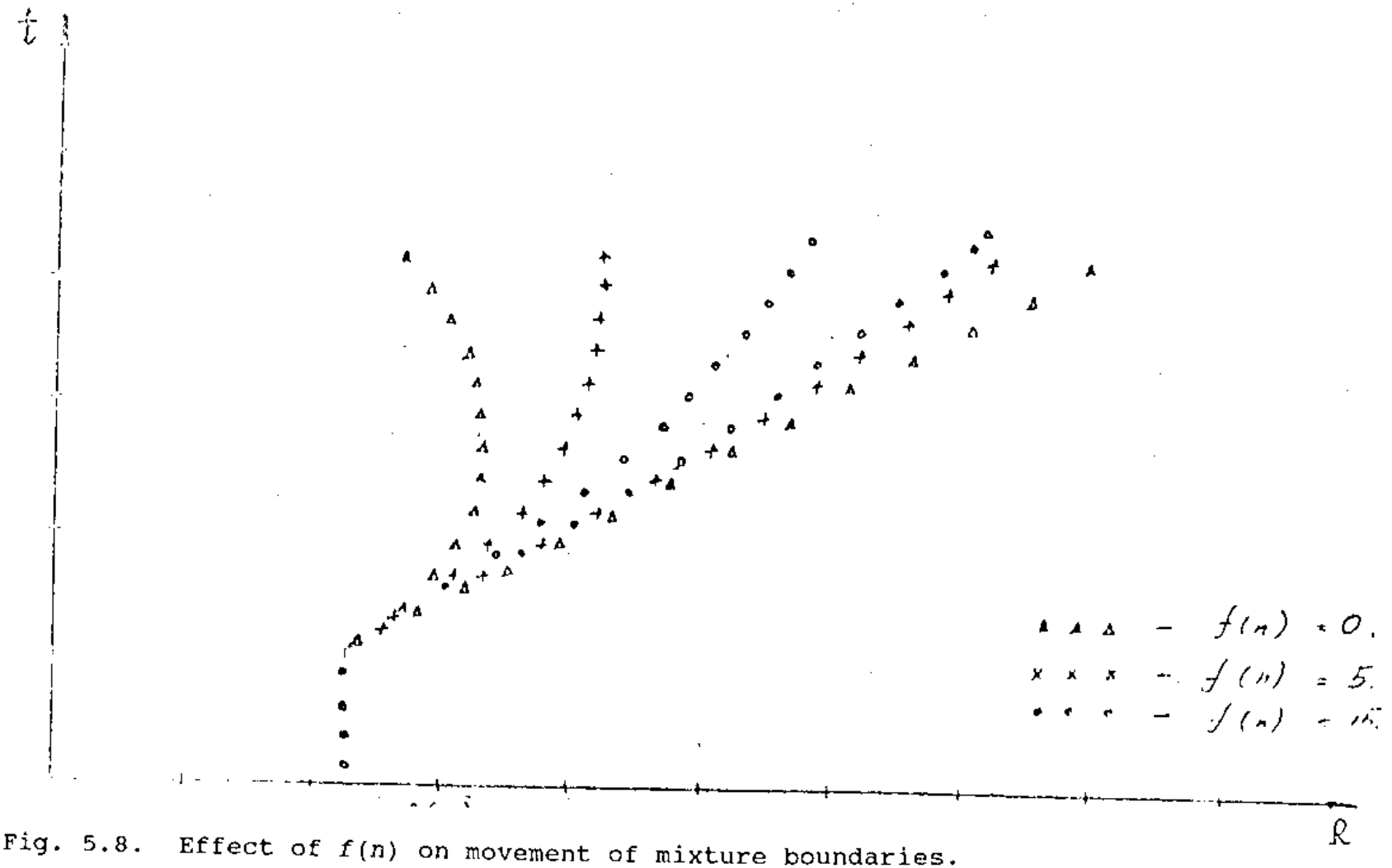

Fig. 5.8. Effect of $f(n)$ on movement of mixture boundaries.

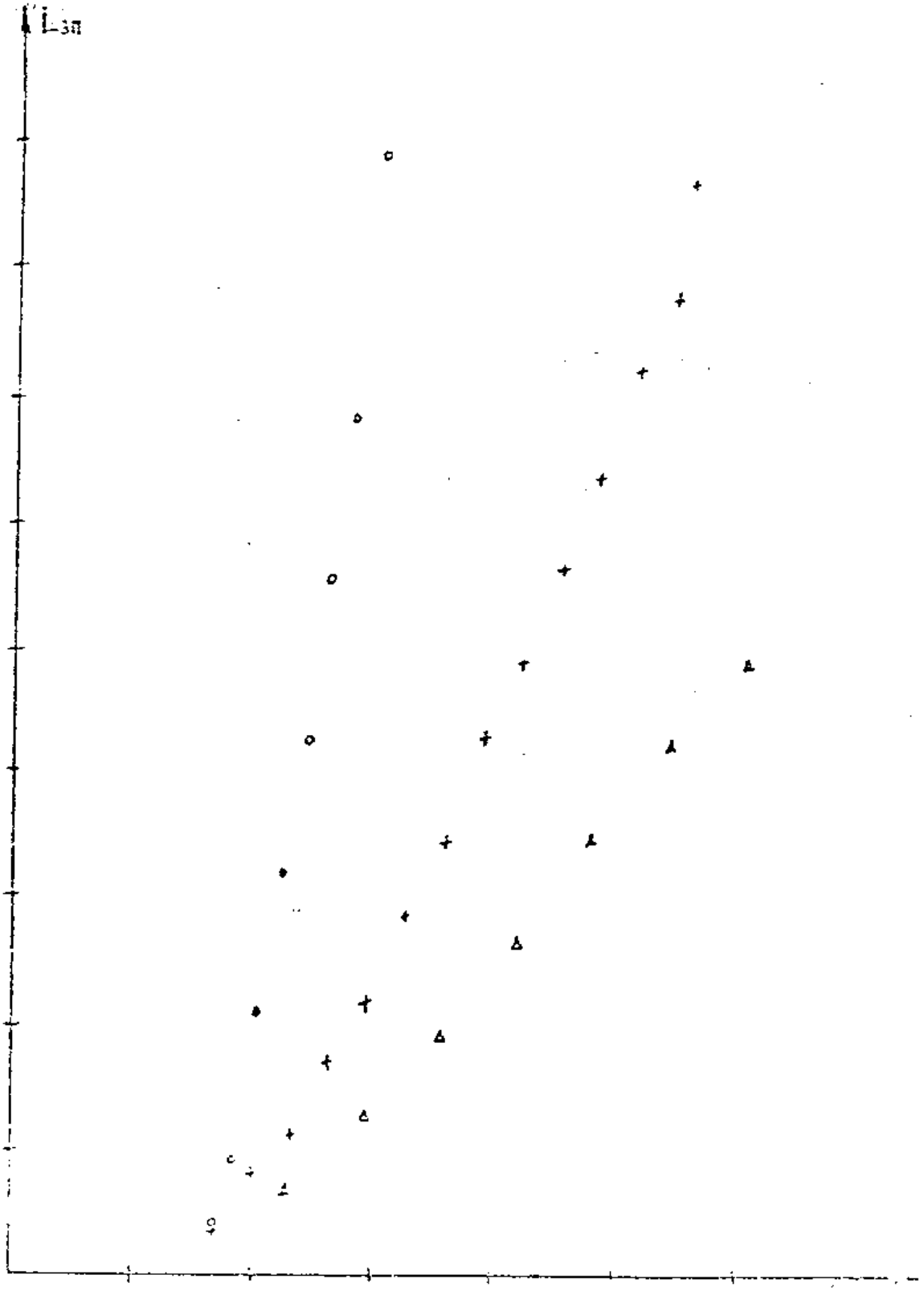

Fig. 5.9.

Function $L_{MZ}(t)$ for various $f(n)$. Ratio of component densities n = 13.5.

o o o – $f(n) = 0$, x x x – $f(n) = 5$,

Δ Δ Δ – $f(n) = 15$.

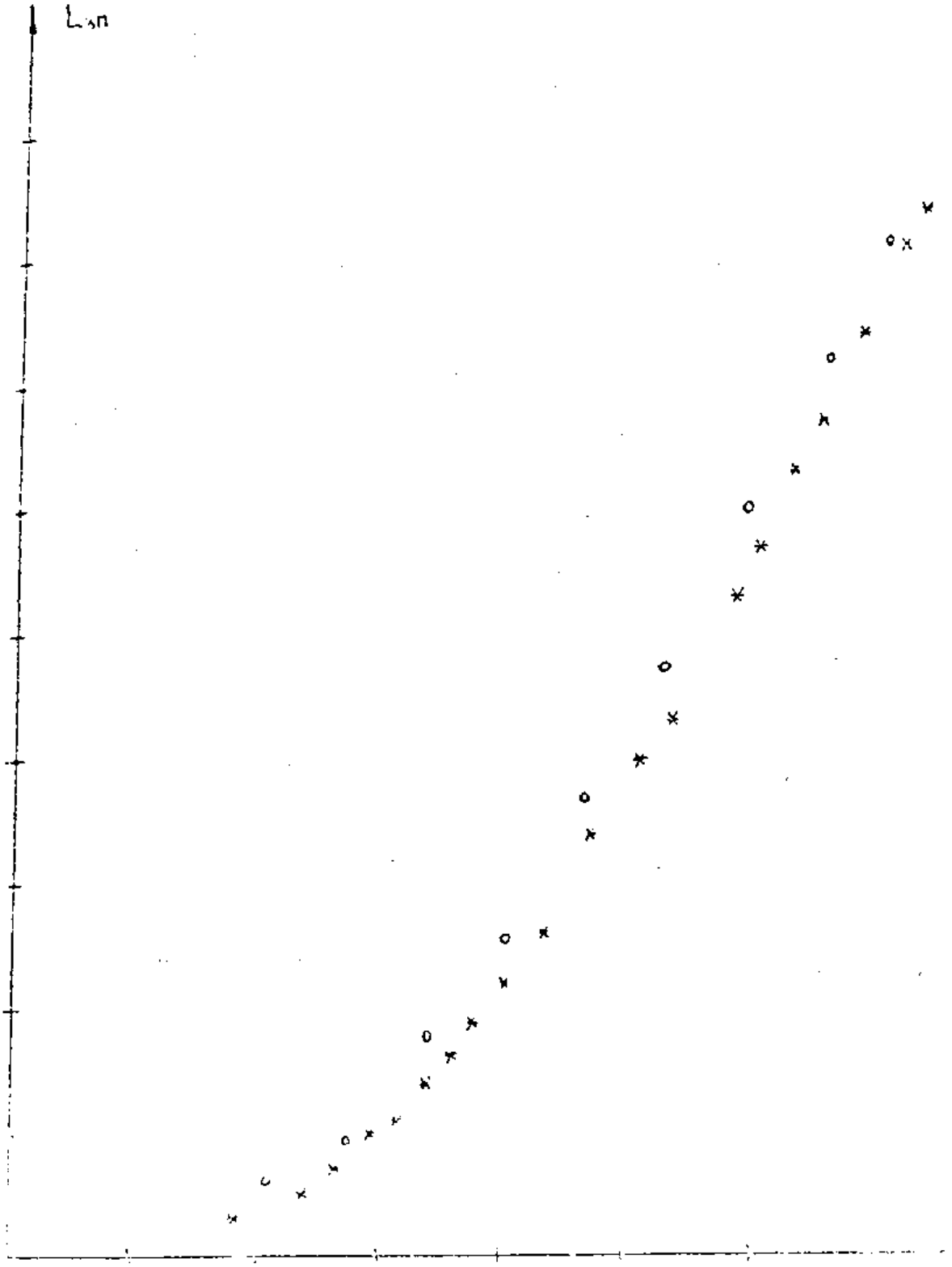

Fig. 5.10. Function $L_{MZ}(t)$. Ratio of component densities

Component n = I3.5.

× × × – experiment;

o o o – numerical calculation.

Experimental investigations of gravitational turbulence for gases with density decreases $n = 13.5$ produced the partial density profile of Kr in the MZ.

The experimental and calculated density profiles of Kr obtained using the CMM program with different MDC are plotted in Fig. 5.11. The experimental profile satisfactorily agrees with that calculated. The effect of the type of MDC of the components on the accuracy of the Kr profile description can also be seen. An isothermal calculation at the left boundary gives a more accurate description; an isentropic one is more accurate near the right boundary.

The experimental curve near the CB lies between the limiting cases. This means that the heat exchange between the components in the MZ must be calculated.

Thus, the results suggest that studies on mathematical modelling of turbulent flows of multicomponent media within the framework of the CMM method are promising.

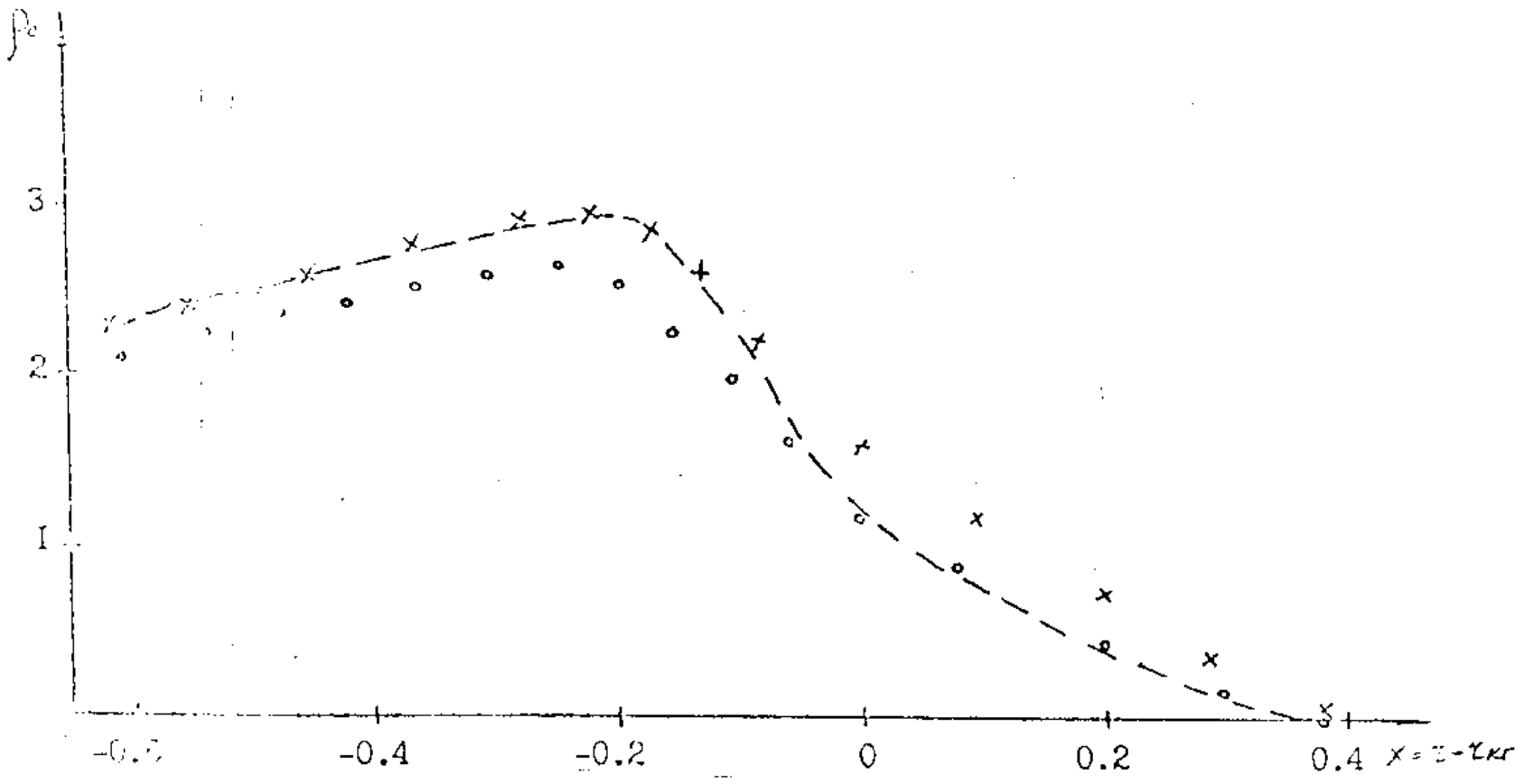

Fig. 5.11. Profile of partial density of the heavy component. ---, — - experiment;', x x - isotherm; oo - isentrope..

References

1. Kh. A. Rakhmatulin, "Principles of gas dynamics of interpenetrating compressed media," *P. M. M.*, **20**, No. 2, (1956).
2. O. V. Buryakov and V. F. Kuropatenko, "Numerical modelling of turbulent flow of a two-component heterogeneous medium taking into account velocity and temperature nonequilibrium of components," VANT Ser. Methods and Programs of Numerical Solution of Mathematical Physics Problems, No. 3 (1986).
3. O. V. Buryakov and V. F. Kuropatenko, "Propagation of rarefaction and shock waves in a heterogeneous mixture of two isothermal gases," VANT Ser. Methods and Programs of Numerical Solution of Mathematical Physics Problems, No. 2(8), (1981).
4. O. V. Buryakov and V. K. Mustafin, "Solution of the piston problem in a heterogeneous mixture of two isothermal gases taking into account the associated-mass effect," VANT Ser. Methods and Programs of Numerical Solution of Mathematical Physics Problems, No. 2 (1988).
5. O. V. Buryakov and V. F. Kuropatenko, "Structure of the shock wave front in a heterogeneous mixture of two isothermal gases with component interaction forces," VANT Ser. Methods and Programs of Numerical Solution of Mathematical Physics Problems, No. 3, (1985).
6. O. V. Buryakov and V. F. Kuropatenko, "Solution of the piston problem in a mixture of two gases," VANT Ser. Methods and Programs of Numerical Solution of Mathematical Physics Problems, No. 1, (1985).
7. O. V. Buryakov and V. F. Kuropatenko, "Automodel rarefaction wave for one model of a heterogeneous mixture of two polytropic gases," VANT Ser. Methods and Programs of Numerical Solution of [words at bottom of R. p. 82].
8. O. V. Buryakov, V. F. Kuropatenko, and V. K. Mustafin, "Shock and rarefaction waves in a heterogeneous mixture of two solids," VANT Ser. Methods and Programs of Numerical Solution

of Mathematical Physics Problems, No. 4, (1988).

9. O. V. Buryakov, V. F. Kuropatenko, and V. K. Mustafin, "Dissipation of an arbitrary explosion at the interface of an isothermal gas and a heterogeneous mixture of two other isothermal gases," VANT Ser. Mathematical Modelling of Physical Processes, No. 2, (1990).
10. O. V. Buryakov and V. F. Kuropatenko, "Solution of the piston problem for a mixture of an isothermal gas with uncompressible particles, taking into account the component velocity nonequilibrium," VANT Ser. Methods and Programs of Numerical Solution of Mathematical Physics Problems, No. 1, (1986).
11. V. F. Kuropatenko, "On difference methods for hydrodynamics equations," in: Works of the Steklov Mathematical Institute, **74**, (1966).
12. Yu. A. Kucherenko et al., "Experimental investigation of gravitational turbulent mixing in the automodel regime," VANT, No. 1, (1988).
13. A. M. Vasilenko et al., Preprint 56, Physics Inst., Acad. Sci., Moscow (1990).

SESSION A

Algorithm Development I

Numerical Modeling of Multi-Dimensional Flows with Large Deformations
Vladimir Volkov, et al. (Chelyabinsk)

Anuchina, N.N., Volkov, V.I., Voronina, V.P., Es'kov, N.S. and Yarlykova, L.S.

Numerical Modeling of Multi-Dimensional Flows with Large Deformations

All-Russian Scientific Research Institute of Technical Physics

Annotation

This report describes a numerical method and its capabilities as it is implemented in the MAX software package. The results from the calculations of a number of problems on vortex flows with large deformations in the separation boundaries of substances are presented as an illustration.

1. Physical processes and mathematical models.

The MAX software package is designed to calculate the following physical processes:

-- adiabatic flows;

-- processes of the development and motion of detonation waves in explosive substances (with kinetic burning propagation and without the allocation of a zone for chemical reactions);

-- viscous fluid flows (the **[TN] equation is integrated)

-- viscous plastic flows;

-- phase transitions (melting, evaporation, polymorphism; modeling using equations of state);

-- motion of energy release unstable in terms of time and varied in terms of space.

2. Numerical method and its capabilities.

Depending on a prior information about the processes taking place in the problems, the system being calculated represents a set of calculated domains. The boundaries of these domains can be contact boundaries (i.e. domains in contact with other domains), external boundaries (free boundaries, rigid walls, boundaries with a prescribed pressure or normal velocity, Eulerian boundaries either with an outflow or influx of the substance) or continuous Eulerian boundaries through which a substance overflows from one computed domain into another.

[TN] Name illegible in original Russian text

A variety of physical regions can be found within a computed domain. There are two ways to describe the contact ruptures: regular and irregular. First let us examine the numerical method with a regular description of the surfaces of the substance interface in the substances where they are mesh lines.

2.1 Regular method

A sort of modification of the arbitrary Lagrangian-Eulerian method proposed by S. Zhert, E. Amsdon and J. Cook [1] is used for calculations within the internal points of the computed domains. The algorithm currently being implemented in MAX differs significantly from the one used originally, although the basic design principles and ideas of the method have been preserved [1]. They consist of the following:

1. Difference equations derived by approximation of the quadrangular mesh of the laws of conservations, i.e. the diagram is a divergent relative to mass, impulse and full energy.
2. Integration is divided into two stages. Lagrangian equations are solved at the first stage, while the second stage takes into account the convective flows between the cells, in the event that the law of motion of the upper mesh does not correspond to the Lagrangian law.
3. The original implicit iteration diagram is used at the Lagrangian stage. The explicit phase is a null iteration. At every iteration the diagram is also implicit, and the iteration process comes together at any time increment .

The modified method has a number of new and important features:

-- Spherical symmetry is preserved at the Lagrangian and Eulerian stages, and the equations thus remain divergent;

-- The difference diagram is more monotonous, and in such problems, like the calculation on the Eulerian mesh of the disintegration of gaps with large drops in density and dispersion into a vacuum, it is more exact.

Each computed domain uses its own arbitrary quadrangular mesh. The contact boundaries between the computed domains are calculated without taking slipping into account. For boundaries of adjacent computed domains that are in contact, a computational algorithm for surface slipping has been developed and implemented . The algorithm fulfills the condition for preserving symmetry.

2.2 Irregular method of calculating contact boundaries

The irregular method is used to calculate significant deformations in the boundaries of substance separation. In this method, particle markers, located directly along the line separating the substances, are used to describe the contact rupture. The markers, whose coordinates are calculated at every increment, determine the location of the contact surface.

In the irregular method the boundary calculations may arbitrarily intersect the Eulerian mesh, thereby forming mixed cells containing several different substances. These cells also introduce an irregularity into the numerical algorithm both at the Lagrangian and Eulerian stages. Various conditions for consistent deformation of the components are employed to calculate the mixture. The conditions for thermodynamic equilibrium of components and the continuity of the velocity vector along the contact boundary are the conditions primarily used.

At the Lagrangian stage, the peculiarity of the mixed cell calculation lies in determining the pressure of the mixture, which is generally found by using iterations. Otherwise, the calculation of such cells essentially does not differ from the calculations of homogeneous cells.

The peculiarities introduced by irregular boundaries at the Eulerian stage considerably complicate the algorithm for calculating convective flows during mesh readjustment. At this stage, first the coordinates of the markers and their position in the mesh are determined. Flows in the neighborhood of mixed cells are calculated by taking into account the direction of the flow, the composition of the substance in the cell, depending on the direction in which the markers are relocated along the Eulerian mesh, and in some instances, depending on the number of markers that have shifted from one cell to another.

During calculation, the rarefaction or thickening of the markers on the separation boundary is monitored. Such markers are eliminated and the addition of new ones is prevented.

The transition to the irregular method of describing the contact boundaries takes place, as a rule, at a certain point in the calculation when large deformations begin to occur and a regular calculation becomes difficult.

Since the irregular method is rather expensive, the program envisages the possibility of reconstructing and recording the flows at every few Lagrangian increments, rather than at every single increment. A calculation of strong deformations of contact surfaces without using markers at all, but using a concentration, is also conceivable.

By using a priori information about processes in convective problems, it is possible to combine Lagrangian (explicit or implicit) and Eulerian calculations, and use the regular or irregular method for describing the contact boundaries in various domains of a given problem or in one in the same domain, but in different time intervals. This approach makes it possible to calculate a wide class of flows while choosing the optimal path for obtaining the necessary precision.

on the following concepts:

1) local component pressures are equal in the MZ;
2) the overall pressure gradient causes different accelerations of components with different densities;
3) the component interaction forces are proportional to the square of the difference of their densities;
4) the linear dimension of heterogeneities in the MZ increases in proportion to the width of MZ;
5) the coefficient of resistivity in the component interaction forces depends on the local decrease of component densities;
6) additional dissipation of energy owing to turbulence is considered in terms of the dissipation of kinetic energy through component force interaction.

A series of calculations was performed using the CMM program. These correspond to experimental setups for mixing of uncompressed liquids and gases [12, 13].

The goal of these calculations was to calibrate the model parameters and to determine its capabilities for modelling flows arising under these experimental conditions.

Let us turn to modelling the experiments of Kucherenko.

The development of R–T instability at the CB of liquids of different densities can be diagrammed as follows:

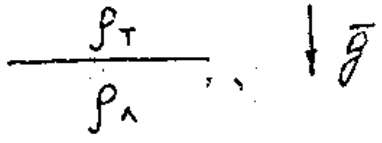

The heavy liquid with density ρ_H lies on the light liquid of density ρ_L in a gravitational field of acceleration g that is directed from the heavy liquid to the light.

Such a physical situation is unstable. If perturbations occur at the surface separating the media, then they will increase with time, the CB will be destroyed and a MZ will arise that will develop on both sides of the initial position of the interface.

It follows from size considerations for a MZ width of L_{MZ}

It follows from size considerations for a MZ width of L_{MZ} that:

$$\frac{L_{MZ}}{2L_{pr}} = A_T f_T(n) \qquad (5.3)$$

where $L_{pr} = gt^2/2$, $n = \rho_H/\rho_L$, and A_H = const.

An analogous relationship is obtained for the depth of penetration of the heavy liquid into the light:

$$\frac{L_{TA}}{L_{pr}} = A_{TA} f_{TA}(n) \qquad (5.4)$$

Coefficients $A_{HL}f_{HL}(n)$ with uncertainty $\sigma_{A_{HL}}$ have been obtained in previous experiments [12] for a series of density decreases n. These data are presented in Table 5.1.

Table 5.1

n	3	4	6	10	13.5	20
$10^2 \cdot A_{TA} f_{TA}$	9.4	13	18	23.6	27.6	29.9
$10^2 \sigma_{A_{TA}}$	0.65	0.3	0.93	0.63	1.3	1.2

Numerical modeling of the previous experiments [12] using the CMM program was carried out with the following setup.

Two substances in a gravitational field of acceleration $g = -1$ have the equation of state

$$p = (\gamma - 1)\rho\varepsilon \; ; \quad \gamma = \frac{5}{3} . \qquad (5.5)$$

The heavy substance lies on the light one, as diagrammed in Fig. 5.2.

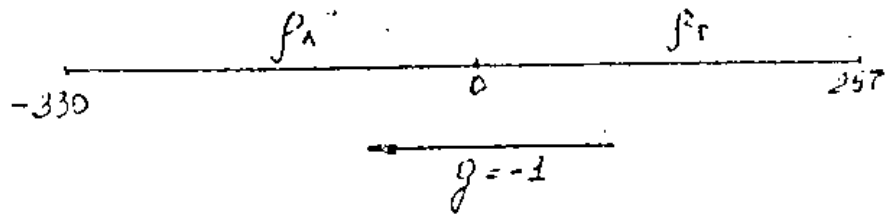

Fig. 5.2

Initially, the system is in equilibrium and the component velocities are $u_H = u_L = 0$. The initial distributions of the specific internal energies are:

$$E_A(x) = E_{0A} + \frac{g}{\gamma - 1}(x - x_0);$$
$$E_T(x) = E_{0T} + \frac{g}{\gamma - 1}(x - x_0), \qquad (5.6)$$

and determine the pressure profiles in the heavy and light layers corresponding to the pressure distribution in an uncompressed liquid placed in a gravitational field of acceleration g.

The temperatures of the substances are identical at the CB.

The criterion for the loss of stability in this problem occurs at the initial time point. According to the CMM method, an elementary MZ is formed at $t = 0$. Its size is equal to twice the maximal range of the difference grids in the substances adjoining the CB.

The parameter $f(n)$ in eq. (5.2) for each decrease of densities was selected to describe satisfactorily the experimental data for the movement of the penetration front of the heavy component into the light. The initial data and the selected parameters $f(n)$ for decreases $n = 3$, 4 and 13.5 are listed in Table 5.2.

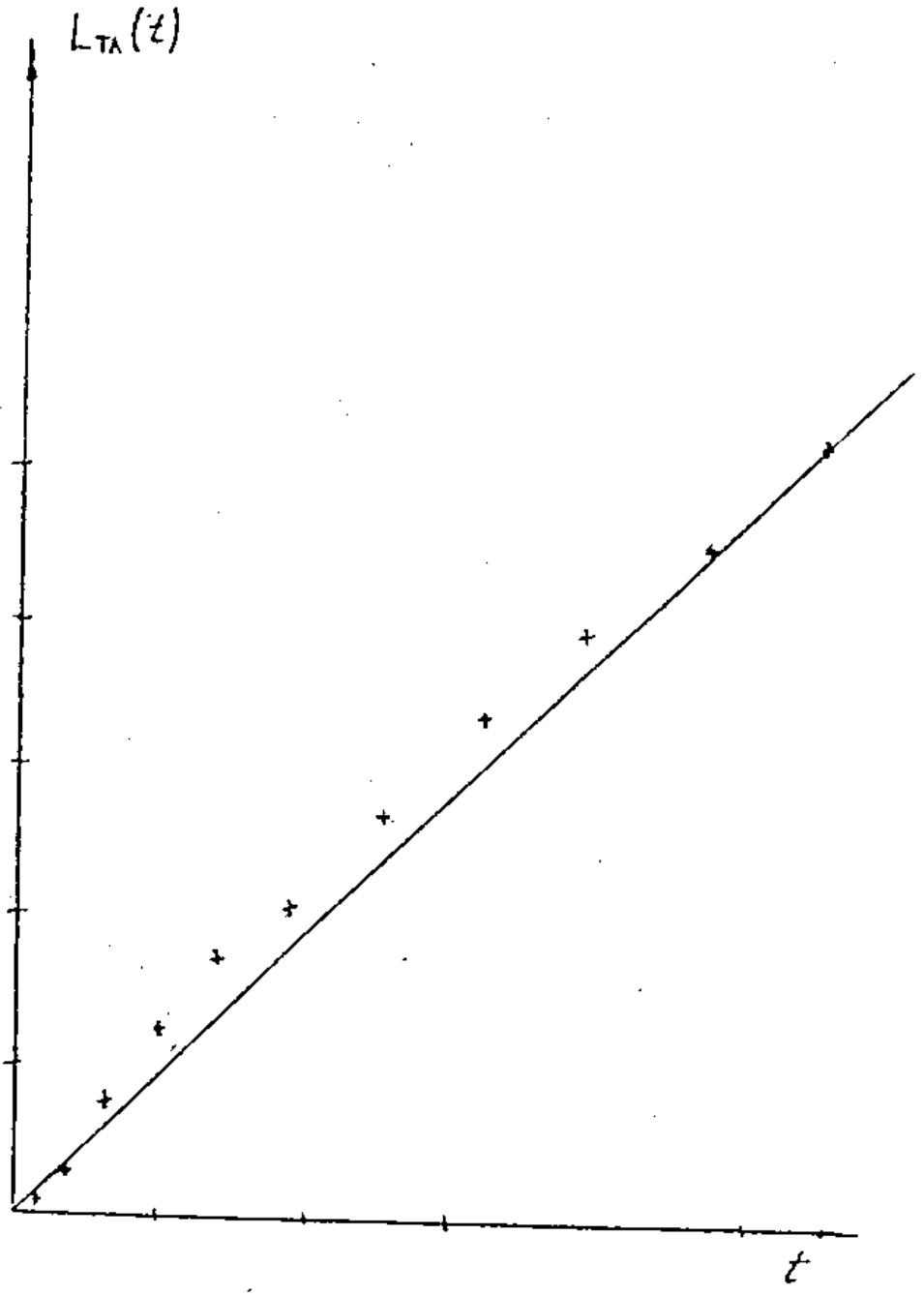

Fig. 5.3.

Function $L_{HL}(t)$. Ratio of component densities $n = 3$.

——— – experiment, × × × – numerical calculation, $f(n) = 32.7$.

Table 5.2

n	ρ_1	ρ_T	E_{01}	E_{0T}	$f(n)$
3	0.68	2.04	I350	450	32.7
4	0.68	2.72	I800	450	28
I3.5	I	I3.5	6075	450	I9.I

The corresponding calculated and experimental dependences of the penetration depths $L_{HL}(x)$ are plotted in Figs. 5.3-5.5. The experimental data are satisfactorily described at the selected $f(n)$. The following function was constructed from these values using the method of indefinite coefficients

$$f(n) = \frac{59.63}{n - 1.17} + 15.29 \qquad (5.7)$$

This function is plotted in Fig. 5.6. Calculations were performed for density decreases n = 6, 10 and 20 in order to check the generality of the constructed function. The values $f(n)$ were chosen according to the constructed function (5.7).

The values $f(n)$ calculated using eq. (5.7) and selected $f(n)$ that ensure the best agreement with the experiment for decreases n = 6, 10 and 20 are listed in Table 5.3.

Table 5.3

n	ρ_1	ρ_T	E_{01}	E_{0T}	$f(n)$ selected	$f(n)$ by formula
6	0.68	4.08	2700	450	24.3	23.3
I0	I.35	I3.5	4500	450	2I.28	20.3
20	0.68	I3.5	9000	450	I8	I8.I

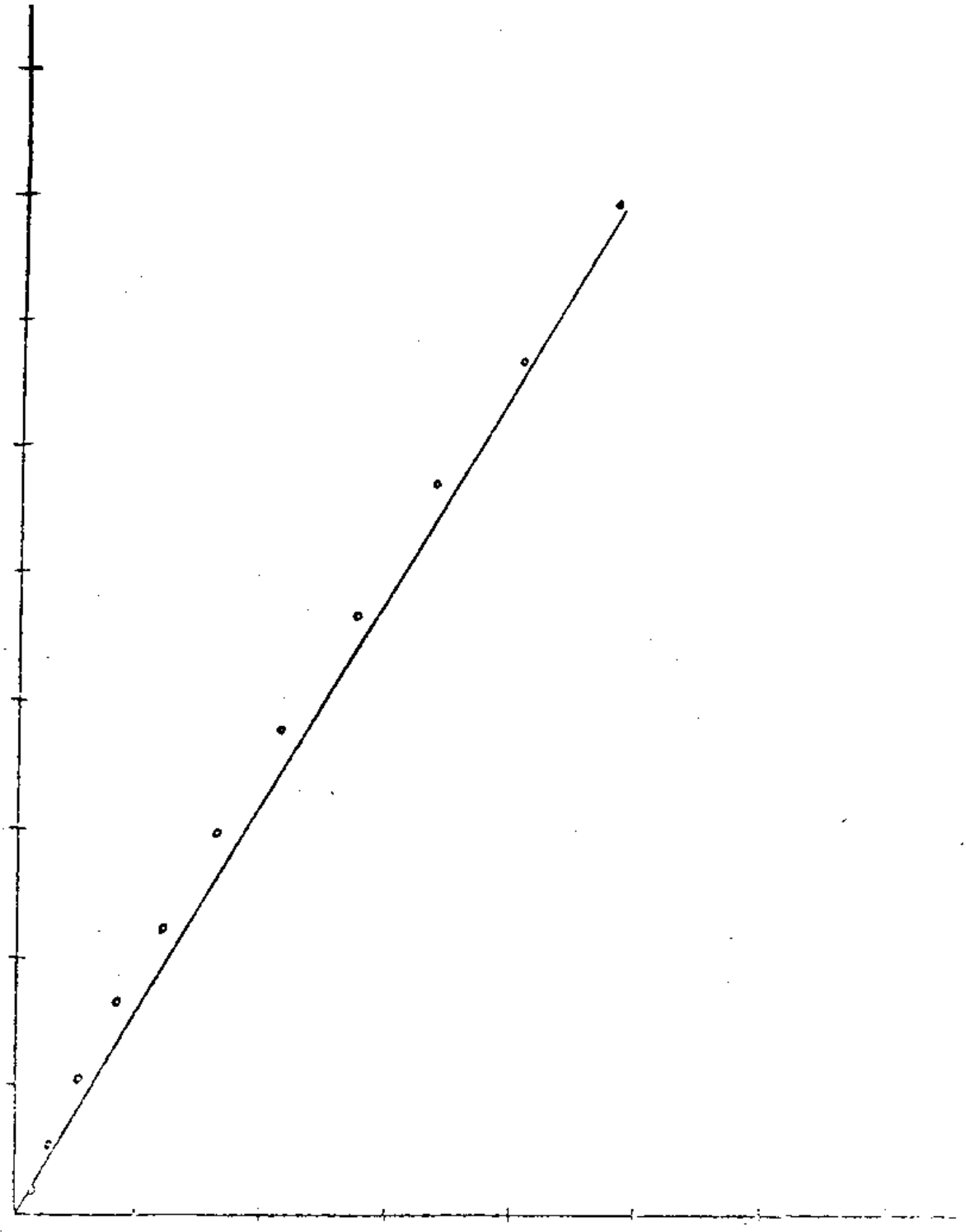

Fig. 5.4.

Function $L_{HL}(t)$. Ratio of component densities n = 13.5. ——— – experiment, ∘ ∘ ∘ – numerical calculation, $f(n)$ = 19.1.

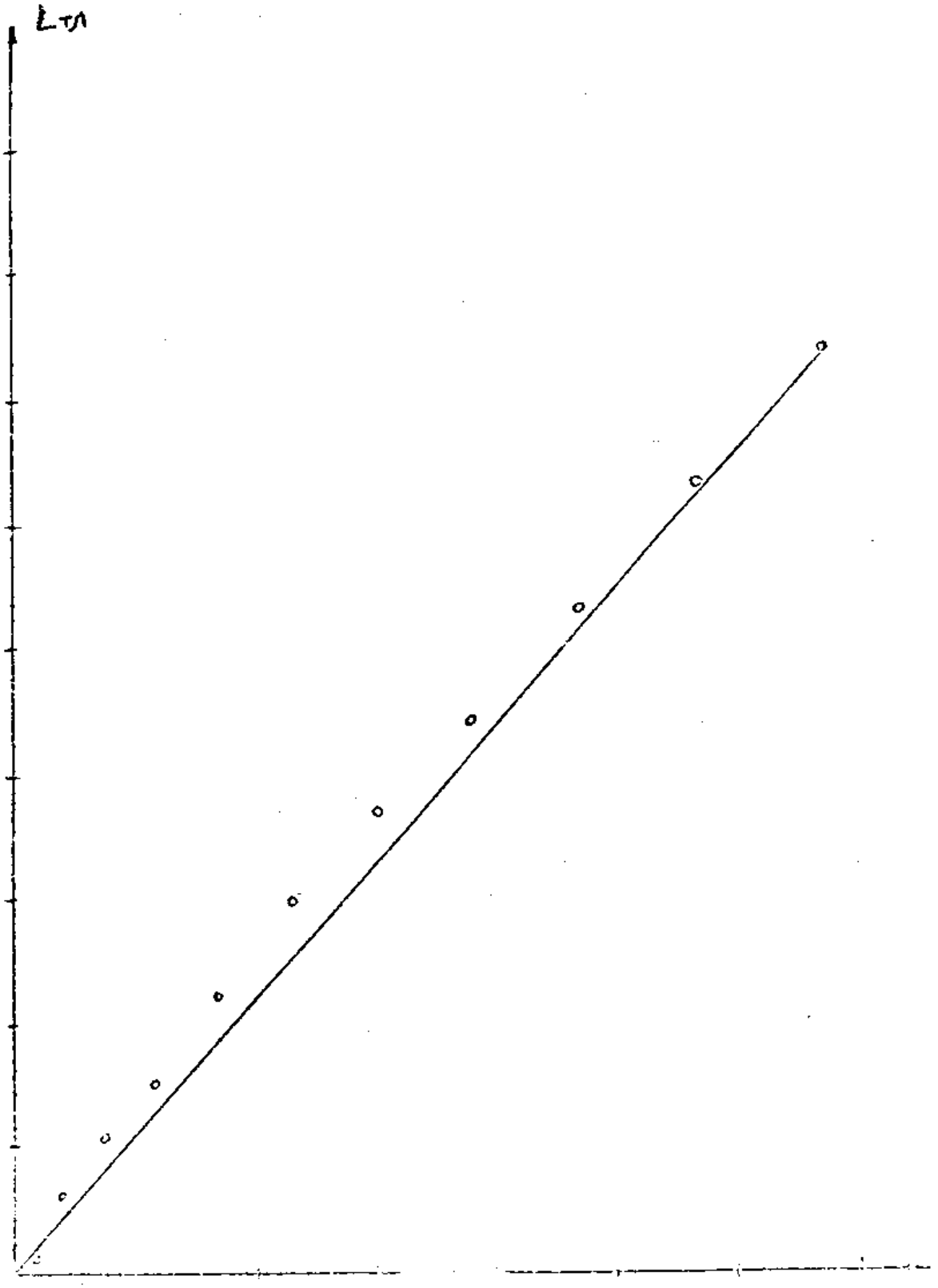

Fig. 5.5.

Function $L_{HL}(t)$. Ratio of component densities $n = 4$.

———— – experiment, • o o – numerical calculation, $f(n) = 28$.

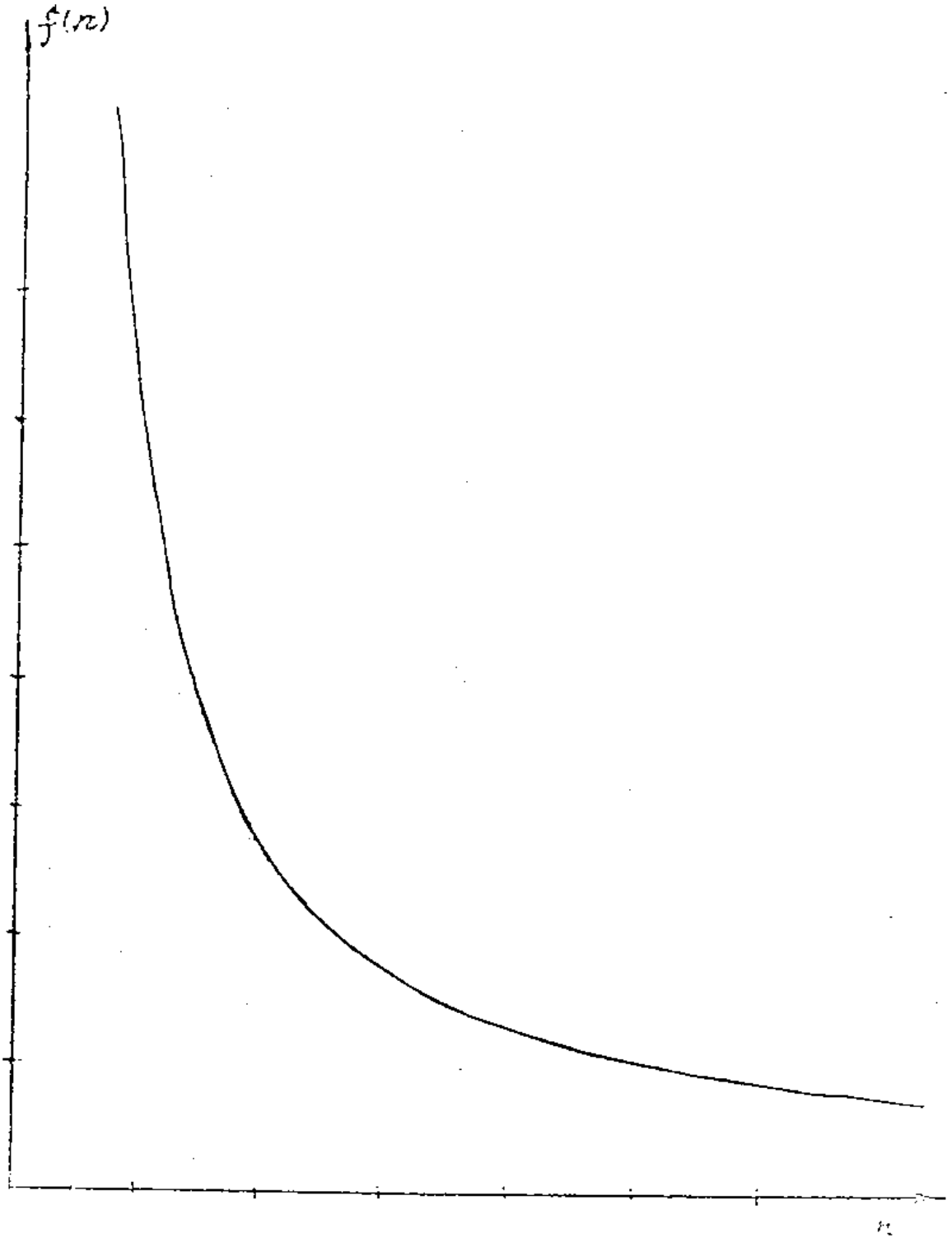

Fig. 5.6. Function $f(n)$.

The values selected and obtained from the formula differ by less than 4.7%.

The constructed function $f(n)$ was used in calculations corresponding to the experimental setup for gas mixing [13].

Previous experiments [13] on the gravitational instability at the interface of inert gases of different density under the influence of a non-steady-state SW were carried out in an electromagnetic shock tube (EMST). The shock tube and the placement of the dividers are diagramed in Fig. 5.7. The first section was filled with He. The second and third sections were filled with different monatomic gases (He, Kr, Xe, Ar). The gas in the second section was heavier than in the third. The physical description of the flow in the EMST is as follows. A SW formed in the discharge section of the EMST passes successively CB1 and CB2. At the moment the SW exits CB2, a sequential explosive discharge occurs. This forms a loading wave advancing in the direction opposite to the origin of the shock tube. The CB2 initially experiences a shock acceleration in the positive direction and then, entering the active zone of the loading wave, experiences an acceleration in the negative direction. This leads to an unstable state of the CB and mixing.

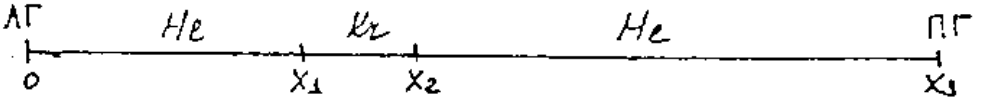

Figure 5.7

For a density decrease $n = 13.5$, the mathematical statement of the problem corresponding to the experimental setup has the following form:

[Equation missing?]

The pressure at the left boundary $p(t)$ is given as a function of time t, selected from the coincidence condition of the calculated and experimental trajectory of the first SW in He. The right boundary is a rigid wall. The gases are described by the state equation

$$P=(\gamma-1)\rho E \qquad (5.9)$$

The coordinates of the CB, the initial data, and the parameters of the state equations of the gases are given in Table 5.4.

Table 5.4

Boundary Coordinates (dm)	γ	ρ	P
$X_1 = 10.87$	1.63	$1.6\cdot10^{-4}$	0.984
$X_2 = 13.12$	1.689	$3.364\cdot10^{-3}$	0.984
$X_3 = 20$	1.63	$1.6\cdot10^{-4}$	0.984

As noted earlier, the component force interaction, *i.e.*, the parameter $f(n)$, is an important element of the examined mathematical model. The scale of the influence of this parameter is demonstrated in Fig. 5.8, where the z–t diagrams of the component fronts are plotted, and in Fig. 5.9, where the effect of $f(n)$ on the behavior of $L_{MZ}(t)$ is shown.

Experiments on gas mixing were numerically modeled both assuming no heat transfer and assuming local temperature equilibration of components. It was found that the decrease in densities in the mixture zone depend on the choice of conditions of mutual deformation with temperature. In effect, a decrease n = 13.5 in the case of an isentrope changed to n = 19.15 if the calculation was carried out assuming local temperature equilibration. The dependence of the decrease on the heat-exchange conditions between components means that the function $f(n)$ must be used in the general case of calculating the component force interaction. This function depends on the local density decrease n. A function constructed through modeling of experiments on the mixing of uncompressed liquids was used as $f(n)$ [12].

The dependence of the MZ width on time constructed for an isothermal decrease n = 13.5 is plotted in Fig. 5.10. Satisfactory agreement with the experimental curve is seen.

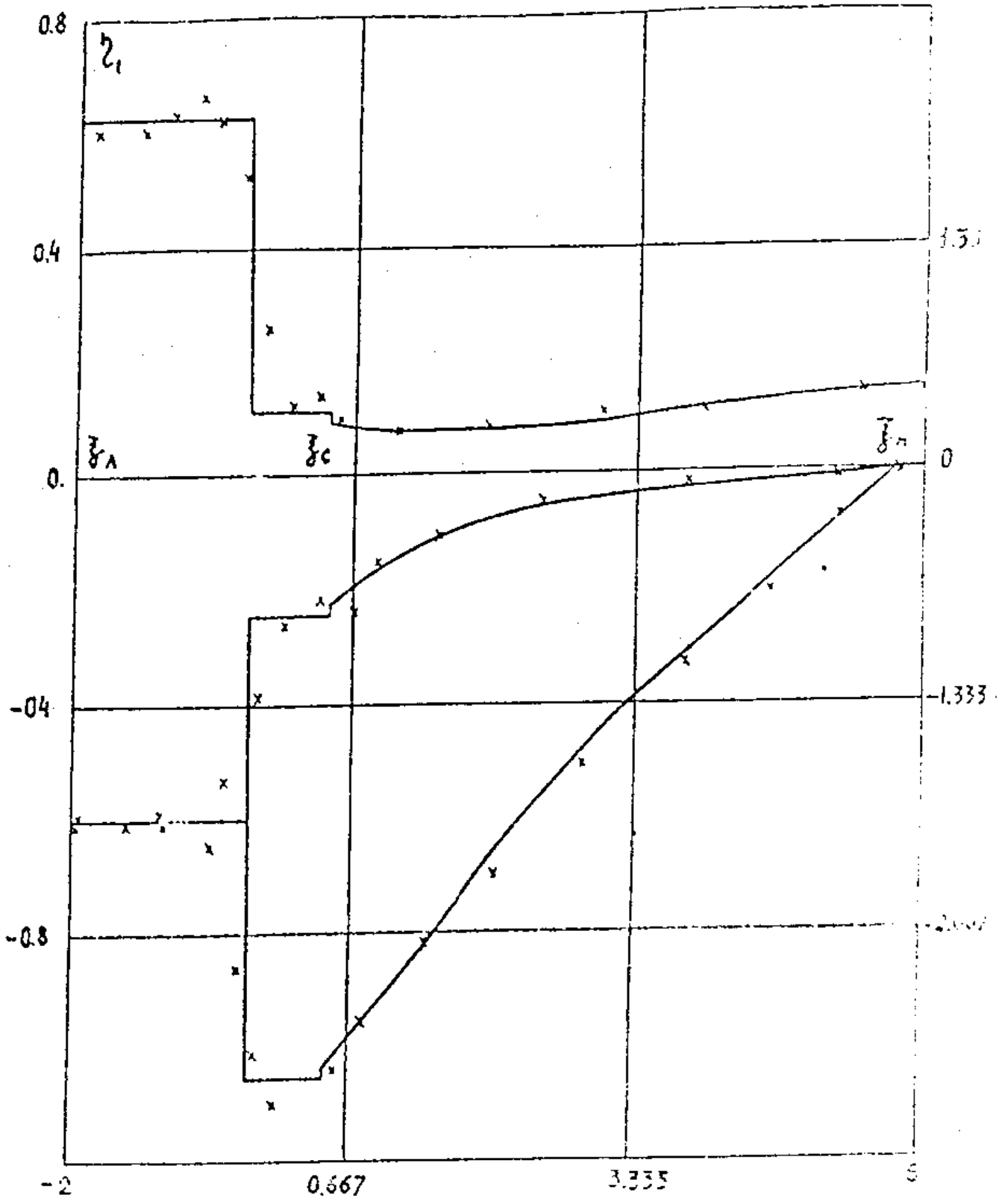

Рис. 4.8

Fig. 4.8.

Solution for a piston moving out of a mixture of two solids. Partial component separation in a rarefaction wave.

———— – precise solution

× × × – numerical solution. $t = 0.3551$

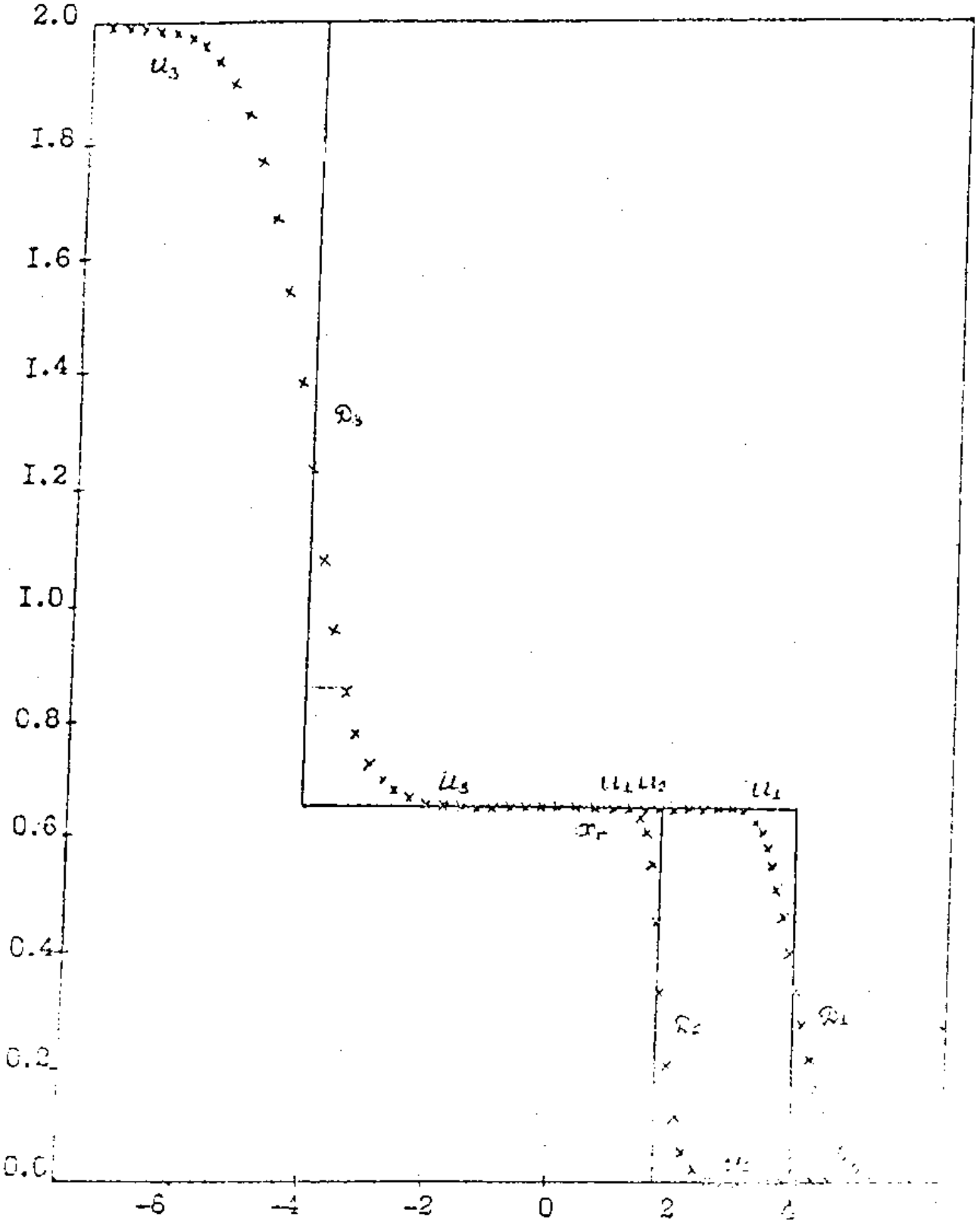

Fig. 4.9.

Explosion dissipation at the boundary of a homogeneous and heterogeneous element. SW–SW configuration.

———— - precise solution × × × - numerical solution.

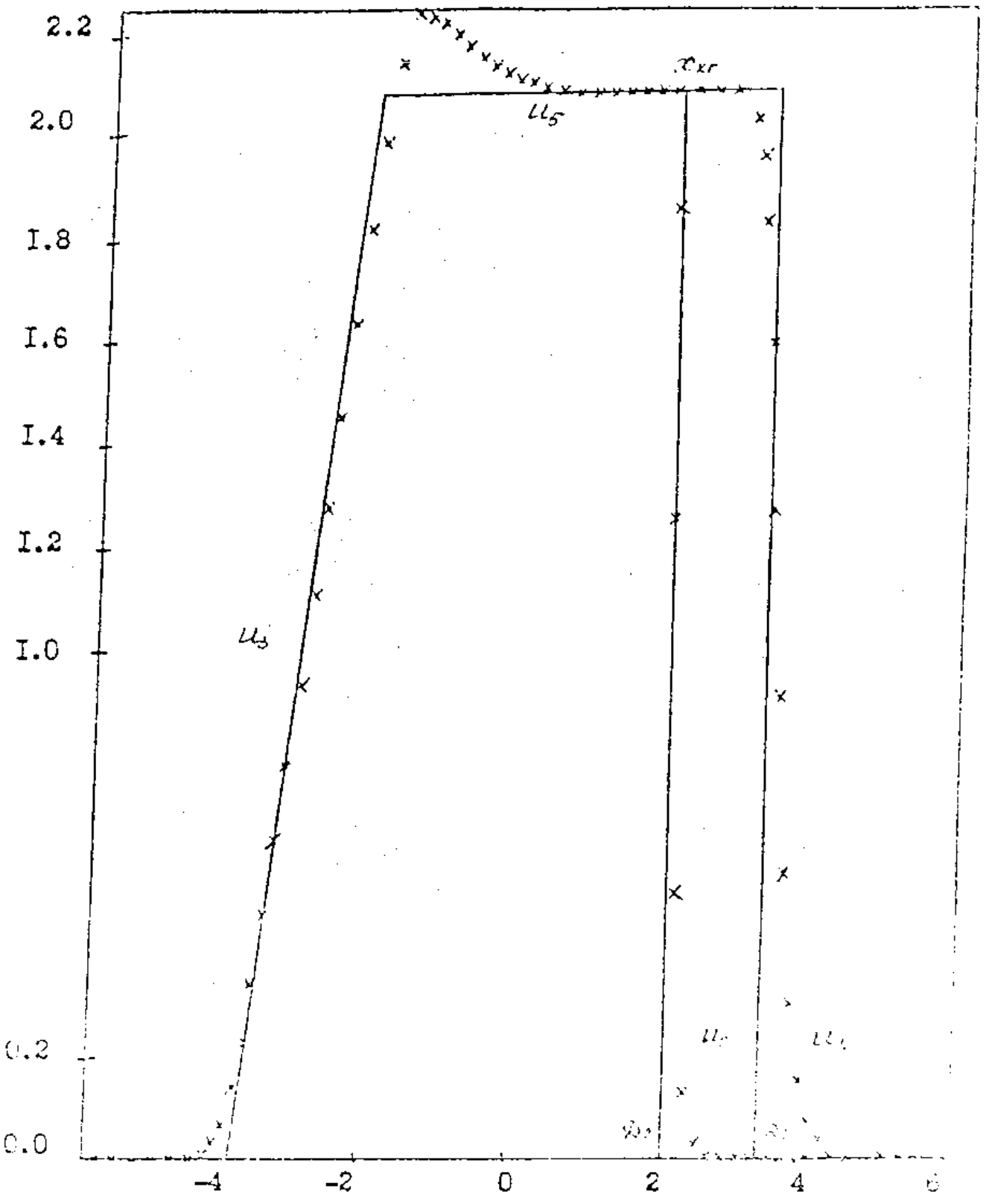

Fig. 4.10.

Explosion dissipation at the boundary of homogeneous and heterogeneous elements. RW–SW configuration.

———— precise solution, * * * numerical solution.

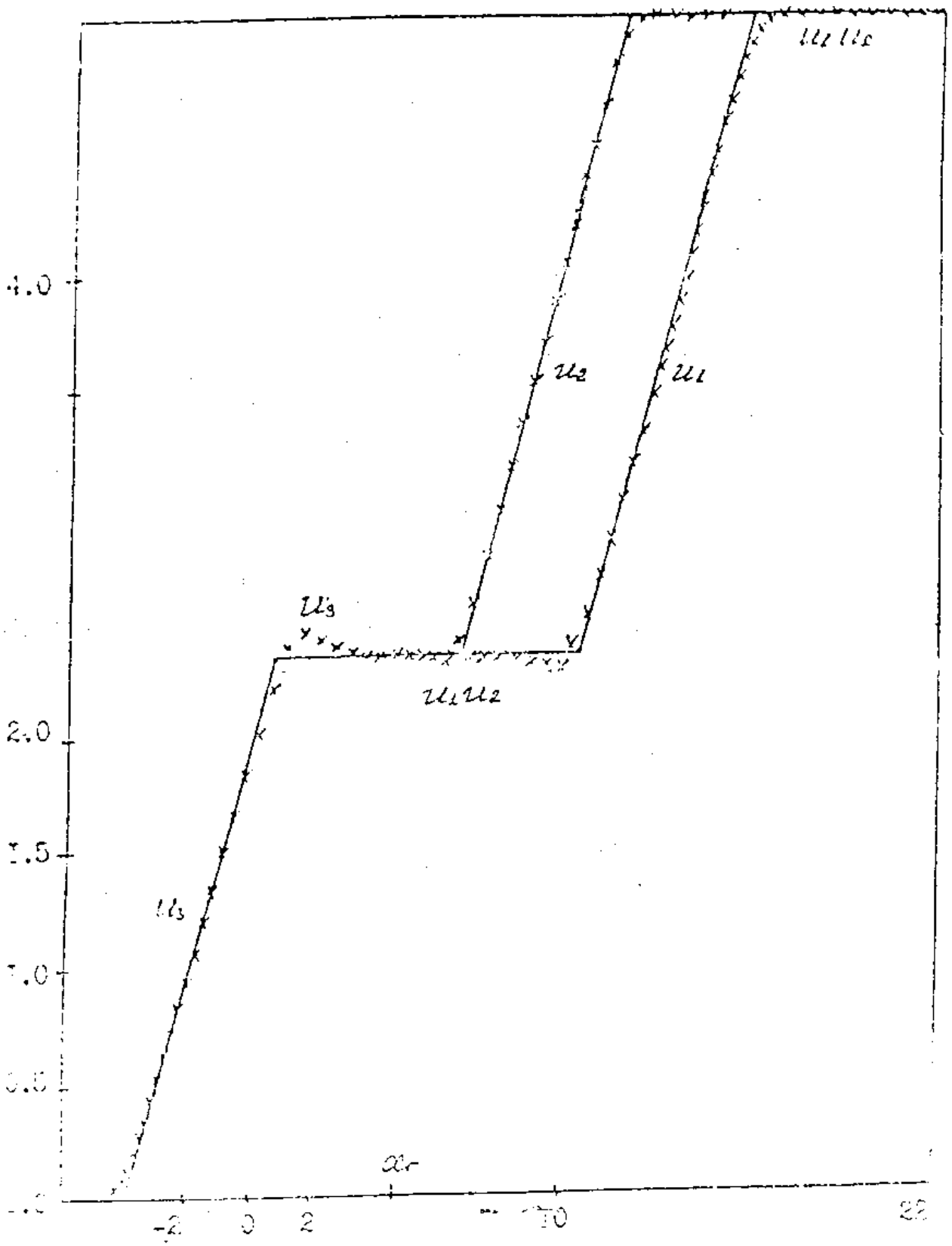

Fig. 4.11.

Explosion dissipation at the boundary of homogeneous and heterogeneous elements. RW–RW configuration.

вида ВР - ВР. ——— precise solution

× × × numerical solution.

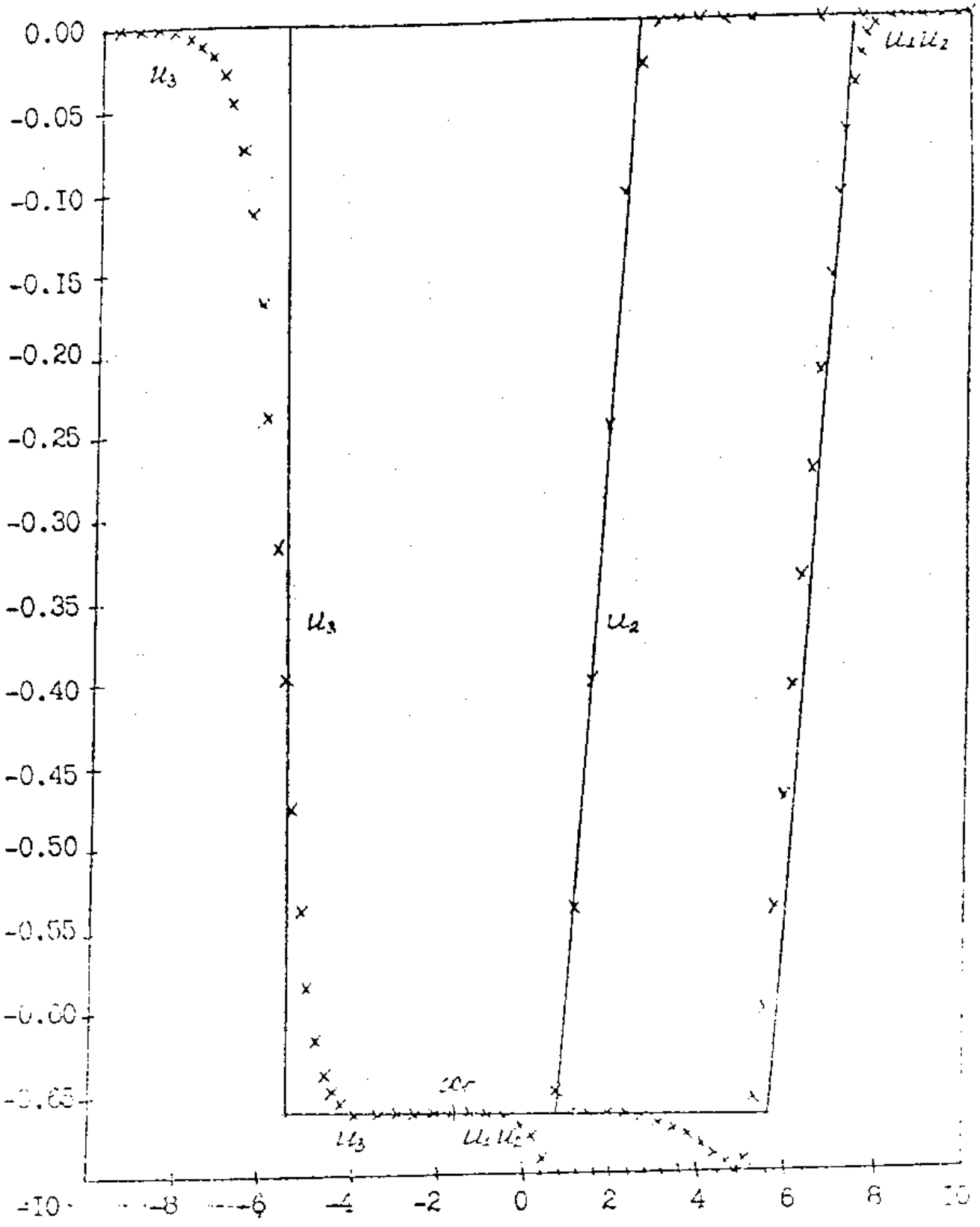

Fig. 4.12.

Explosion dissipation at the boundary of homogeneous and heterogeneous elements. SW–RW configuration.

——— precise solution x x x numerical solution.

gases without component interaction forces:

-SW (Fig. 4.3),

-RW with complete separation (Fig. 4.4),

-SW with partial separation (Fig. 4.5).

3. Solution for piston movement in a mixture of two solids without component interaction forces:

-SW (Fig. 4.6),

-RW with complete separation (Fig. 4.7),

-SW with partial separation (Fig. 4.8).

4. Solution for arbitrary explosion dissipation at a boundary separating an isothermal gas and a mixture of two other isothermal gases:

1) SW–SW configuration (Fig. 4.9)

2) RW–SW configuration (Fig. 4.10)

3) RW–RW configuration (Fig. 4.11)

4) SW–RW configuration (Fig. 4.12)

A comparison of precise and numerical solutions without component force interaction demonstrates the capacities and accuracy of the method with the maximal effects of component velocity inequalities in dynamic processes.

5. Mathematical modelling of the development of a mixing zone (MZ) of substances with Rayleigh–Taylor (R–T) instability

If the component pressures are equal, the relative movement in the mixture arises through the different accelerations acquired by the components with a different density in the overall pressure gradient field.

The investigation of the stability of uni-dimensional hydrodynamic flow enables the required instability condition of the CB to be written as

$$\frac{\partial \rho}{\partial z} \cdot \frac{\partial P}{\partial z} < 0 , \qquad (5.1)$$

where $\partial P/\partial z$ and $\partial \rho/\partial z$ are the pressure and density gradients through the CB.

During random generation of a mixture at the CB, the action of forces that cause a relative movement of components destroys the CB and forms an elementary MZ that is a two-component mixture. After generation, the elementary MZ develops according to features of the mathematical model [eqs. (1.5-1.13)].

In the CMM method, an elementary MZ forms in the CB region after achieving criterion (5.1). Thus, the following are defined:

a) positions of the component mutual penetration fronts;

b) volume concentrations of components;

c) thermodynamic parameters corresponding to accepted MDC of components;

d) characteristic size of heterogeneities.

Information on the individual thermodynamic parameters of the substances on both sides of the CB and that on perturbations at the CB are used as the starting information for obtaining the numerical characteristics of the mixture.

The volume concentration of the right substance in the elementary MZ at the moment it is formed is a parameter of the mathematical model, α_n^0.

The force and energy of component interaction have a determining effect on the integral characteristics of the numerical solutions such as the movements of the component interpenetration fronts, the component concentration profiles in the MZ, etc.

The parameter t_u in eq. (1.9) is represented as

$$\frac{1}{t_u} = \alpha_i \alpha_j \rho F_u,$$

$$F_u = \frac{f(n)\,|u_j - u_i|}{L_{MZ}}; \qquad (5.2)$$

where L_{MZ} is the width of the MZ and $f(n)$ is a dimensionless function depending on the decrease of densities, $n = \rho_H/\rho_L$. Thus, the mathematical model from the CMM method that describes the

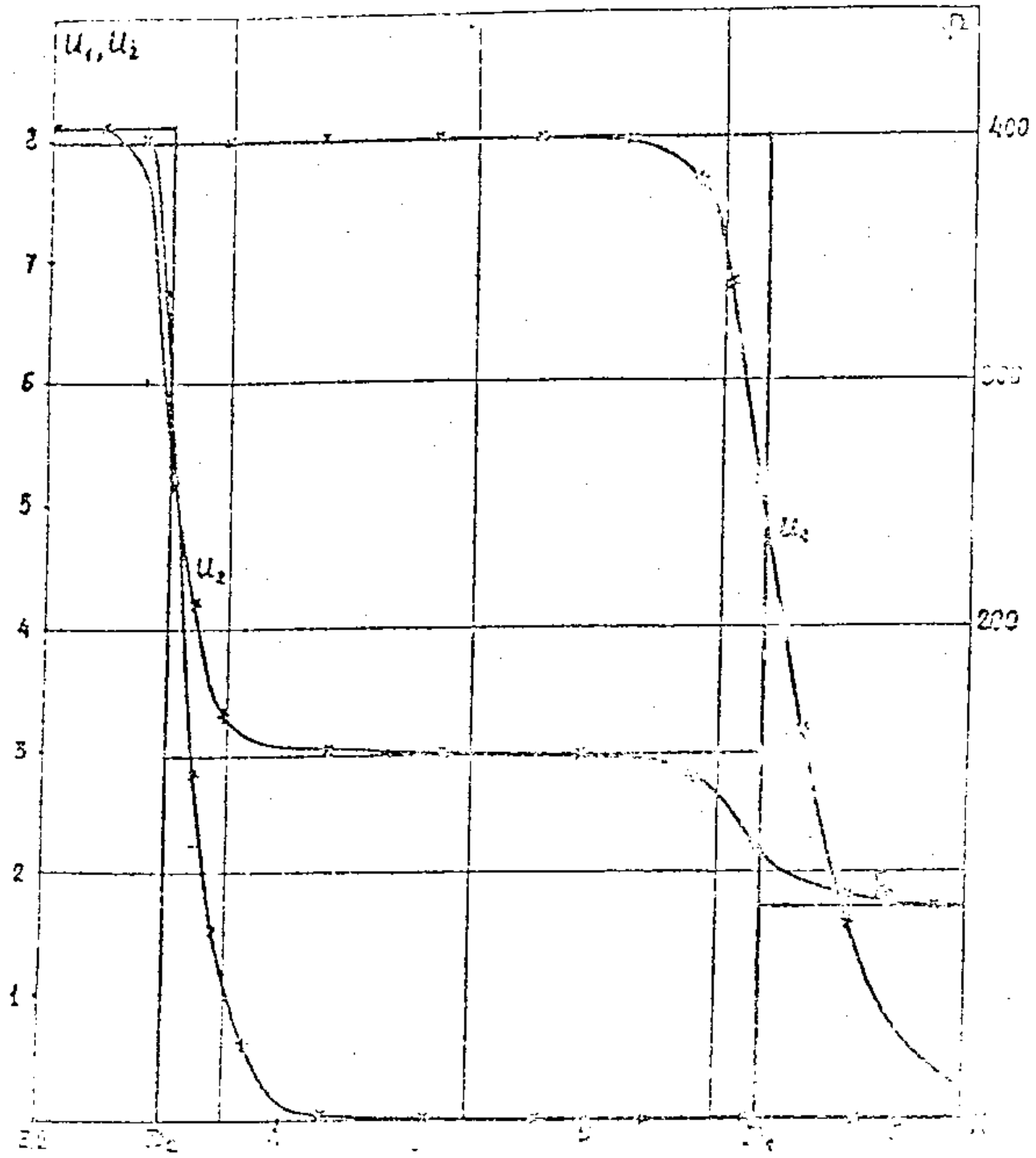

Fig. 4.1.

Solution for a piston moving into a mixture of two isothermal gases for $t = 0.4$.

——— precise solution

—×—×— numerical solution.

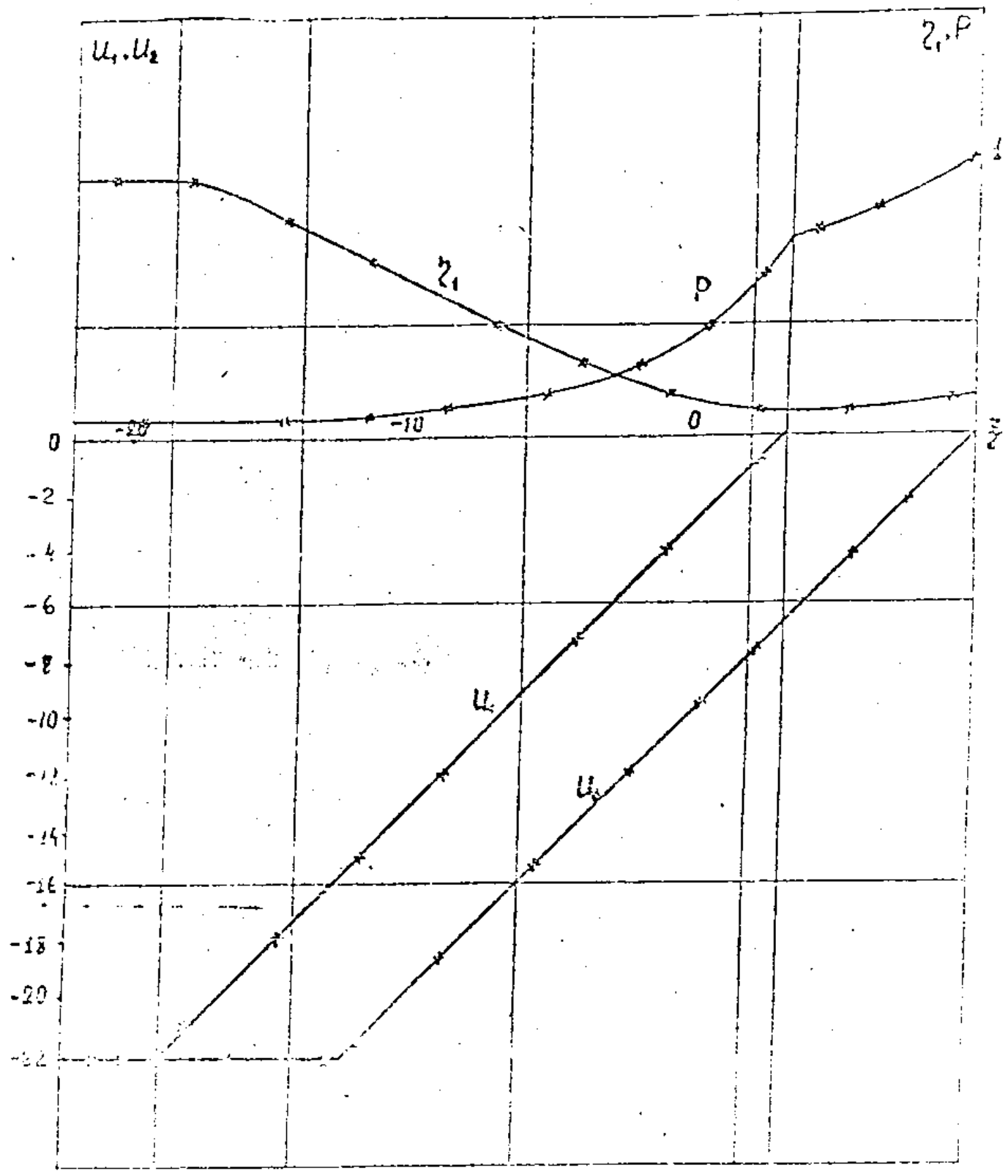

Fig. 4.2.

Solution for a piston moving out of a mixture of two isothermal gases.

——— – precise solution

–×–×– – numerical solution. $t = 0.84$.

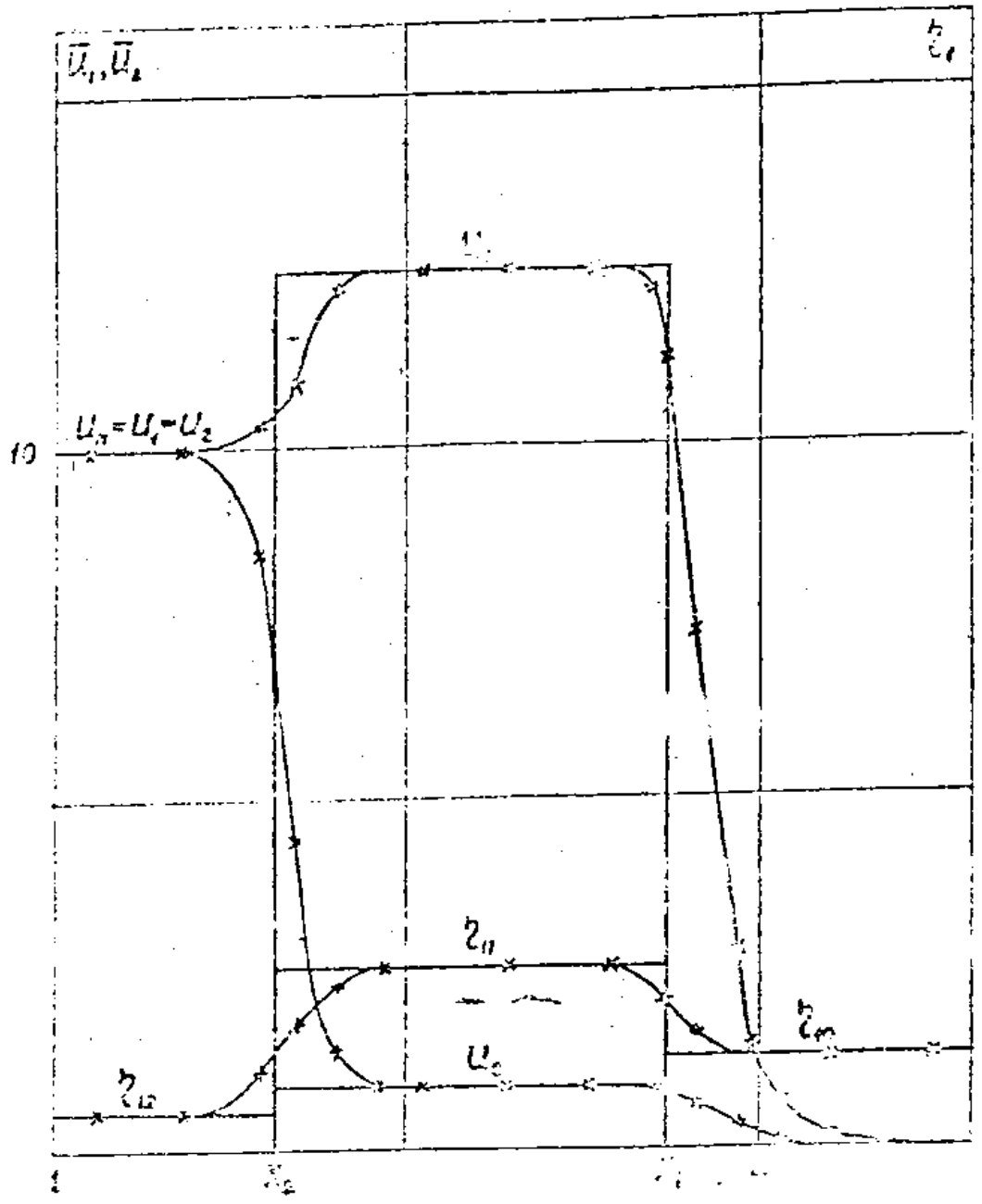

Fig. 4.3.

Solution for a piston moving into a mixture of two polytropic gases for $t = 0.0882$

——— precise solution

—×—×— numerical solution.

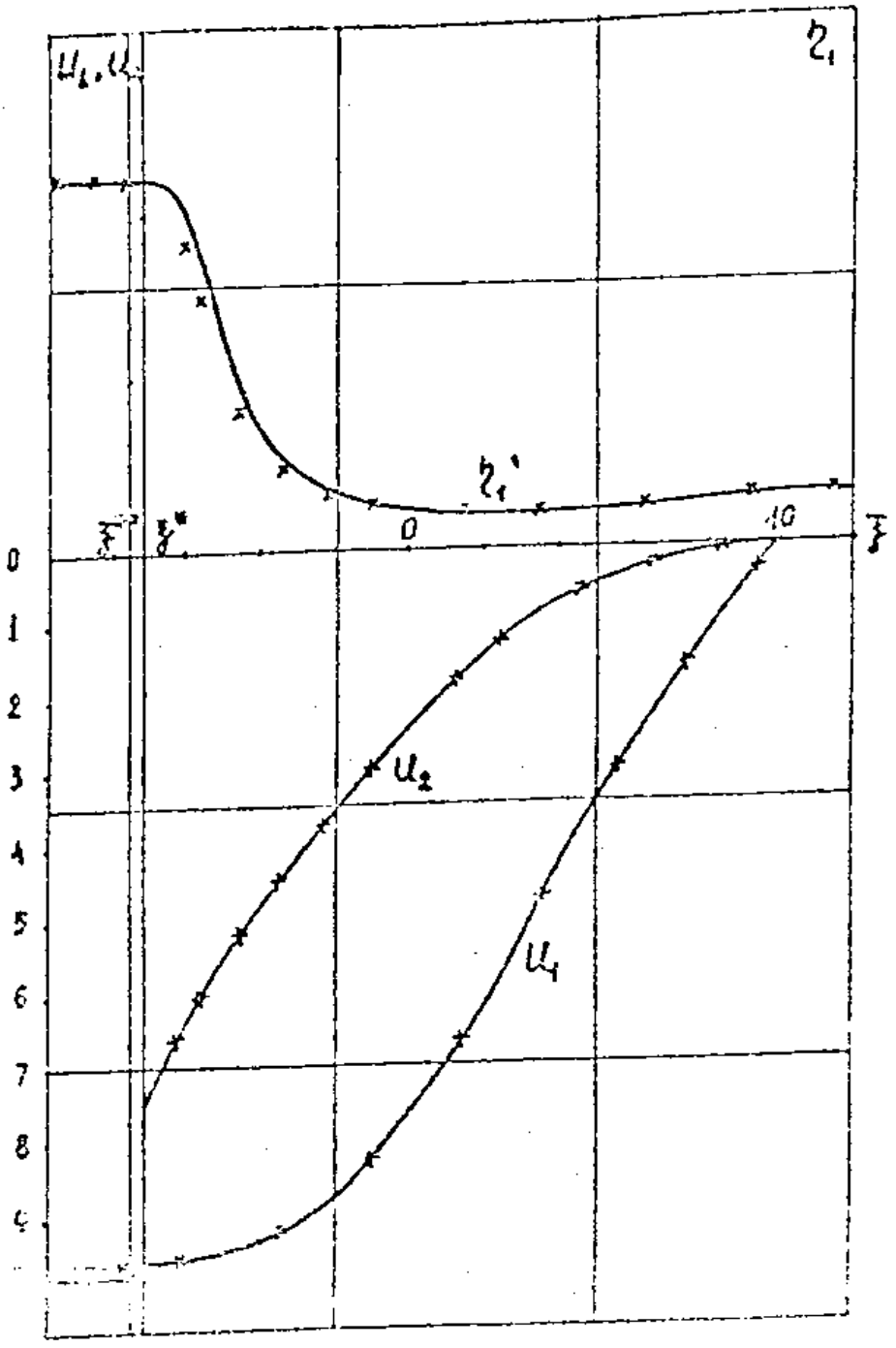

Fig. 4.4.

Solution for a piston moving out of a mixture of two polytropic gases. Complete separation in the rarefaction wave.

——— – precise solution

–×–×– – numerical solution. $t = 0.58023$.

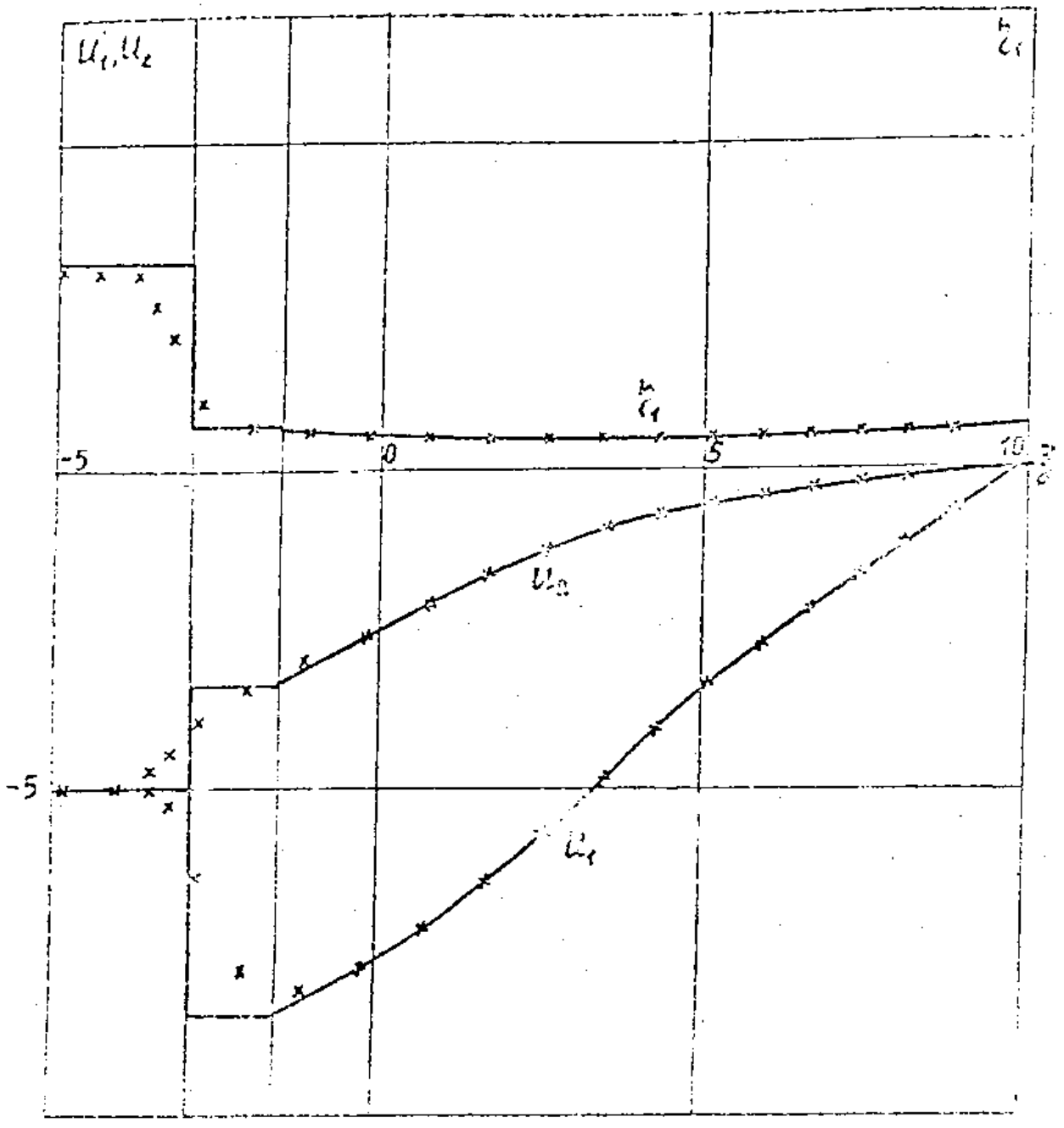

Fig. 4.5.

Solution for a piston moving out of a mixture of two polytropic gases. Partial component separation in a rarefaction wave.

——— – precise solution

× × × – numerical solution. $t = 0.226$.

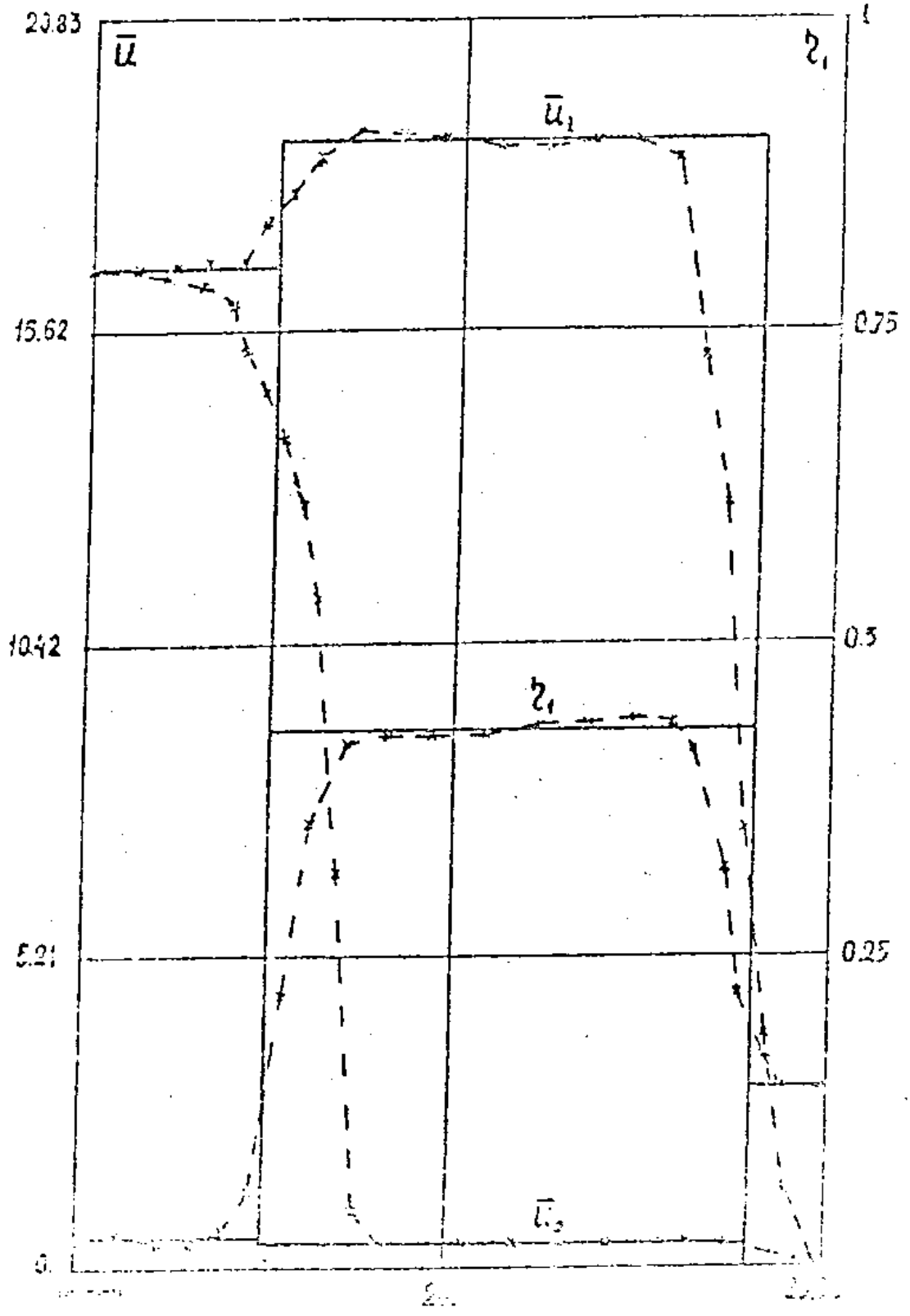

Fig. 4.6.

Solution for a piston moving into a mixture of two solids for t = 0.0231.

⟵——⟶ - precise solution

⟵×—×—×⟶ - numerical solution.

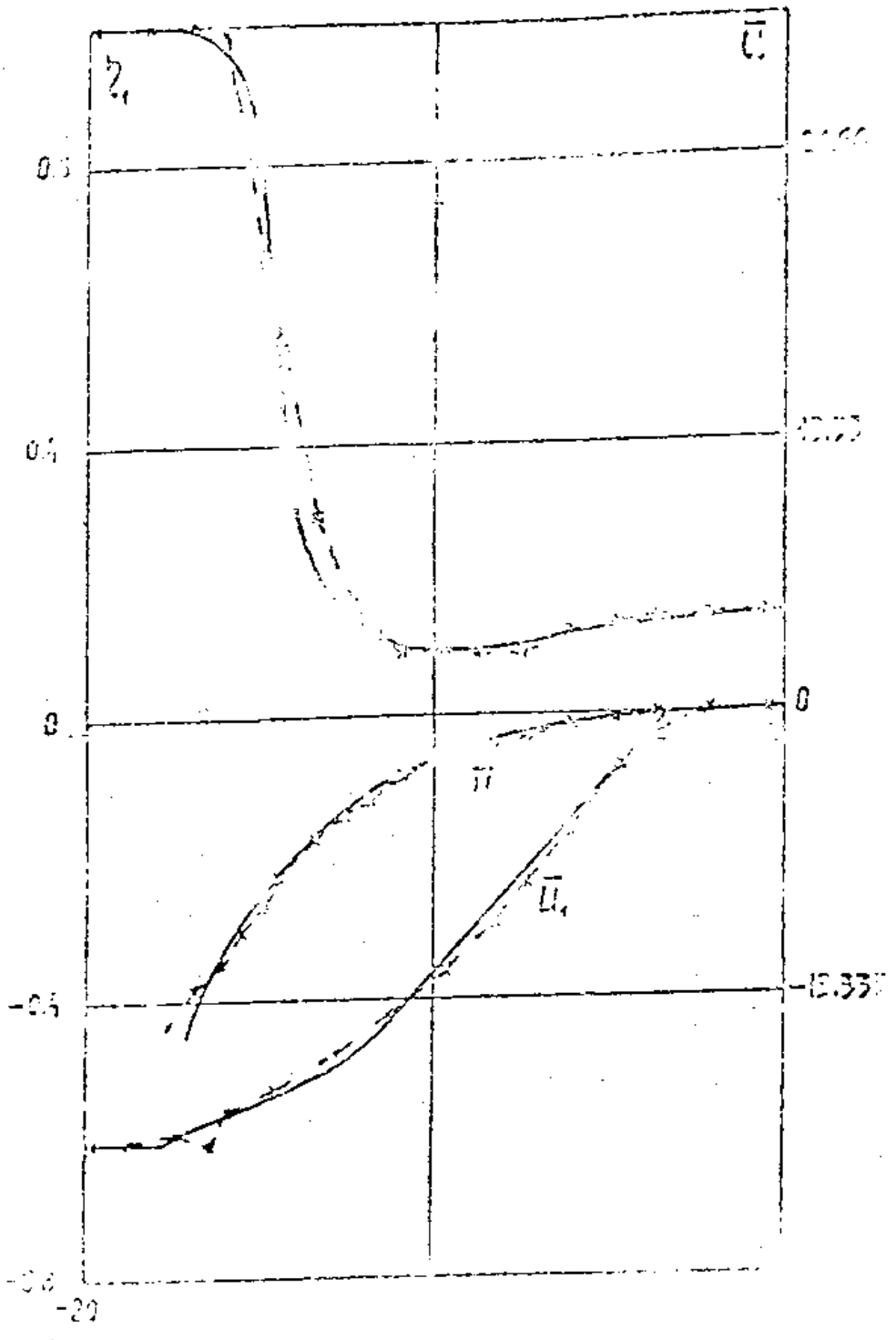

Fig. 4.7.

Solution for a piston moving out of a mixture of two solids. Complete separation in a rarefaction wave.

———— – precise solution

—×—×—×— numerical solution. $t = 0.08462$.

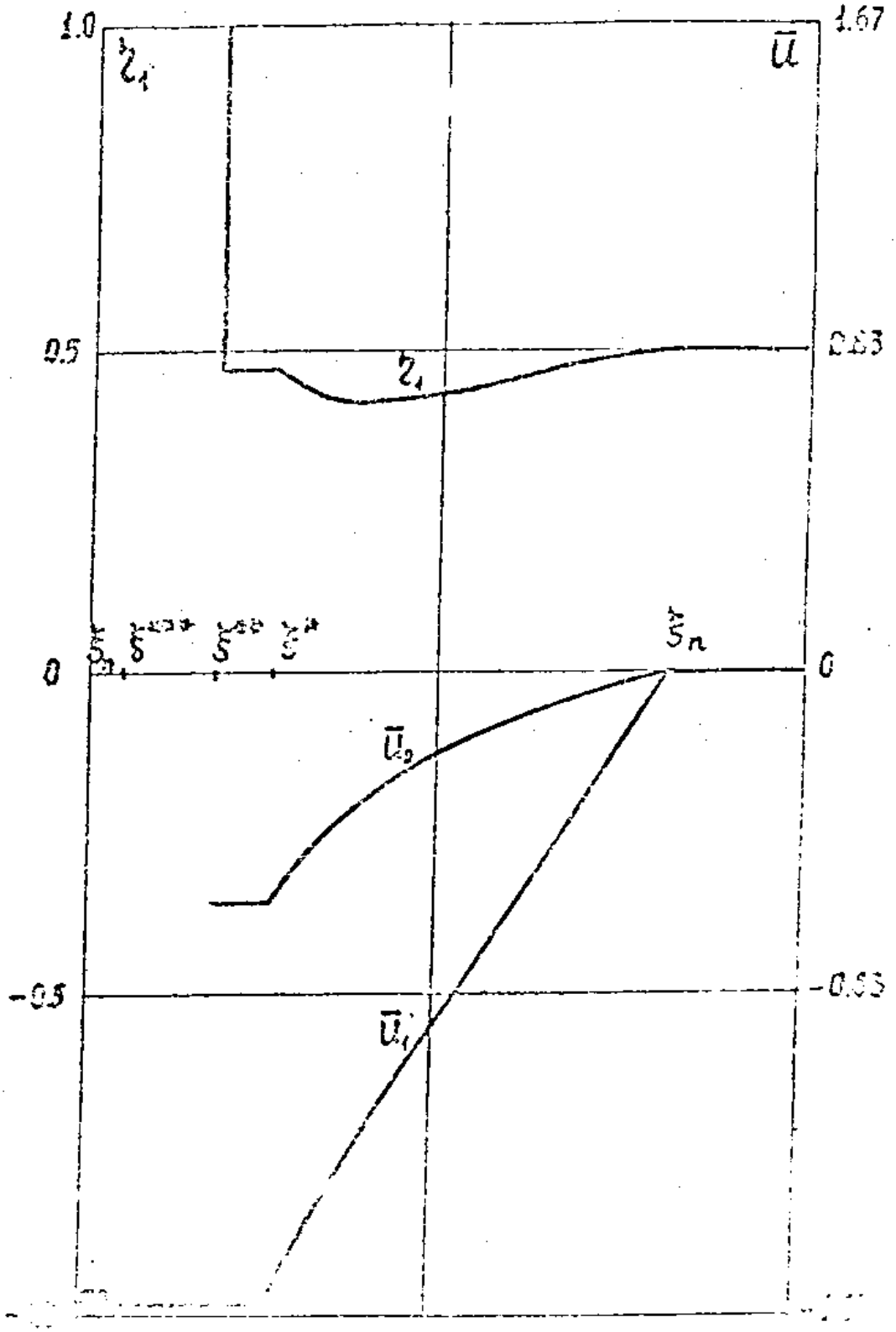

Fig. 2.21.

Automodel rarefaction wave in a mixture of two solids. Complete separation in the region of completely destroyed substance.

$$\gamma_{10} = 0.143, \qquad \bar{u}_0 = -1.6, \qquad \bar{F} = 0.1.$$

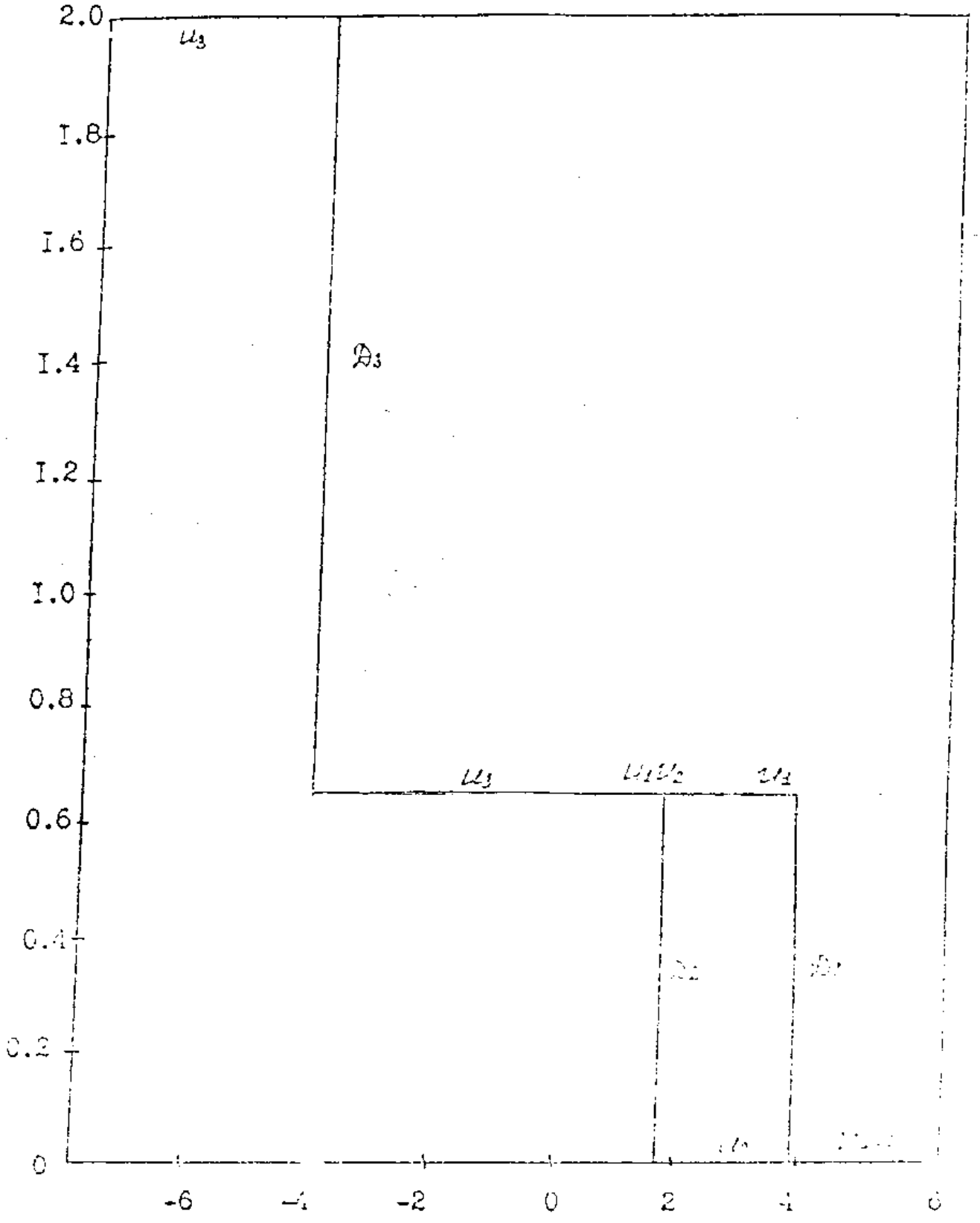

Fig. 2.22.

Explosion dissipation at the boundary of a homogeneous and heterogeneous element. Velocity profiles for the SW–SW configuration.

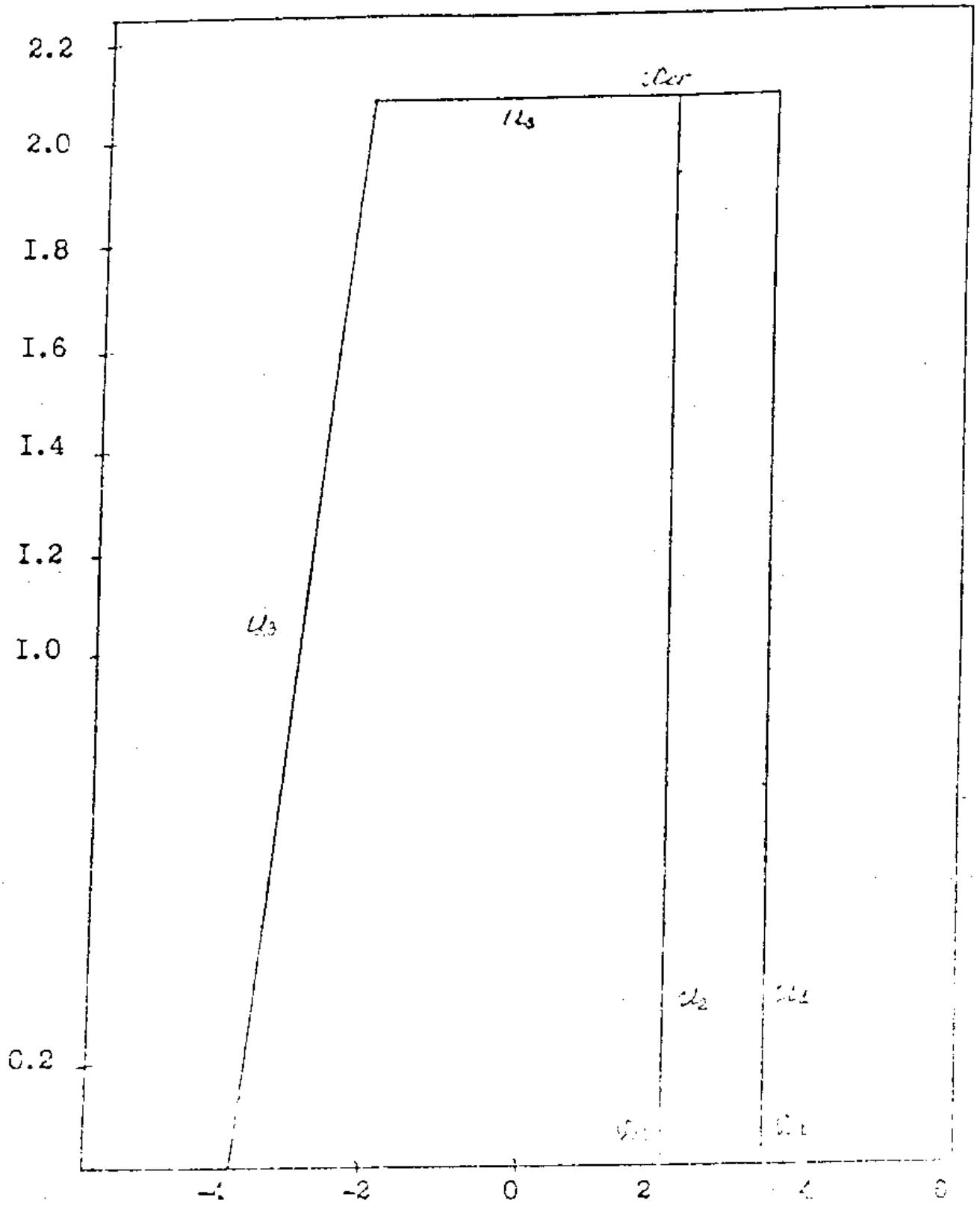

Fig. 2.23.

Explosion dissipation at the boundary of a homogeneous and heterogeneous element. Velocity profiles for the RW–SW configuration.

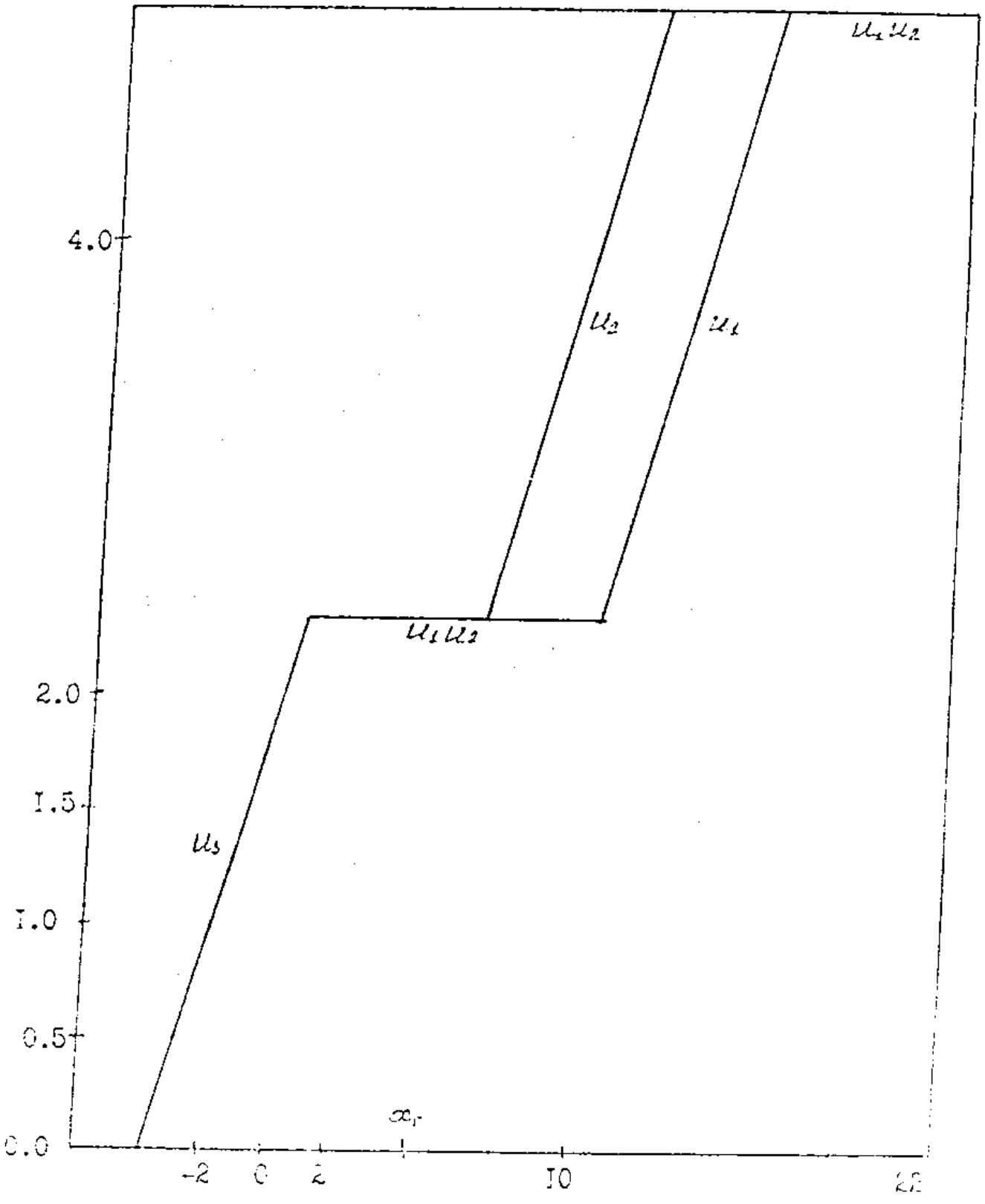

Fig. 2.24.

Explosion dissipation at the boundary of a homogeneous and heterogeneous element. Velocity profiles for the RW–RW configuration.

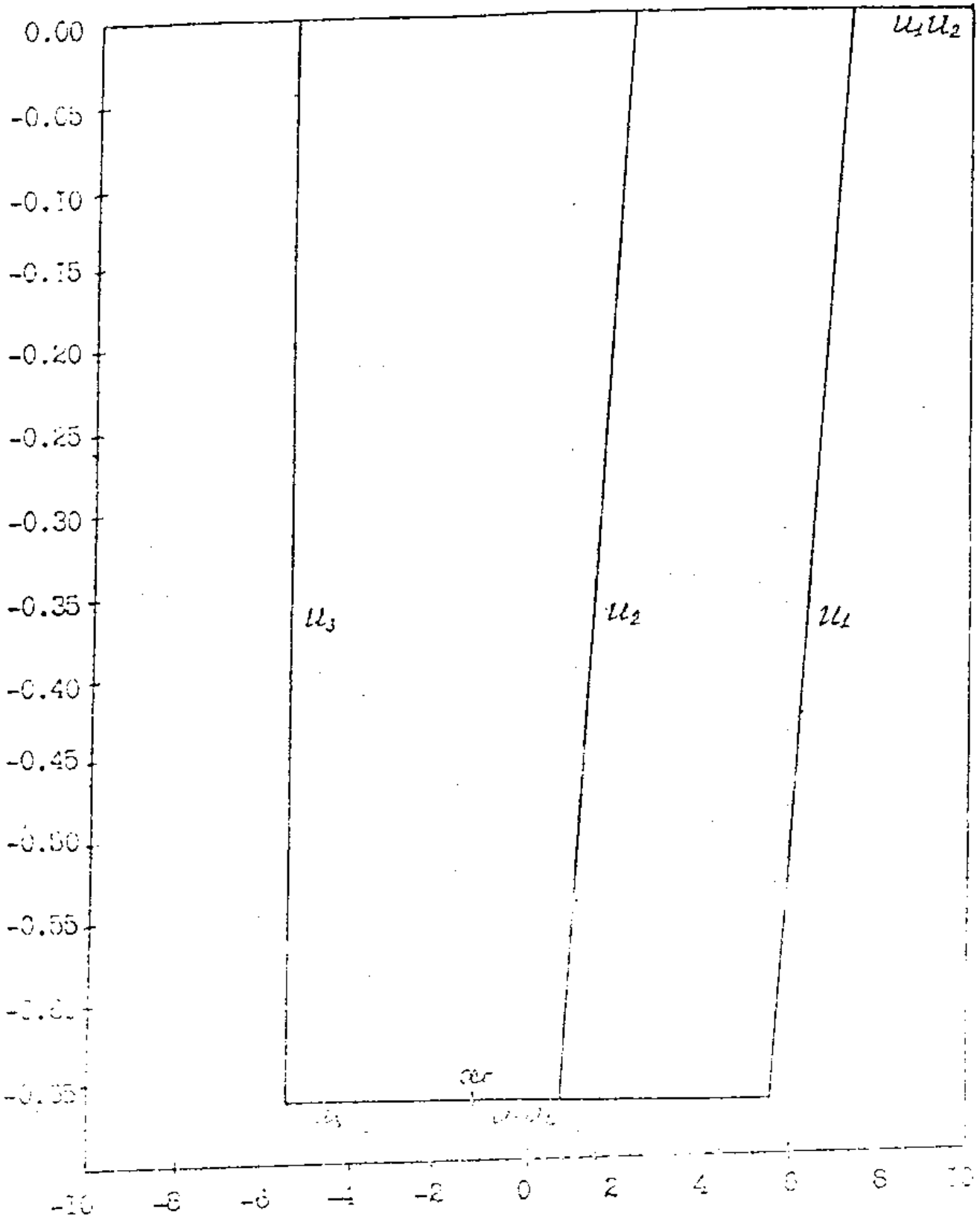

Fig. 2.25.

Explosion dissipation at the boundary of homogeneous and heterogeneous elements. Velocity profiles for the SW–RW configuration.

3) A RW–RW configuration. In this instance, a typical RW expands in a homogeneous substance; a combination of two RW into the mixture (see Fig. 2.24).

4) A SW–RW configuration. A SW occurs in a homogeneous substance during this type of dissipation; a combination of two RW in a mixture (see Fig. 2.25).

The velocity of the CB is determined by the pressure equalization on both sides of it. Determining the type of explosion dissipation by solving the corresponding problem with a one-dimensional description for the mixture is an important element of the algorithm for solving the problem of the dissipation of an arbitrary explosion. In the examined instances for the chosen parameters, assuming a different type of explosion dissipation (even for a two-velocity description of the mixture) always led to an incompatible system of equations.

In conclusion, we note the precise solution of the piston problem for a mixture of isothermal gas with uncompressible particles that was previously obtained [10].

Studies on precise solutions of interesting applied problems are presently continuing. It seems to us that efforts here must increase and that they will be generously repaid through a deepened understanding of the physical nature of complicated processes occurring in systems with nonequilibrated mixtures of substances.

3. Numerical method

The layers comprising the multilayered system will be called elements.

Two types of elements are permitted: heterogeneous and homogeneous.

A homogeneous element is a layer of homogeneous substance without internal boundaries.

In principle, the following types of heterogeneous elements are possible:

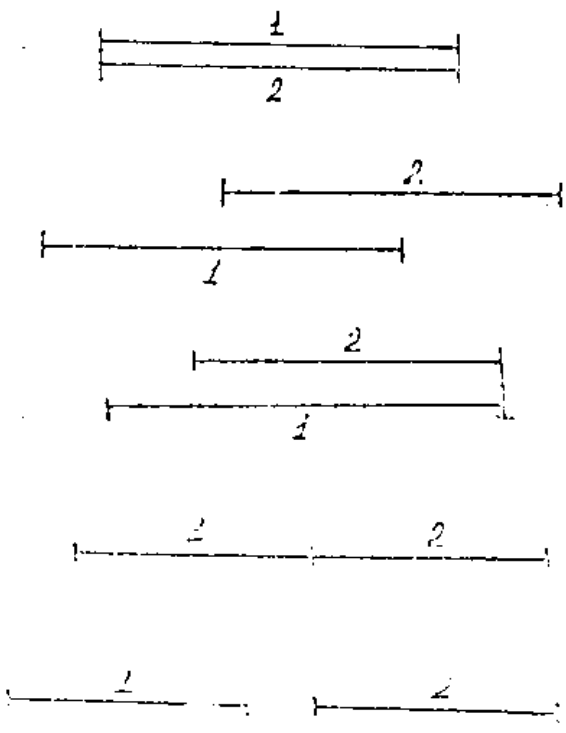

a) -left and right component boundaries coincide;

b) -two substances overlap in a certain region, representing a mixture;

c) -only the right boundaries coincide;

d) -a CB occurs between two substances;

e) -an evacuated gap occurs between two substances.

The difference method for calculating a homogeneous element consists of the following [11]

$$u_x^{n+1} = u_x^n - \tau \frac{p''_{(x-0.5)} - p''_{(x-0.5)}}{0.5\left(m''_{x-0.5} + m''_{x-0.5}\right)} + \tau g \qquad (3.1)$$

where $m^{n}_{k+0.5} = \rho^{n}_{(k+0.5)} \left(r^{n}_{k+1} - r^{n}_{k}\right)$,

(3.2)

$$r_k^{n+1} = r_k^n + u_k^{n+1} \cdot \tau \quad ,$$

$$\rho^{n+1}_{(k+0.5)} = \frac{M_{k+0.5}}{\left(r^{n+1}_{(k+1)}\right)^{\nu} - \left(r^{n+1}_{k}\right)^{\nu}} \quad , \tag{3.3}$$

where $M_{k+0.5} = L_{\nu} \cdot \rho^{n}_{k+0.5} \cdot \left[\left(r^{n}_{(k+1)}\right)^{\nu} - \left(r^{n}_{k}\right)^{\nu}\right]$,

$$L_{1\nu} = \begin{cases} 1 & , \ \nu = 1 \\ \pi & , \ \nu = 2 \\ \frac{4\pi}{3} & , \ \nu = 3 \end{cases}$$

The cells containing the SW and those containing the RW differ in the numerical method.

If $\Delta u = u_{k+1} - u_k \geq 0$, then the cell is considered to contain a RW. In this instance, $\rho^{n+1}_{k+0.5}$ and $E^{n+1}_{k+0.5}$ are obtained by integrating isentropic equations with the necessary precision:

$$\frac{dr}{dt} = -\frac{\rho}{\rho^2} \frac{\partial p}{\partial L} = D,$$

$$p = f_p(\rho, E, \Phi) \quad . \tag{3.4}$$

If $\Delta u = u_{k+1} - u_k < 0$, then a SW is considered to lie in the interval. In this instance, $\rho^{n+1}_{(k+0.5)}$ is determined by numerically solving a system of equations resulting from relationships on the surface of a strong explosion:

$$\left[\left(\bar{P}^{n+1}-P^{n}\right)\left(\bar{V}^{n+1}-V^{n}\right)\right]_{(k+0.5)}=-(\Delta u)^{2}$$

$$E^{n+1}_{(k+0.5)}=E^{n}_{(k+0.5)}+0.5(\Delta u)^{2}-P^{n}_{(k+0.5)}\left(V^{n+1}-V^{n}\right)_{k+0.5} \qquad (3.5)$$

$$\bar{V}^{n+1}_{(k+0.5)}=\frac{1}{\bar{P}^{n+1}_{(k+0.5)}}$$

$$\bar{P}^{n+1}_{(k+0.5)}=f_{p}\left(\bar{\rho}^{n+1}_{k+0.5},\ \bar{E}^{n+1}_{k+0.5},\ \bar{\Phi}^{n+1}\right)$$

Then, $E^{n+1}_{(k+0.5)}$ is found using the formula

$$E^{n+1}_{k+0.5}=E^{n}_{k+0.5}-0.5\left[\bar{P}^{n}_{(k+0.5)}+\bar{P}^{n+1}_{(k+0.5)}\right]\left[V^{n+1}_{k+0.5}-V^{n}_{k+0.5}\right] \qquad (3.6)$$

The difference method for calculating a heterogeneous element consists of the following.

Numerical integration of a system of equations for mathematical models of multicomponent and heterogeneous media uses the following breakdown of physical processes [2].

STAGE 1. The motion and deformation of a component is calculated taking into account the force interaction from another component in Lagrangian coordinates. This produces individual (inconsistent with mutual deformation) component parameters.

STAGE 2. The spatial correspondence of components is determined in Euler coordinates. Their individual thermodynamic states are then converted locally into a state satisfying the MDC.

For each component, an individual Lagrangian coordinate system is introduced that is related to the velocity field of this component.

Each component is viewed as a spatial region. A two-component mixture is considered a combination of such regions superimposed on each other.

A unique difference grid is constructed for each component.

The values of the other component in a mixture are defined on the grid of each mixture component, in addition to the values of that component. The values are obtained by interpolating the values of the second component determined from its own grid onto the grid of the other component.

The difference grid of the component can consist of three types of ranges:

1) pure range,

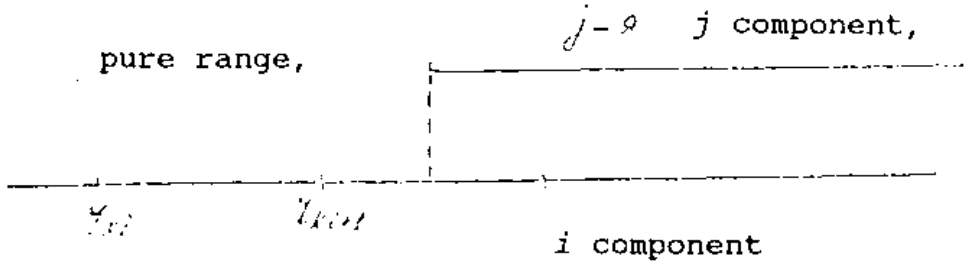

2) mixed range,

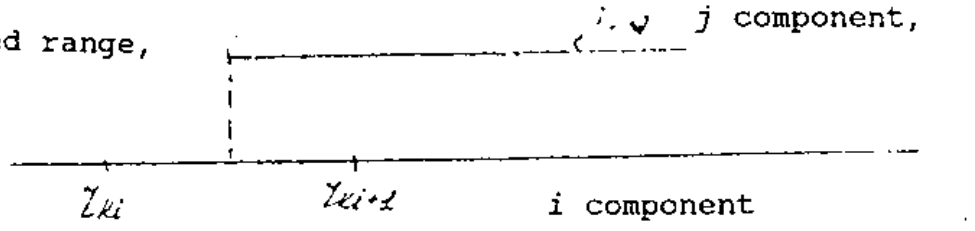

3)

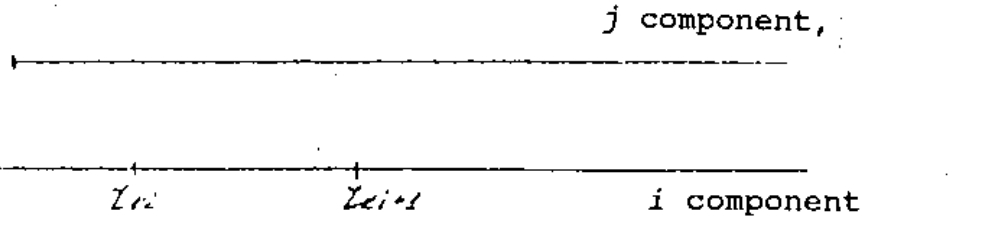

heterogeneous range,

The difference method for calculating the heterogeneous range generalizes the previous schematic [11] for a two-component medium. The difference system for calculating the component velocities has the following form:

$$u_{ki}^{n+1} = u_{ki}^{n} - \tau f_{ki}^{n} - \tau K_{kji}^{n} \frac{u_{ki}^{n} - u_{kj}^{n} - \tau\left(f_{ki}^{n} - f_{kj}^{n}\right)}{\left[\beta + \tau\left(K_{kij}^{n} + K_{kji}^{n}\right)\right]} + g\tau \qquad (3.7)$$

$$u_{kj}^{n+1} = u_{kj}^{n} - \tau f_{kj}^{n} + \tau K_{kij}^{n} \frac{u_{ki}^{n} - u_{kj}^{n} - \tau(f_{ki}^{n} - f_{kj}^{n})}{[1 + \tau(K_{kji}^{n} + K_{kij}^{n})]} + g\tau \quad (3.8)$$

where for a heterogeneous medium

$$f_{ki}^{n} = \bar{I}_{ki}^{n} \frac{\bar{P}_{(k+0.5)i}^{n} - \bar{P}_{(k-0.5)i}^{n}}{0.5(m_{(k+0.5)i}^{n} + m_{(k-0.5)i}^{n})},$$

$$\bar{I}_{ki}^{n} = (u_{ki}^{n} + u_{ki}^{n}) - \bar{I}_{ki}^{n} \frac{\bar{\rho}_{ki}^{n}}{\rho_{kij}^{n}} \cdot \frac{\bar{P}_{(k+0.5)i}^{n} - \bar{P}_{(k-0.5)i}^{n}}{i\, m_{(k+0.5)i}^{n} + m_{(k-0.5)i}^{n}},$$

$$m_{(k+0.5)i}^{n} = \rho_{(k+0.5)i}^{n} \left(\frac{1}{\rho_{(k+1)i}^{n}} + \frac{1}{\rho_{ki}^{n}} \right),$$

$$\rho_{ki}^{n} = \frac{M_{(k+0.5)i} + M_{(k-0.5)i}}{(\gamma_{(k+1)i})^{2} + (\gamma_{(k-1)i})^{2}},$$

$$\rho_{kij}^{n} = \frac{M_{(k+0.5)i} + M_{(k-0.5)i}}{(\gamma_{(k+1)i})^{2} + (\gamma_{(k-1)i})^{2}},$$

$$\xi_{kj}^{n} = \begin{cases} \dfrac{2\rho_{(k+1)i}^{n} - 2u_{kj}^{n}}{m_{(k+0.5)i}^{n}}, & u_{kj}^{n} - u_{ki}^{n} < 0 \\ \dfrac{u_{kj}^{n} - u_{(k-1)j}^{n}}{m_{(k-0.5)i}^{n}}, & u_{kj}^{n} - u_{ki}^{n} > 0 \end{cases}$$

$$\bar{I}_{ki}^{n} = \frac{D_{(k-0.5)i}^{n} \bar{I}_{(k-0.5)i}^{n} + D_{(k+0.5)i}^{n} \bar{I}_{(k+0.5)i}^{n}}{D_{(k-0.5)i}^{n} + D_{(k+0.5)i}^{n}},$$

$$\bar{\alpha}_{xj}^{n} = 1 - \bar{\alpha}_{xi}^{n} ;$$

$$\rho_{(x\pm0.5)i}^{n} = \frac{M_{(x\pm0.5)i}}{\rho_{(x\pm0.5)i}^{n}} .$$

[There is some printing below these equations that is too faint to read]

New coordinates for nodes and dissipation of kinetic energy in steps of t are calculated after determining the velocities:

$$x_{xi}^{n+1} = x_{xi}^{n} + \tau u_{xi}^{n+1} \qquad (3.9)$$

$$\Delta Q_{xji}^{n+1} = k_{xji}^{n} \left(u_{xi}^{n+1} - u_{xj}^{n+1}\right)^2 \cdot \tau \qquad (3.10)$$

After this, individual thermodynamic component parameters are calculated. Thus, it is assumed

$$\frac{\partial \rho_{xi}^{*}}{\partial t} = 0 \quad ; \quad \frac{\partial \alpha_i}{\partial t} = 0 \qquad (3.11),$$

i.e., only force interaction of components is considered. Within its own grid, each component at this stage is deformed as if the other component were not present.

The system for calculating the individual thermodynamic parameters is the same as that for a homogeneous element (different systems of equations are solved for $\Delta u_i = u_{(x+1)i}^{n+1} - u_{xi}^{n+1} < 0$ and $\Delta u_i \geq 0$).

The second step of the calculation is carried out after this. It consists essentially of determining the parameters of the mixture and components that satisfy their MDC using the individual component parameters at a given point.

In order to avoid inaccuracies in the interpolation, the MDC are calculated for each component.

After completing the second step, all thermodynamic parameters acquire new values:

$$\bar{u}^{n+1},\ p_i^{n+1}=p_{ij}^{n+1},\ E_i^{n+1},\ E_{ij}^{n+1}$$

$$\bar{r}^{n+1},\ \bar{r}_i^{n+1}=\bar{r}_{ij}^{n+1},\ \bar{\varepsilon}^{n+1},\ \bar{\varepsilon}_{ij}^{n+1}$$

This finishes the calculation cycle.

Averaging is first carried out for mixed ranges. Then, the algorithm for the heterogeneous range is used.

Step limitations

An investigation of the stability of the difference schemata leads to the following limitations on the time step t (Curant's condition):

a) for a homogeneous element

$$\tau \le \frac{m_k}{a_k + 4\rho_k z / |\Delta u_k|} \qquad (3.12)$$

where m_k is the planar mass of the range and a_k is the mass velocity of sound,

$$z = \begin{cases} 1, & \Delta u_k < 0 \\ 0, & \Delta u_k \ge 0 \end{cases},$$

$$\Delta u_k = u_{k+1} - u_k ;$$

b) for a heterogeneous element

$$\tau \le \frac{h_k}{c_k} \cdot \frac{L_k h_k + 4G_k}{4G_k} \qquad (3.13)$$

where

$$G_k = \rho c_k \left(\tau |\Delta u_k| z + c_k\right).$$

h_k is the spatial step in the k interval of the i component, c_k is the velocity of sound in the k interval of the i component,

$$\mathcal{I} = \begin{cases} 1, & \Delta u_k < 0 \\ 0, & \Delta u_k \geq 0 \end{cases},$$

$$\Delta u_k = u_{k+1} - u_k .$$

$$L_k = \frac{K'}{\rho c_0} .$$

(the extent of force interaction of components is taken as $R_i = K(u_j - u_i)$, with the index i, determining that h_k, G_k, L_k, u_k, and C_k belong to the i component, omitted).

Numerical calculations indicate that $\Gamma = 4$ in eq. (3.13) is sufficient to ensure that the numerical estimation is stable for SW of arbitrary intensity.

The accuracy and the stability criteria are considered in determining t. There are limitations on the deformation range and limitations on the change of volume concentration of a component in the range. There are also limitations requiring that the mixture boundary after one time step should traverse less than one range of a component entering the heterogeneous mixture or exiting it.

4. Numerical solutions by the CMM method of certain mechanics problems of two-velocity heterogeneous media with precise solutions

The CMM program executing the CMM method is written in FORTRAN for an ES (1066) computer. The accuracy and capacities of the method are demonstrated below in the figures, where precise and numerical solutions of the following problems already known to you are presented.

1. Solution for piston movement in a mixture of two isothermal gases without component interaction forces:
   -SW (Fig. 4.1),
   -RW (Fig. 4.2).
2. Solution for piston movement in a mixture of two polytropic

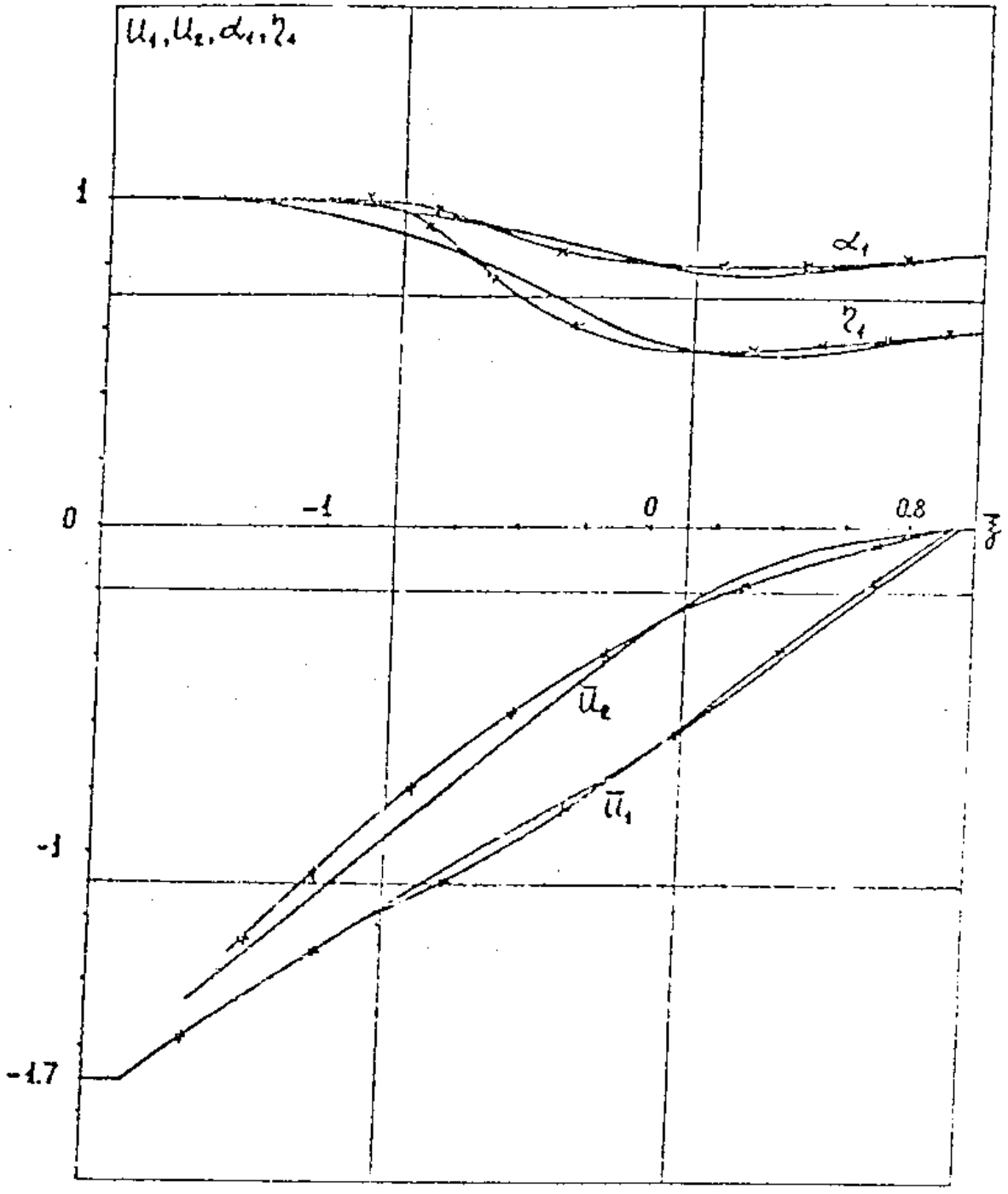

Fig. 2.14.

Automodel rarefaction wave in a mixture of two polytropic gases. Complete separation in a rarefaction wave $k = 2$,

$\chi^n = 0.1$; $\rho_{10} = 0.8889$; $\rho_{20} = 0.5506$; $\gamma_{10} = 0.6$; $U_n = -1.7$.

——— - solution for a multicomponent medium model with α_i under a pressure gradient sign

—×—×— - solution for a heterogeneous medium model with α_i before a pressure gradient sign.

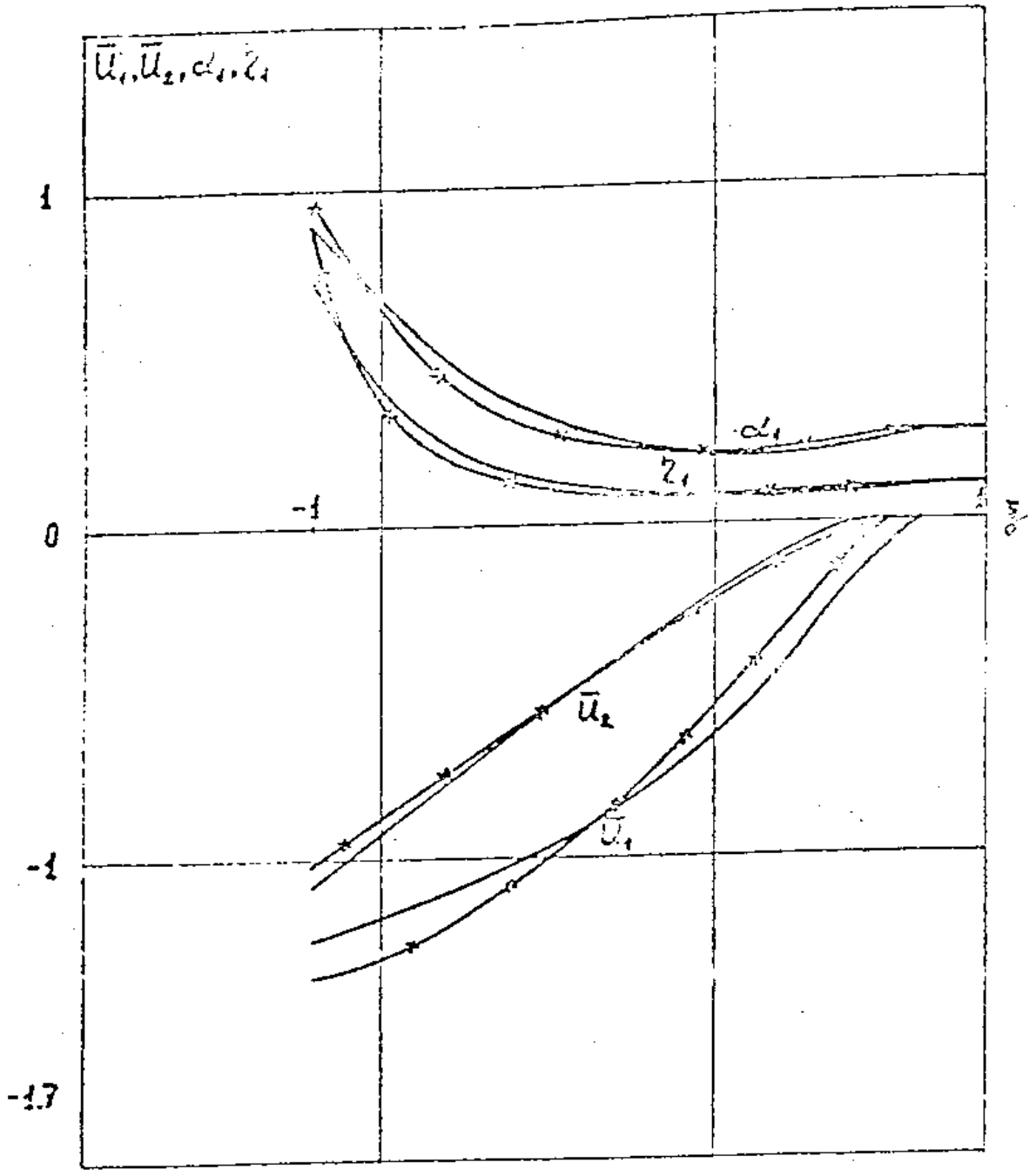

Fig. 2.15.

Automodel rarefaction wave in a mixture of two polytropic gases. Complete separation in a rarefaction wave. n = 2;

$\bar{x}^0 = 0.1$; $\bar{\rho}_{10} = 0.1$; $\bar{\rho}_{20} = 0.26$; $\bar{p}_0 = 2.301$;

$\bar{u}_n = -1.7$. Portion of the solution

——— - solution for a multicomponent medium model with α_i under a pressure gradient sign

—x—x— - solution for a heterogeneous medium model with α_i before a pressure gradient sign.

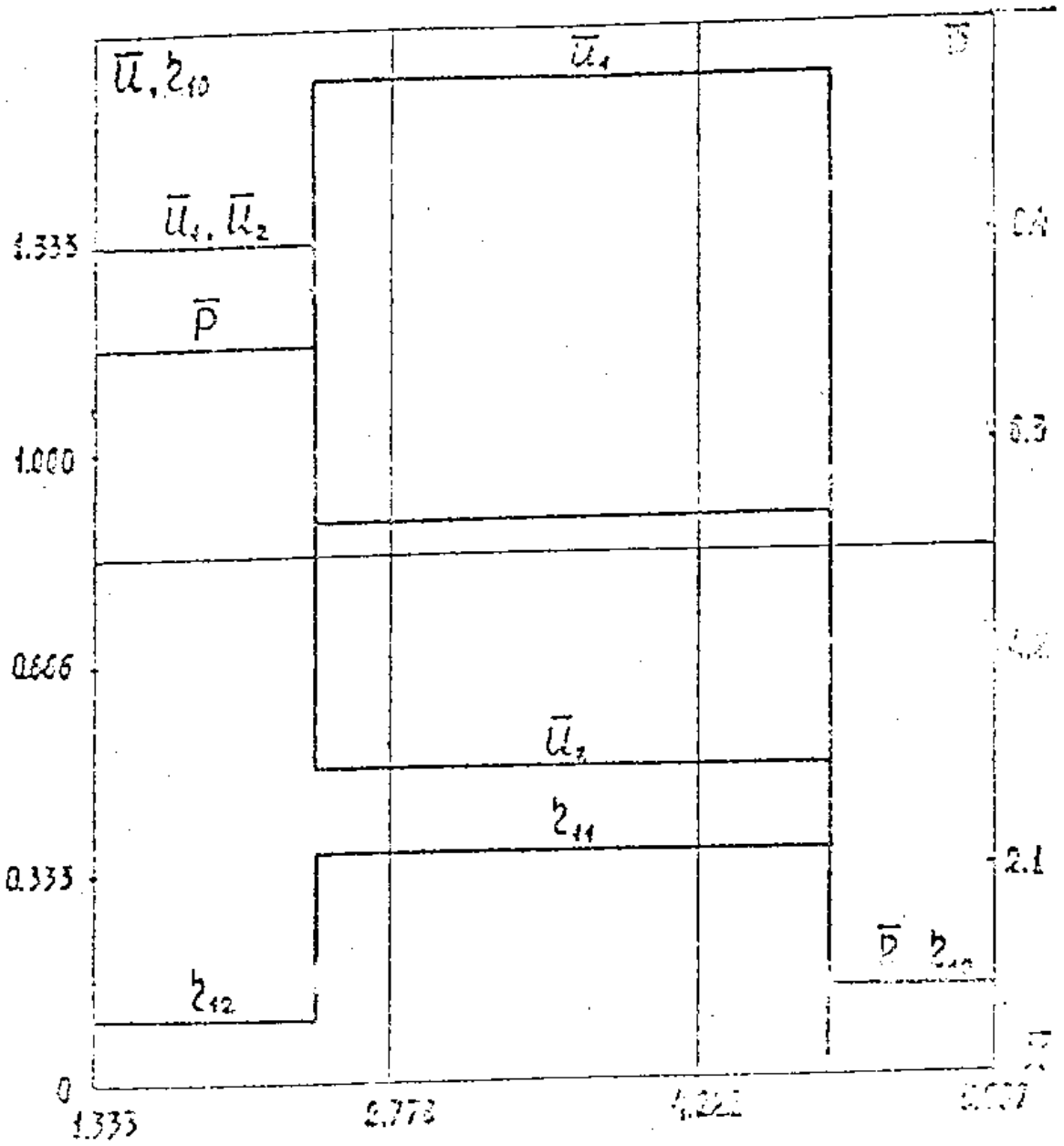

Fig. 2.16.

Shock wave in a mixture of two solids

$\zeta_{10} = 1.143$, $\bar{u}_0 = 1.3333$, $\frac{\lambda}{q} = 1$. Dimensionless coordinate: $\bar{x} = \frac{x}{c_{0,2}\,t}$.

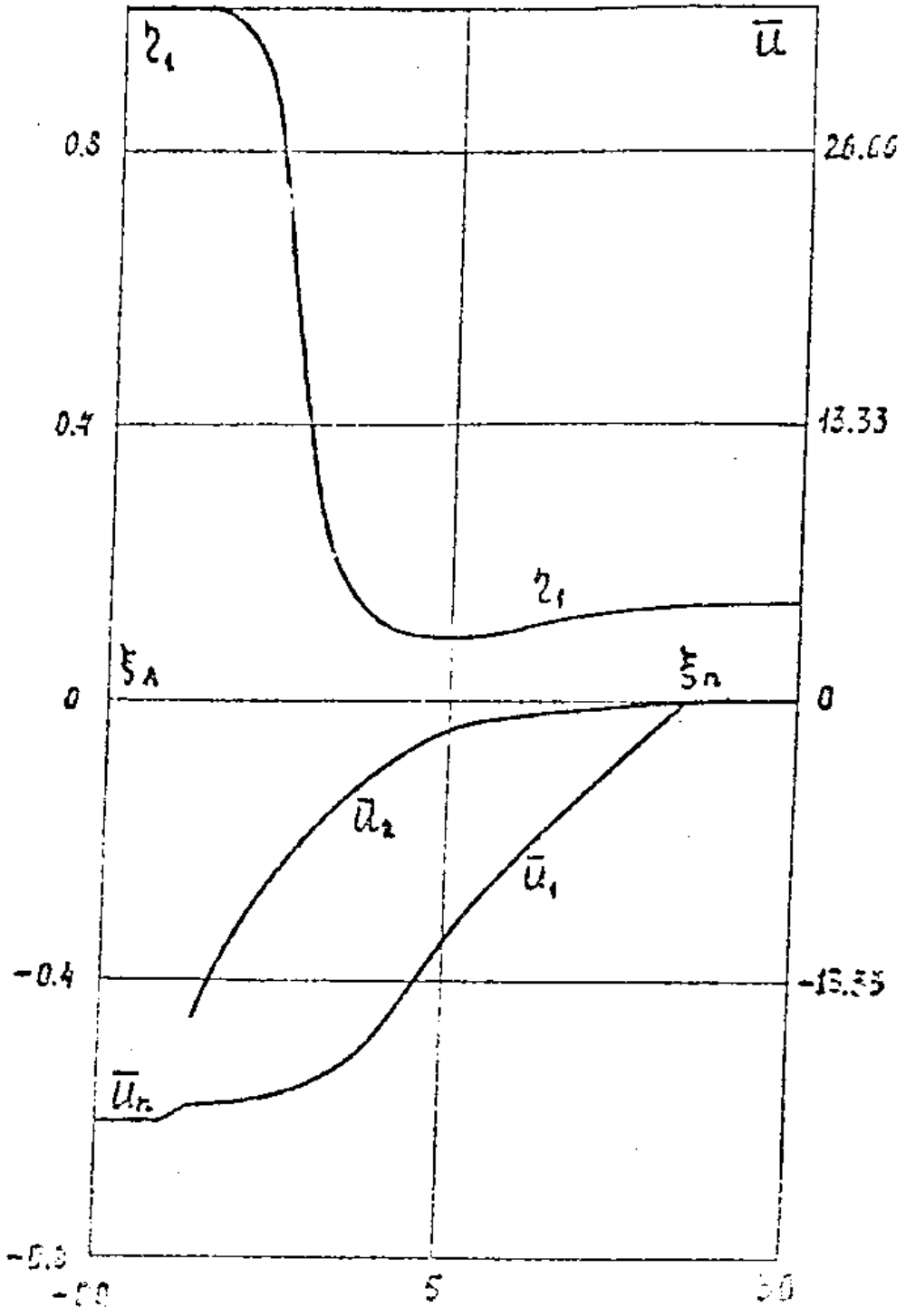

Fig. 2.17.

Automodel rarefaction wave in a mixture of two solids. Complete component separation. $\alpha_{10} = 0.143$,

$\bar{u}_n = -20$, $\bar{F} = 0$ $(\tau \to \infty)$

or the limiting velocity for dispersion into the void (see Fig. 2.18).

2) At a certain point ζ^*, the velocity of the light component reaches that of the piston whereas the mass concentration of the heavy component and the pressure still have not become zero. In this instance, the solution consists of two elements. These are a RW solution and two strong explosions (see Fig. 2.19).

3) At a certain point ζ^*, the mixture pressure becomes equal to zero. This means that the material is destroyed and the component velocities reach the limiting values.

In the region $[\zeta_n, \zeta^*]$, the solution can be different, depending on the piston velocity. A situation analogous to that depicted in Fig. 2.20 arises at significant velocities u_n. If $|u_2^{lim}| < |u_n| < |u_1^{lim}|$, then a SW moving away from the piston arises (see Fig. 2.21). The point ζ^{***} is determined from the mass-conservation condition in the explosion

$$\rho_{02}(u_n - D) = \rho_{01}^*(u_1^* - D), \quad (\zeta^{***} = D)$$

The calculation of the CB between homogeneous substances and mixtures is a serious methodical problem during construction of numerical algorithms for solving the problem of the movement of multilayered systems with substance mixtures.

In order to understand the specific principles associated with this problem, the problem of the dissipation of an arbitrary explosion at the boundary of an isothermal gas and a mixture of two other isothermal gases was solved [9].

Depending on the parameters of the gases, four types of dissipation of the arbitrary explosion are possible.

1) A SW–SW configuration. In this instance, a SW travels in a homogeneous gas whereas two strong explosions are disseminated at different velocities into the mixture. (see Fig. 2.22).

2) A RW–SW configuration. A RW occurs in a homogeneous gas during this type of explosion dissipation. A combination of two strong explosions moves through a mixture (see Fig. 2.23).

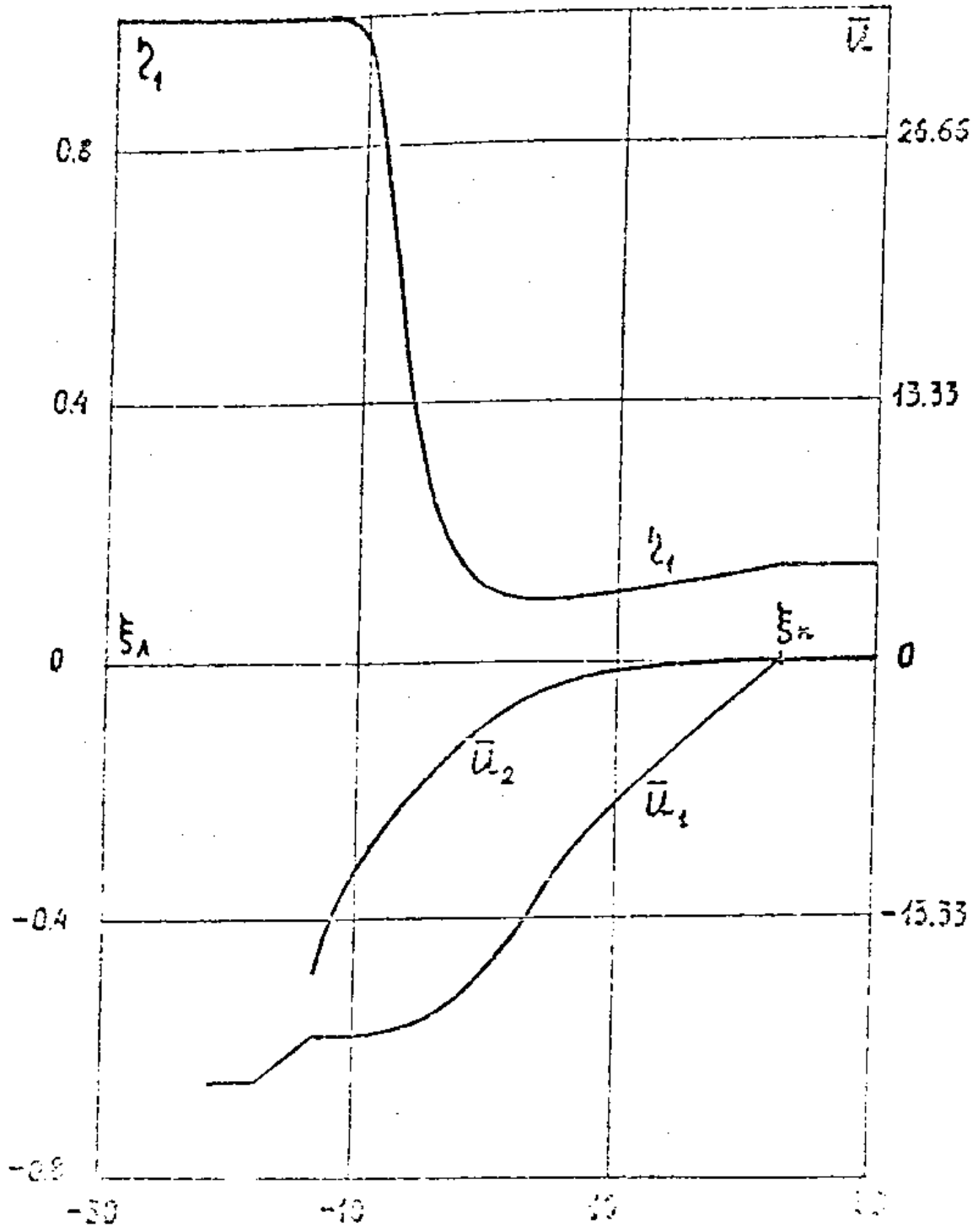

Fig. 2.18.

Automodel rarefaction wave in a mixture of two solids. Complete component separation with formation of an evacuated region near the piston. $\zeta_{10} = 0.143, \quad \bar{u}_n = -30, \quad F = 0 \ (\tau = \infty)$

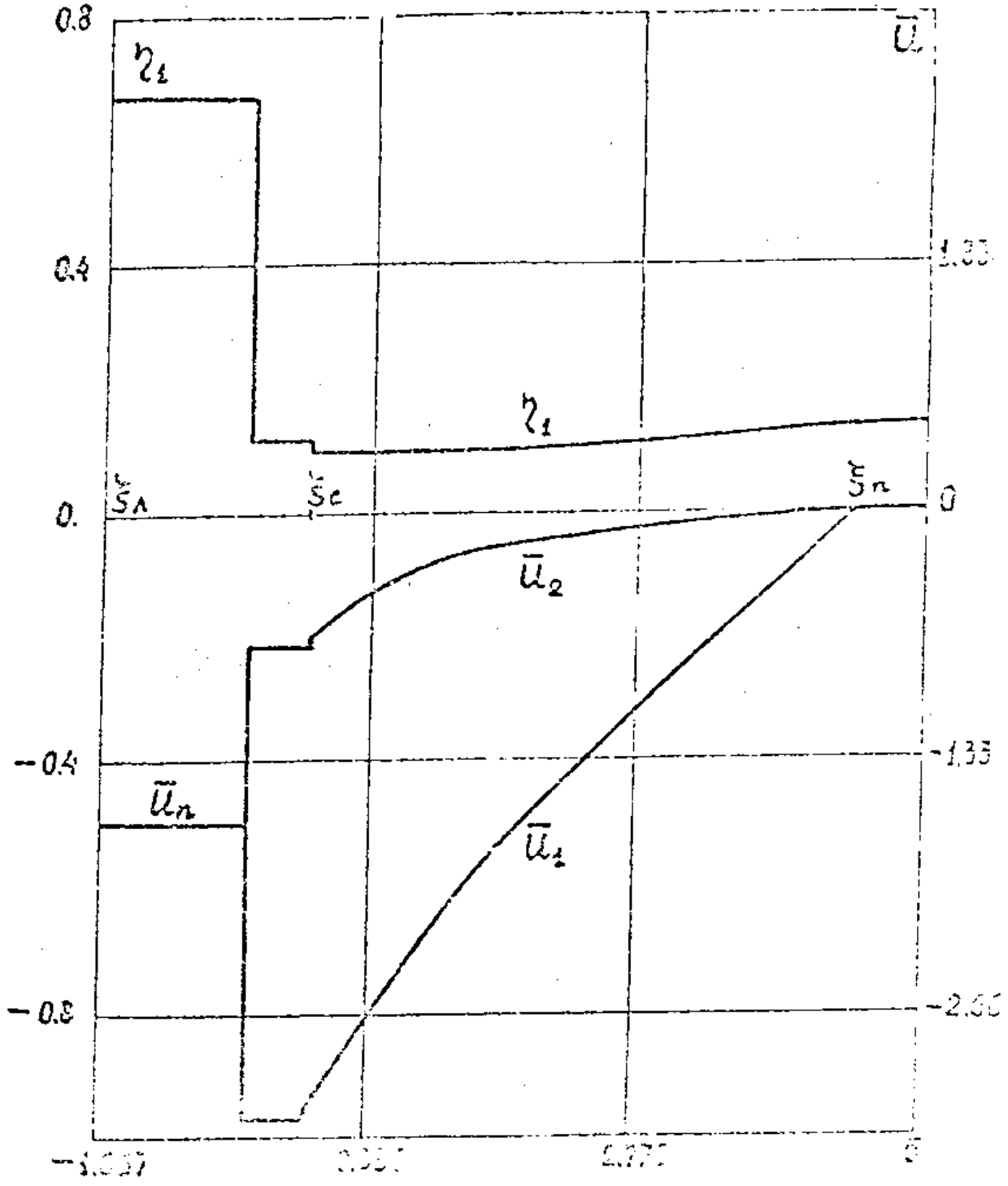

Fig. 2.19.

Partial component separation in an automodel rarefaction wave in a mixture of two solids | $\gamma_{10} = 0.143$,

$\bar{u}_n = -1.6667$, $\bar{F} = 0.1$.

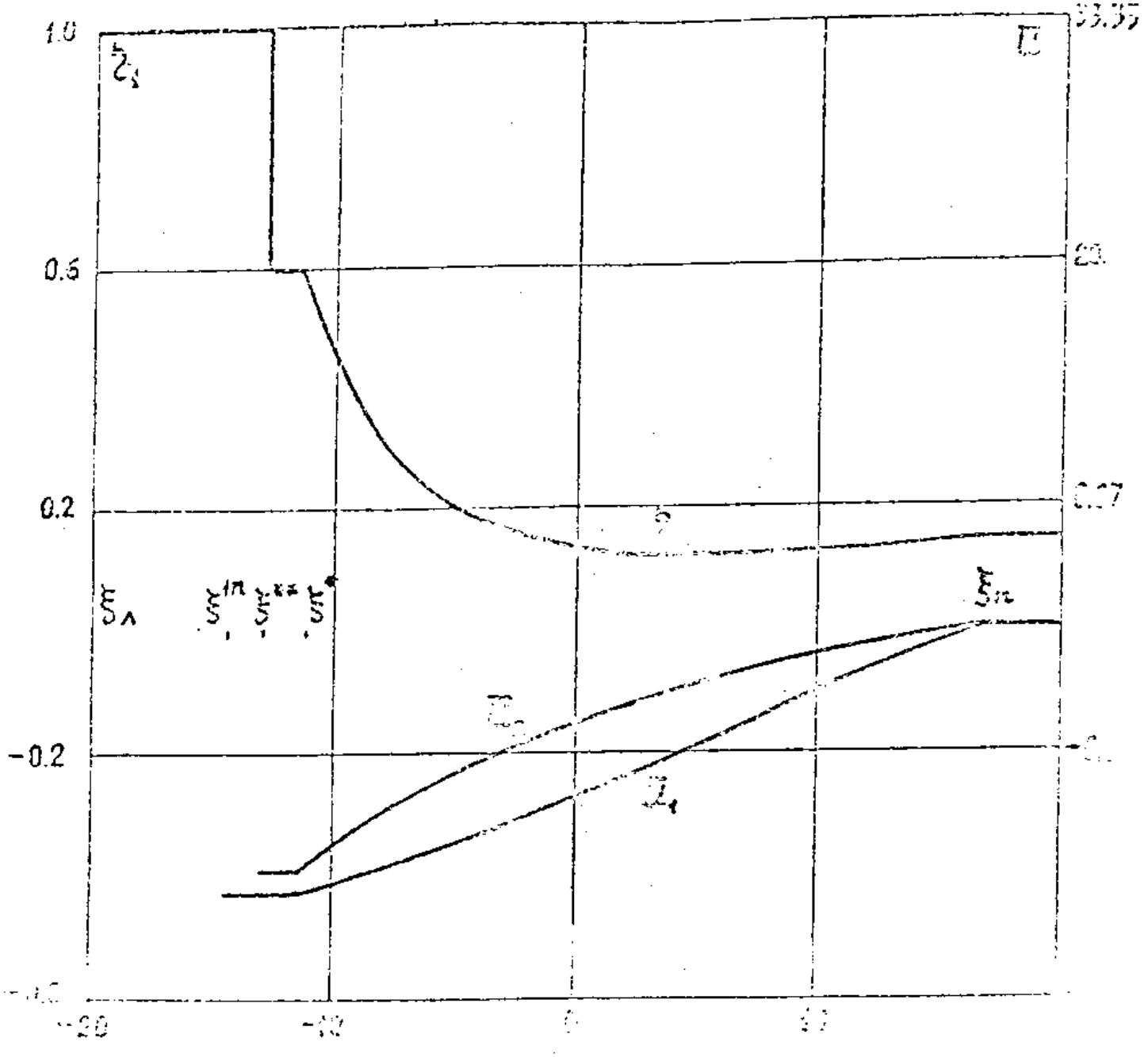

Fig. 2.20.

Automodel rarefaction wave in a mixture of two solids. Component velocity reaches limits, evacuated region forms near the piston

$\bar{\zeta}_{10} = 0.143$, $\bar{U}_\Lambda = -\infty$, ...

$\bar{F} = 1$.

The force R_i has the nature of a viscous friction owing to the difference in the component velocities. The variables t^u_{ij}, t^p_{ij}, and t^T_{ij} are the relaxation times of the velocity, pressure, and temperature, respectively.

The first term in the right part of eq. (1.10) is the power of the interaction forces on movement related to the velocity field of the i component. The existence of interaction forces leads to the dissipation of the kinetic energy of the heterogeneous medium per unit time by $(u_j - u_i)R_i$. The dissipated kinetic energy completely converts to heat. The distribution of this heat across the components is regulated by the coefficient b_i.

The velocities and temperatures of the components continue to relax for certain finite times. In a number of instances, it can happen that t^u_{ij} is much less or, conversely, much greater than other characteristic times of the hydrodynamic flow to be calculated. In the first instance, a one-velocity model of the heterogeneous medium should be used; in the second, pulse exchange due to force interaction of components is not considered. The first possibility occurs at rather small t^u_{ij}; the second, at rather large t^u_{ij}. The actual type of t^u_{ij} function does not need to be known in these instances.

Analogously, t^T_{ij} can be much less or much greater than the characteristic times of the hydrodynamic flow to be calculated.

In the first instance, the local temperatures of the components should be assumed to be equal; in the second, heat exchange between components is not considered. Both these models are also contained as limits in the equation given above. The first occurs at rather small t^T_{ij}; the second, at rather large t^T_{ij}. The correct type of t^T_{ij} function need not be known in these instances.

Expressions for t^u_{ij} and t^T_{ij} in terms of macroscopic parameters of the heterogeneous medium and components should be constructed on the basis of an analysis of the physical properties of the actual substance mixture involved in the actual physical process. This is a rather complicated problem.

The mutual deformation conditions (MDC) of the components, i.e., the conditions for determining the volume concentrations of components in a unit volume of substance mixture during its deformation, must be found in order to complete the mathematical model of a heterogeneous medium.

In the general case, all types of inequality appear in the mutual movement of components. Velocity and temperature inequalities and the corresponding relaxation processes are considered in the mathematical model in terms of the right sides of the equations for R_i and Φ_i.

The relaxation of the component pressures on a microscopic level has a wave hydrodynamic nature and occurs during a finite time determined by the velocities of sound and the particle diameters.

In a number of practical scientific problems, the pressure-relaxation time turns out to be much less than the relaxation times of the velocity, temperature and other characteristic times of the flow to be examined.

In these instances, the local component pressures can be assumed to be equal

$$P_1 = P_2 \qquad (1.11)$$

In the CMM method, this limiting instance is used to describe the component MDC with respect to pressure.

The condition (1.11) occurs in a certain thermodynamic process that results in the individual thermodynamic states of the components changing to states that satisfy this condition.

The nature of this thermodynamic process is determined by the extent of heat exchange between the components and the accepted physical model of the actual relaxation process.

The basic types of MDC of components in the CMM method are:

1) Local pressures and temperatures of components are equal.

The thermodynamic parameters of the components are obtained from known densities, specific internal energies of the mixture, and mass concentrations of components by solving the following system of algebraic equations

$$\frac{1}{\rho} = \frac{\eta_1}{\rho_1} + \frac{\eta_2}{\rho_2}$$

$$E = \eta_1 E_1 + \eta_2 E_2$$

$$P_i = f_{P_i}(\rho_i, E_i, \Phi_i)$$

$$T_i = f_{T_i}(\rho_i, E_i, \Phi_i) \qquad (I.12)$$

$$(i = 1, 2)$$

$$P_1 = P_2 \qquad T_1 = T_2$$

2) Pressures equalize without heat exchange between components.

The pressures equalize along component isentropes.

$$\frac{1}{\rho} = \frac{\eta_1}{\rho_1} + \frac{\eta_2}{\rho_2}$$

$$dE_i - \frac{P_i}{\rho_i^2} d\rho_i = 0$$

$$P_i = f_{P_i}(\rho_i, E_i, \Phi_i) \qquad (I.13)$$

$$T_i = f_{T_i}(\rho_i, E_i, \Phi_i) \qquad (i = 1, 2)$$

$$P_1 = P_2$$

3) Pressures equalize through heat exchange between components due to their temperature difference.

The algorithm for this type of MDC is as follows.

Initially, the component pressures are equalized along their isentropes without considering heat exchange [the system of eqs. (1.13) is solved].

Then, the resulting thermodynamic parameters are used to calculate the increase (decrease) of the component internal energies due to heat exchange in the examined time interval.

Next, the components are converted from these new individual

states to the final states (movement along the isentropes), for which the system of eqs. (1.13) is again solved.

2. Precise solutions of certain mechanics problems for two-velocity multicomponent and heterogeneous media

Let us discuss analytical and precise solutions obtained by us for a characteristic class of problems, the qualitative features of which had a significant effect on our concepts of the physics of SW processes in substance mixtures and the method of constructing the numerical method. The precise solutions have intrinsic value since they are ideal tests for monitoring the accuracy of the numerical methods for solving the most common systems of equations for mathematical models of multicomponent and heterogeneous media.

An analytical solution for piston movement has been obtained for a multicomponent mixture of two isothermal gases in the one-dimensional case without component interaction forces [3]. It was demonstrated that the solution in variables of ρ_{Ci} and u_i for the rarefaction wave (RW) is a combination of two rarefaction waves that expand independently, each for its own component (see Fig. 2.1).

The RW contains both a zone where the mixture is substantially depleted of the light component and a zone where the mixture is substantially enriched in it. The components of isothermal gases are not completely separated in the RW. For the instance where the piston plunges into the mixture, the solution is obtained as two strong explosions that expand independently for each component. After the first strong explosion, the mixture is substantially enriched in the light component; after the second, in the heavy one. The strong explosions propagate with different velocities and diverge with time in space (see Fig. 2.2).

This same problem has been examined [4] taking into account the "associated-mass" effect. The qualitative features of the solution for a SW with pulse exchange between components that is proportional to the difference of their velocities is as follows.

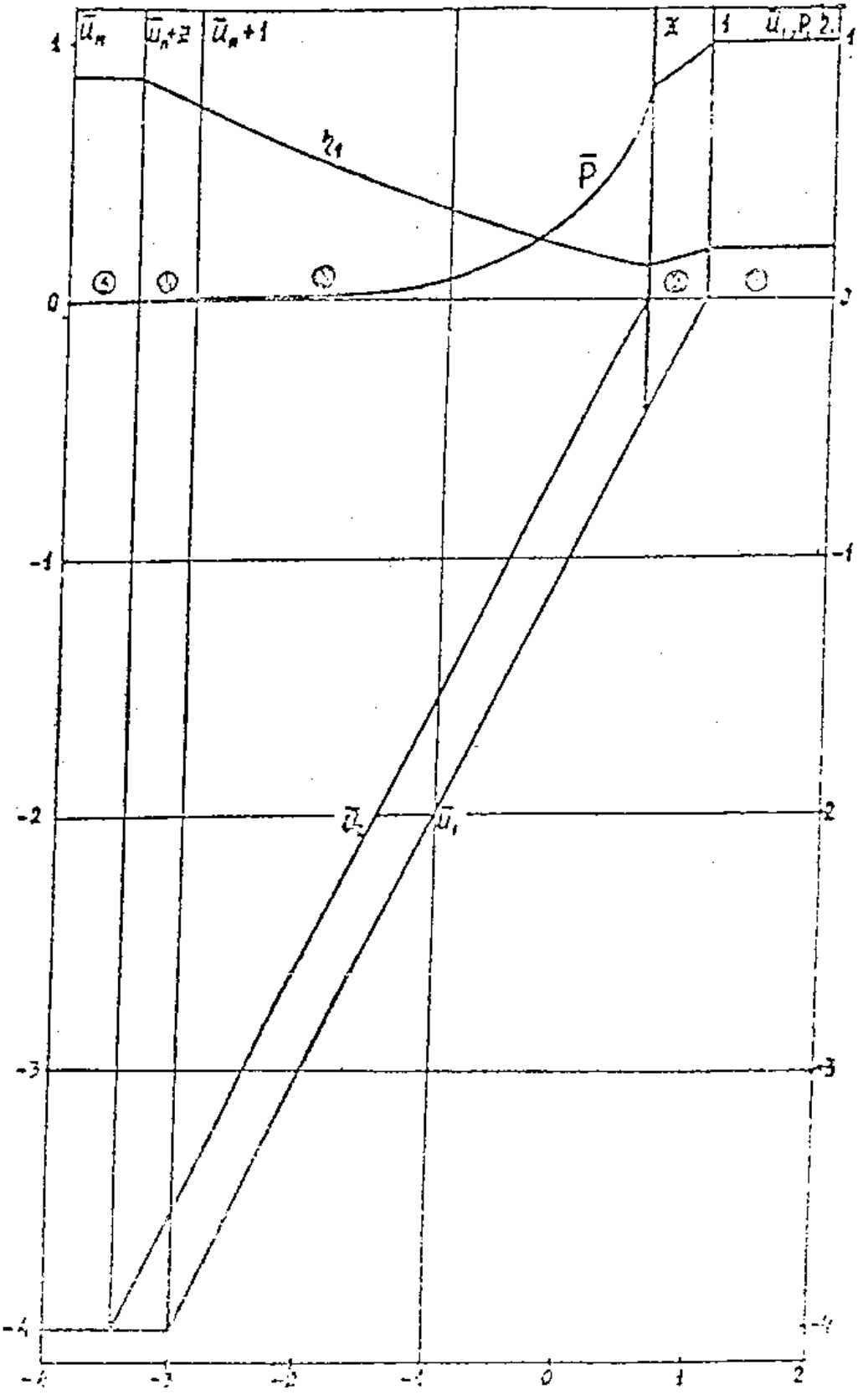

Fig. 2.1.

Rarefaction wave in a mixture of two isothermal gases

$\bar{x}^* = 0.3, \quad \eta_{10} = 0.2, \quad \bar{u}_n = -1, \quad \bar{\rho}_{c_{10}} = 0.4545, \quad \bar{\rho}_{c_{20}} = 1.8181$

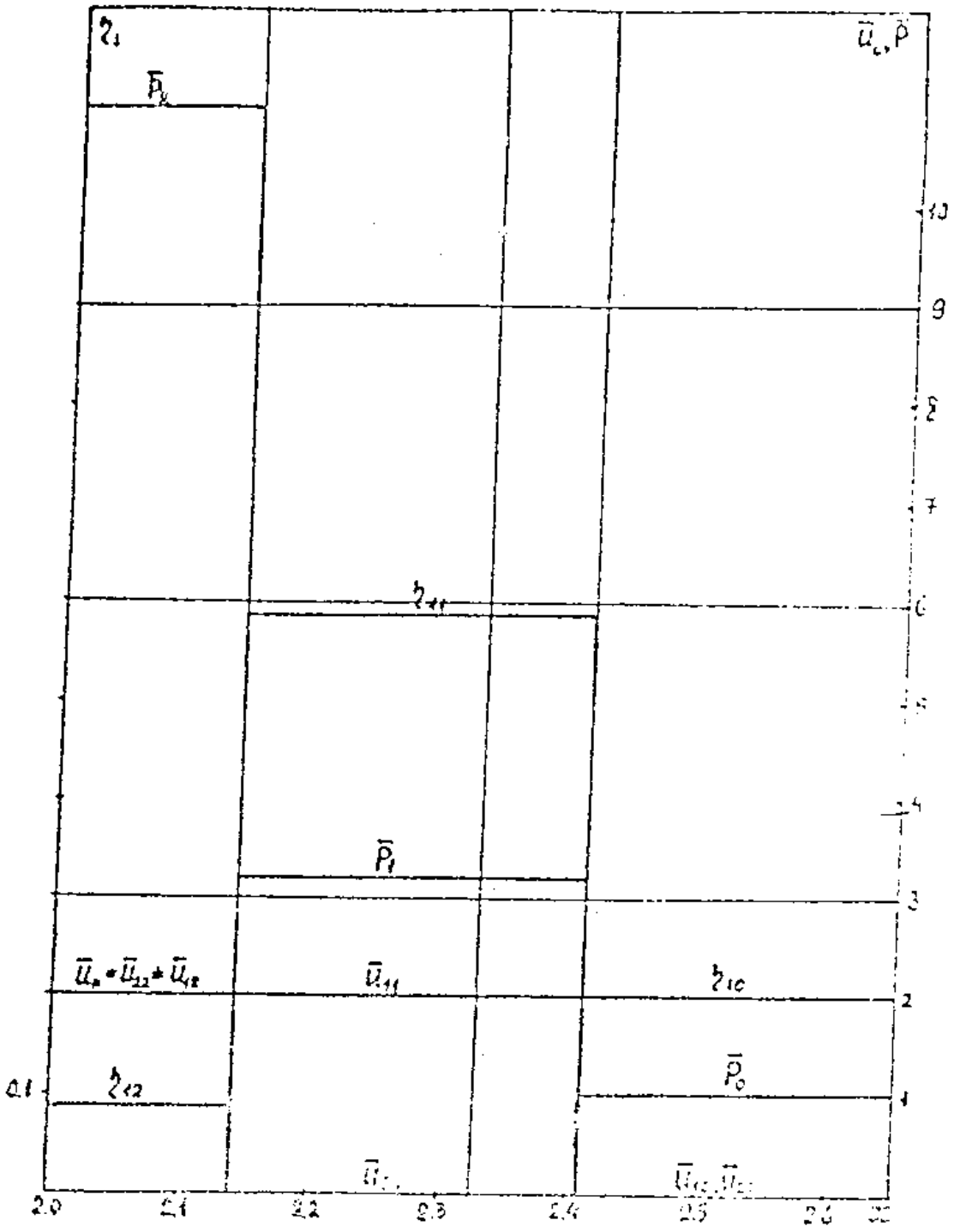

Fig. 2.2.

Solution for a piston moving into a mixture of two isothermal gases

$\xi^2 = 0.3$; $\zeta_{10} = 0.2$; $\bar{u}_n = 2$;

$\bar{Q}_{c_{10}} = 0.4545$; $\bar{Q}_{c_{20}} = 1.8181$; $t = 1$.

A strong explosion with a substantial jump in the parameters of the light component migrates through the mixture in the initial state. The heavy component reacts to a lesser extent to this explosion (see Fig. 2.3). A region of constant flow substantially enriched in the light component follows this explosion. This region expands up to the second strong explosion in which the parameters of the heavy component substantially change. A region of constant flow near the piston follows the second explosion. Here, the mixture is substantially enriched in the heavy component. The velocities of the explosions are different. It is characteristic of the first strong explosion that the rate of the light component behind its front is greater than that of the piston. For the second strong explosion, the velocity of the light component characteristically drops although the pressure in the medium increases.
[Fig. 2.3]

Three situations can arise for the RW:

1) At a certain point ζ^*, the mass concentration of the heavy component reverts to zero whereas the velocity of the light component has still not reached the piston velocity. The components can be completely separated in the RW (see Fig. 2.4).

2) At a certain point, the velocity of the light component reaches that of the piston whereas the mass concentration of the heavy component has still not reverted to zero. In this instance, the solution is a combination of the RW previously described and the sum of two strong explosions. The intersection of these solutions is unambiguously determined (see Fig. 2.5).

3) At a certain point, the velocities of the light and heavy components become equal and the piston velocity is still not reached (see Fig. 2. 6).

As the interaction forces approach infinity, all solutions for both the SW and the RW approach a form corresponding to a one-velocity mixture with the corresponding averaged parameters.

The structure of the SW front in a mixture of two isothermal gases with a strong component interaction proportional to the difference of their velocities has been investigated [5].

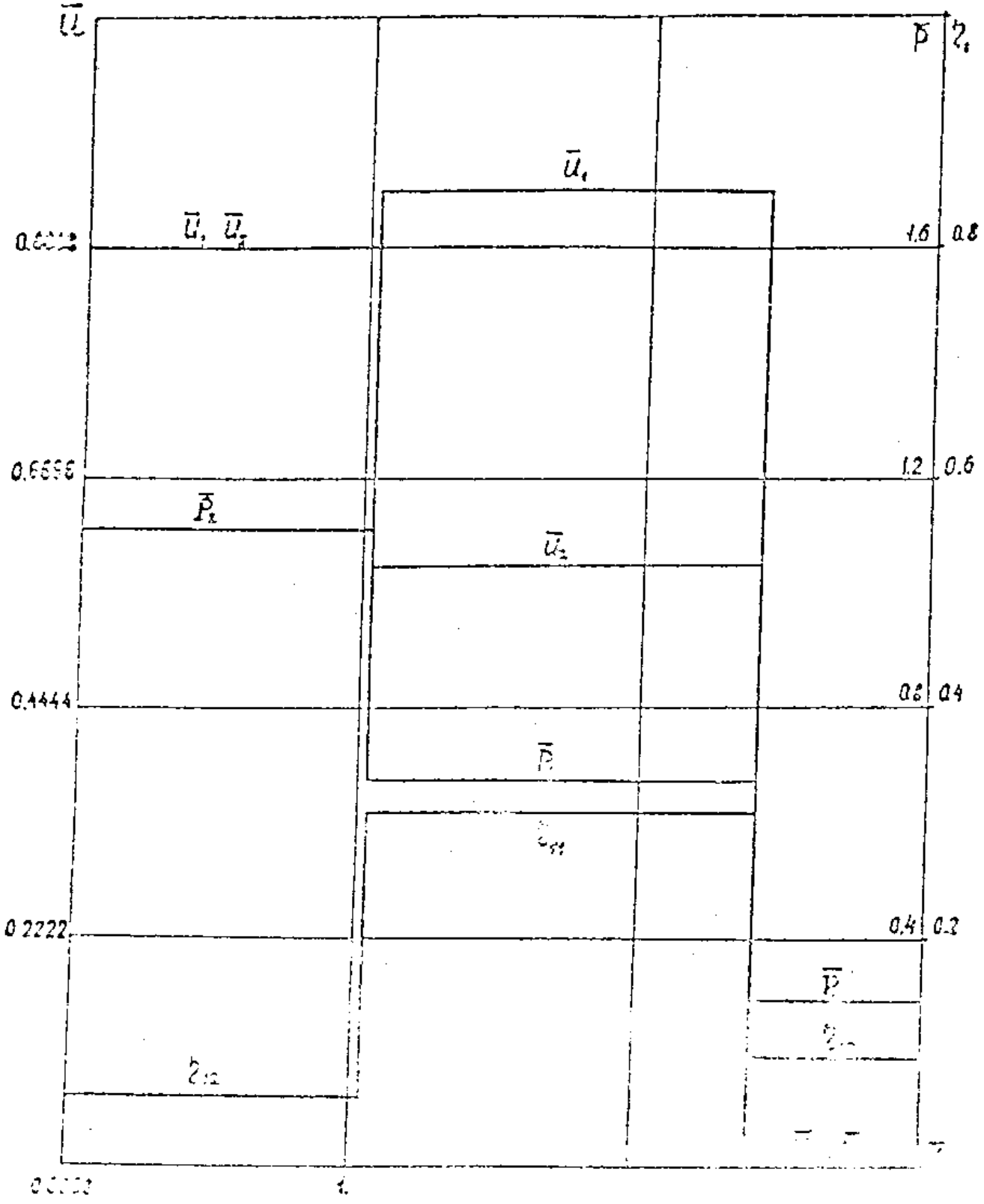

Fig. 2.3.

Shock wave in a mixture of two isothermal gases taking into account the "associated-mass" effect $\rho_{10} = 0.143$; $\Pi^2 = 0.1111$; $\bar{u}_0 = 0.6666$; $\bar{F} = 2.381$. Dimensionless coordinate: $\bar{x} = \frac{x}{c_1 t}$.

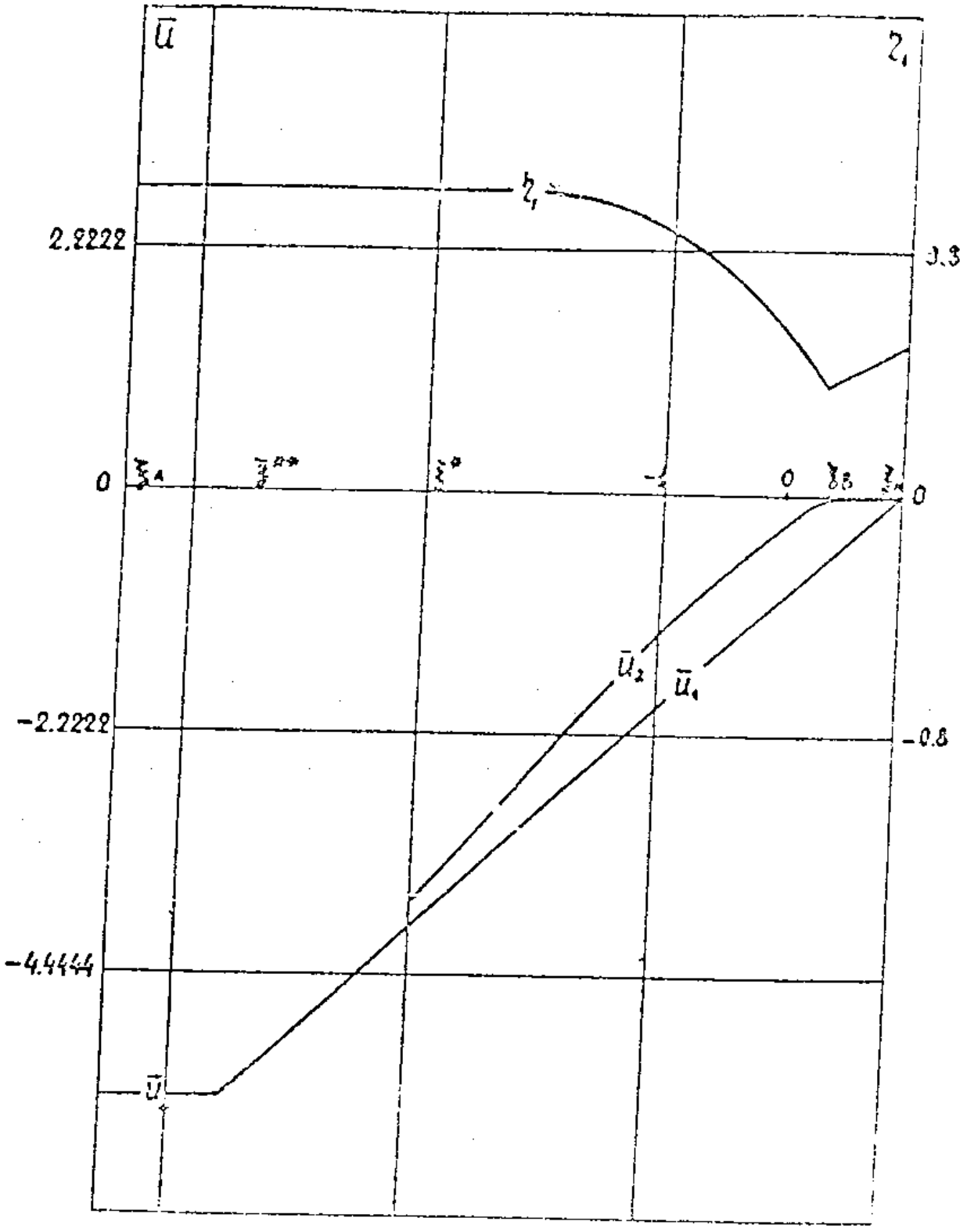

Fig. 2.4.

Automodel rarefaction wave in a mixture of two isothermal gases with component force interaction taking into account the associated-mass effect. Complete separation of components in a rarefaction wave. $\zeta_{10} = 0.5$; $\Xi^2 = 0.IIIII$; $\bar{U}_n = -5.5555$; $\bar{F} = 0.000555$.

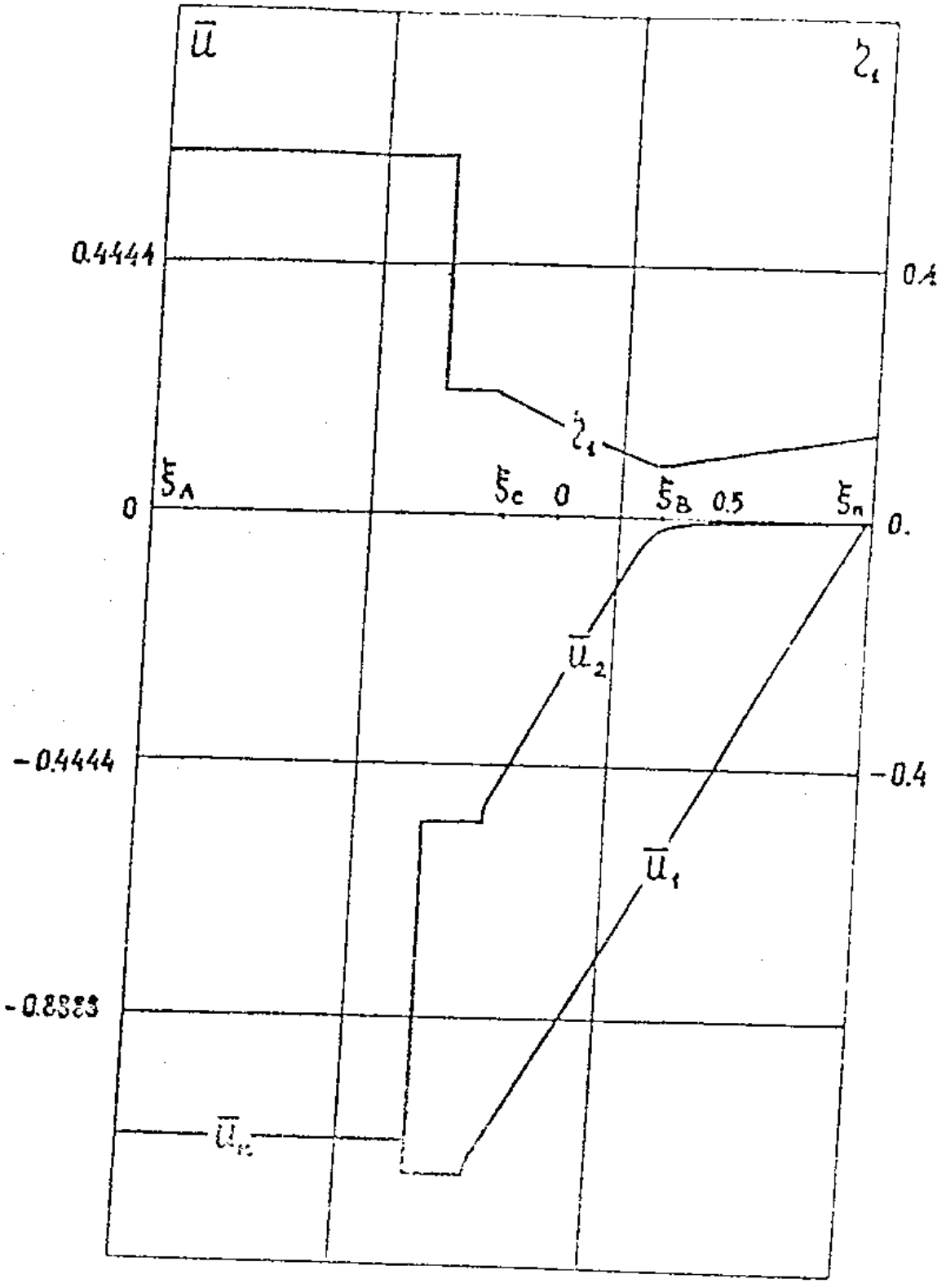

Fig. 2.5.

Automodel rarefaction wave in a mixture of two isothermal gases with component force interaction taking into account the associated-mass effect. Partial separation of components in a rarefaction wave. $\zeta_{10} = 0.143$; $\xi^* = 0.IIIII$; $\bar{u}_n = -I.IIII$; $\bar{F} = 0.004762$.

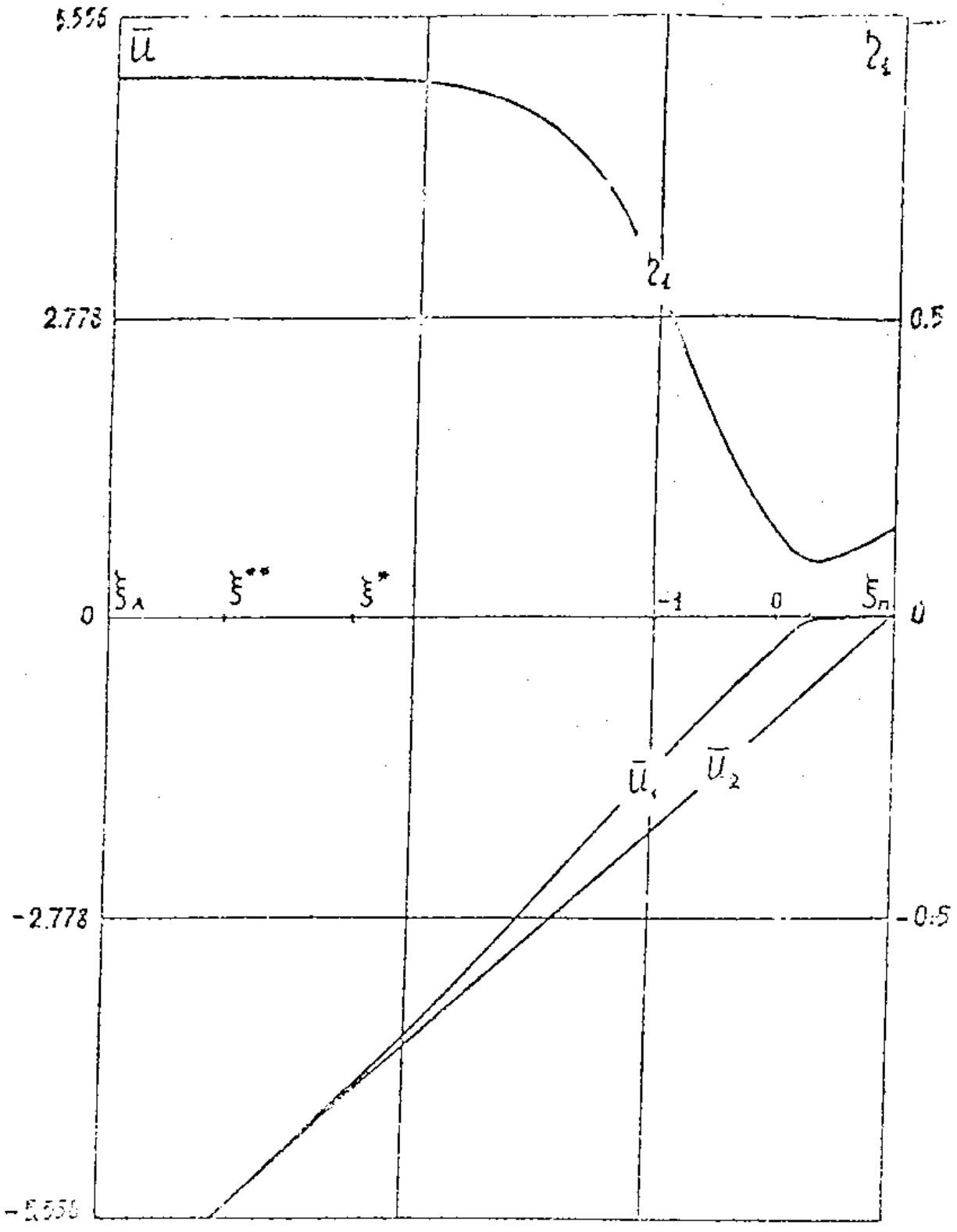

Fig. 2.6.

Automodel rarefaction wave in a mixture of two isothermal gases with component force interaction taking into account the associated-mass effect. Transition of two-velocity flow into one-velocity.

$\zeta_{10} = 0.143$; $\varkappa^2 = 0.11111$; $u_n = -5.5555$;

$\overline{F} = 0.004762$.

Depending on the relationship of the problem parameters, four types of SW front structure are possible:

1) a strong explosion in the light component and a region of continuous flow in front of it (see Fig. 2.7);

2) a strong explosion in the heavy component and a region of continuous flow in front of it (see Fig. 2.8);

3) two strong explosions in the components and a region of continuous flow between them (see. Fig. 2.9);

4) a purely continuous flow (see Fig. 2.10).

A precise solution of the piston problem for a mixture of two polytropic gases without component interaction forces has been obtained [6].

In this instance, in contrast with the mixture of isothermal gases, the components affect each other even without strongly interacting.

The qualitative picture of flow in the SW (see Fig. 2.11) is similar to the case of isothermal gases with pulse exchange between components owing to their different velocities.

Two situations can arise for RW.

1) At a certain point ζ^*, the mass concentration of the heavy component reverts to zero whereas the velocity of the light component has still not reached the piston velocity. In this instance, the components can be completely separated in the RW (see Fig. 2.12).

2) At a certain point ζ^*, the velocity of the light component reaches the piston velocity whereas the mass concentration of the heavy component has still not reverted to zero. This should produce a SW moving away from the piston. Thus, the solution in this instance will contain elements of a solution that is a RW in a heterogeneous medium and a solution that is a sum of two strong explosions. The intersection point ζ_c of these solutions is determined from the condition that the SW parameters, taken at this point as the initial state of the heterogeneous medium, ensure an expansion velocity of the first strong explosion of ζ_c (see Fig. 2.13)

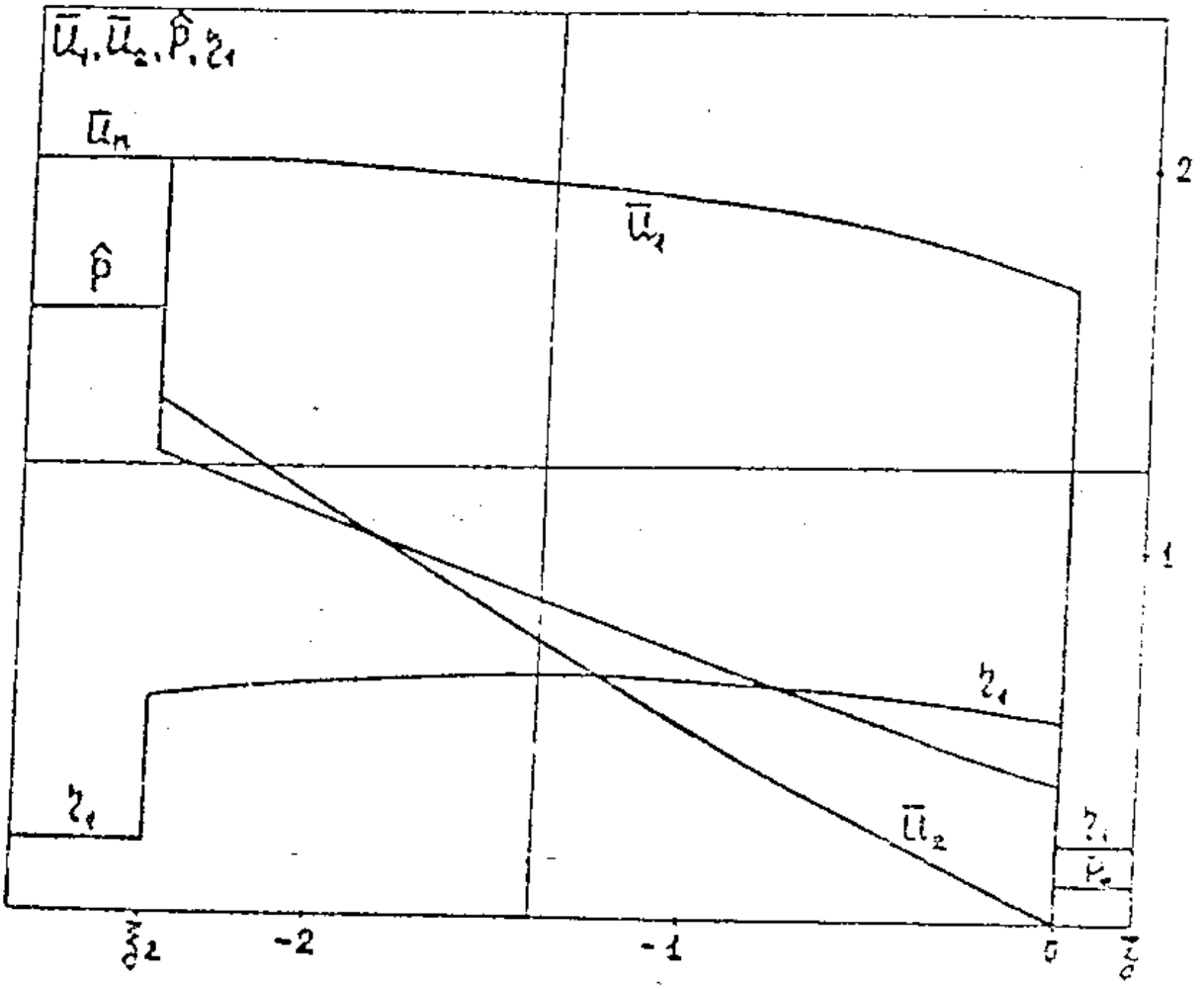

Fig. 2.7.

First type of shock-wave structure front in a mixture of isothermal gases

$z_{10} = 0.2$; $\hat{p} = 0.1$; $\bar{u}_n = 2$; $\varrho_{1n} = 0.0711$;

$\varrho_{e2} = 0.2857$; $\bar{F} = 1$.

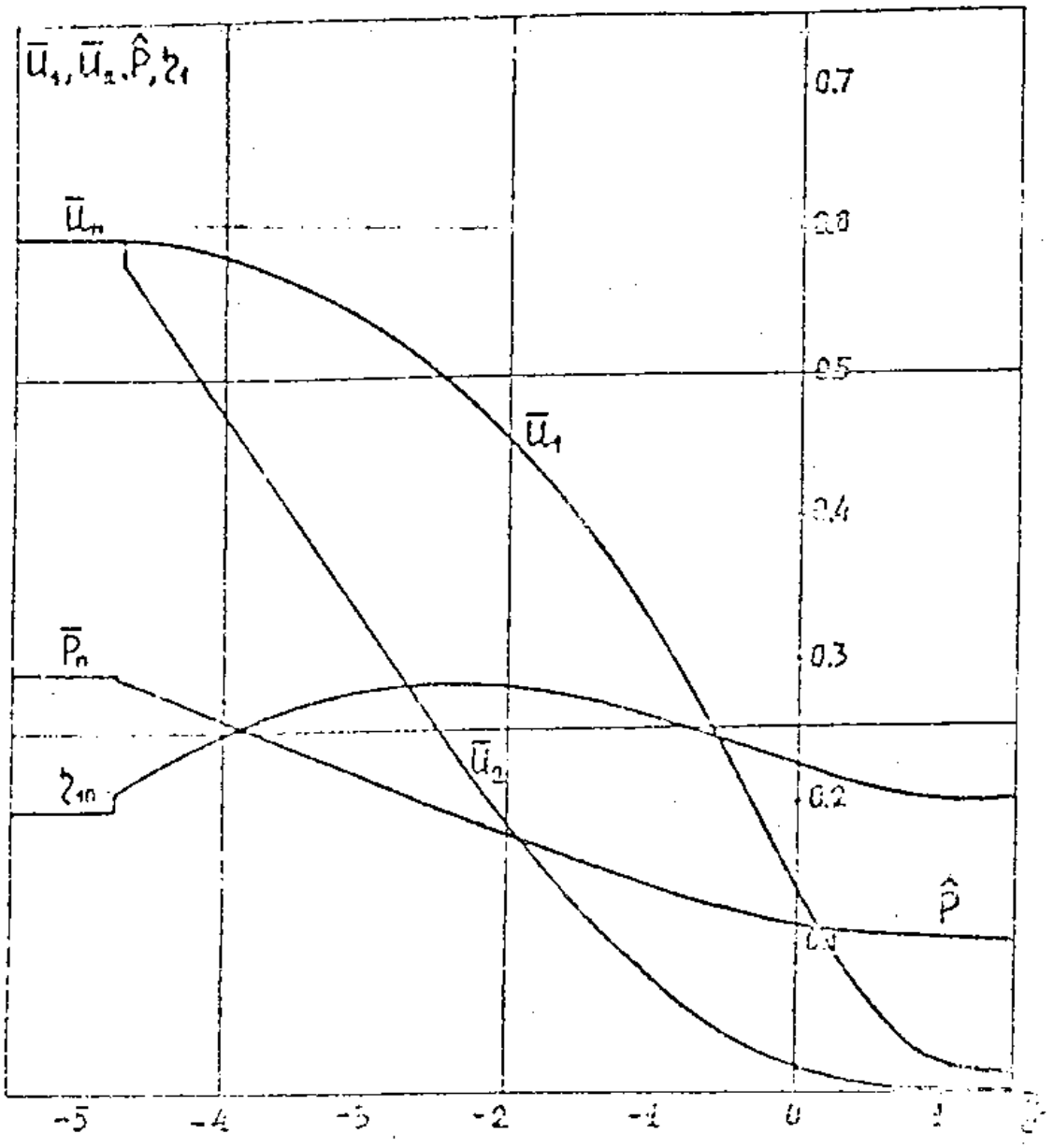

Fig. 2.8.

Second type of shock-wave structure front in a mixture of two isothermal gases

$\gamma_{10} = 0.2$; $\bar{u}_{2n} = 0.1$; $\bar{u}_n = 0.6$;

$\rho_{c10} = 0.0714$; $\rho_{c20} = 0.2857$; $\bar{F} = 1$.

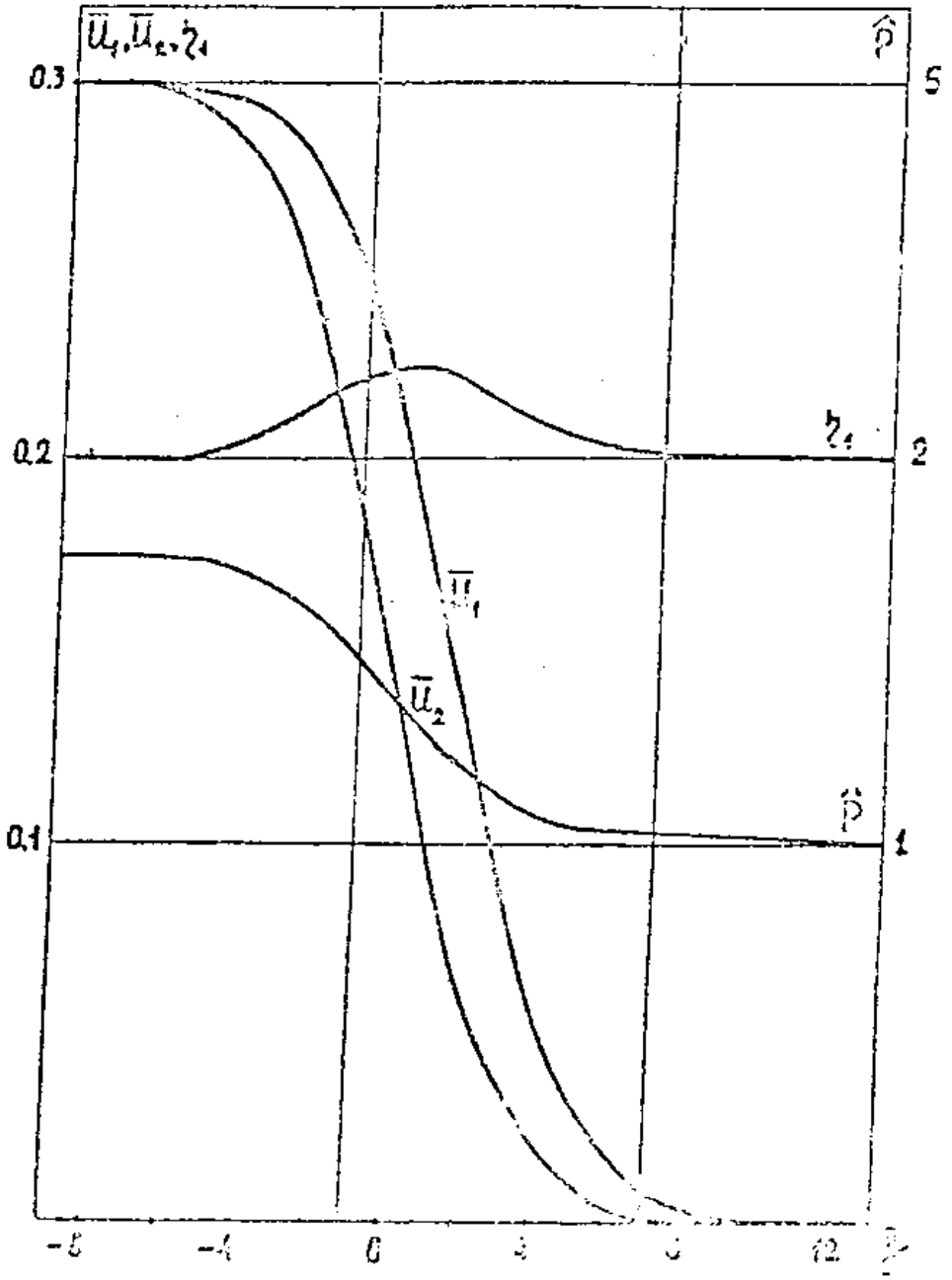

Fig. 2.9.

Third type of shock-wave structure front in a mixture of two isothermal gases

$$\gamma_{1*} = 0.2; \quad \xi^f = 0.1; \quad \bar{u}_n = 0.6;$$

$$\rho_{c1*} = 0.0714; \quad \rho_{c2*} = 0.2857; \quad \bar{F} = 1.$$

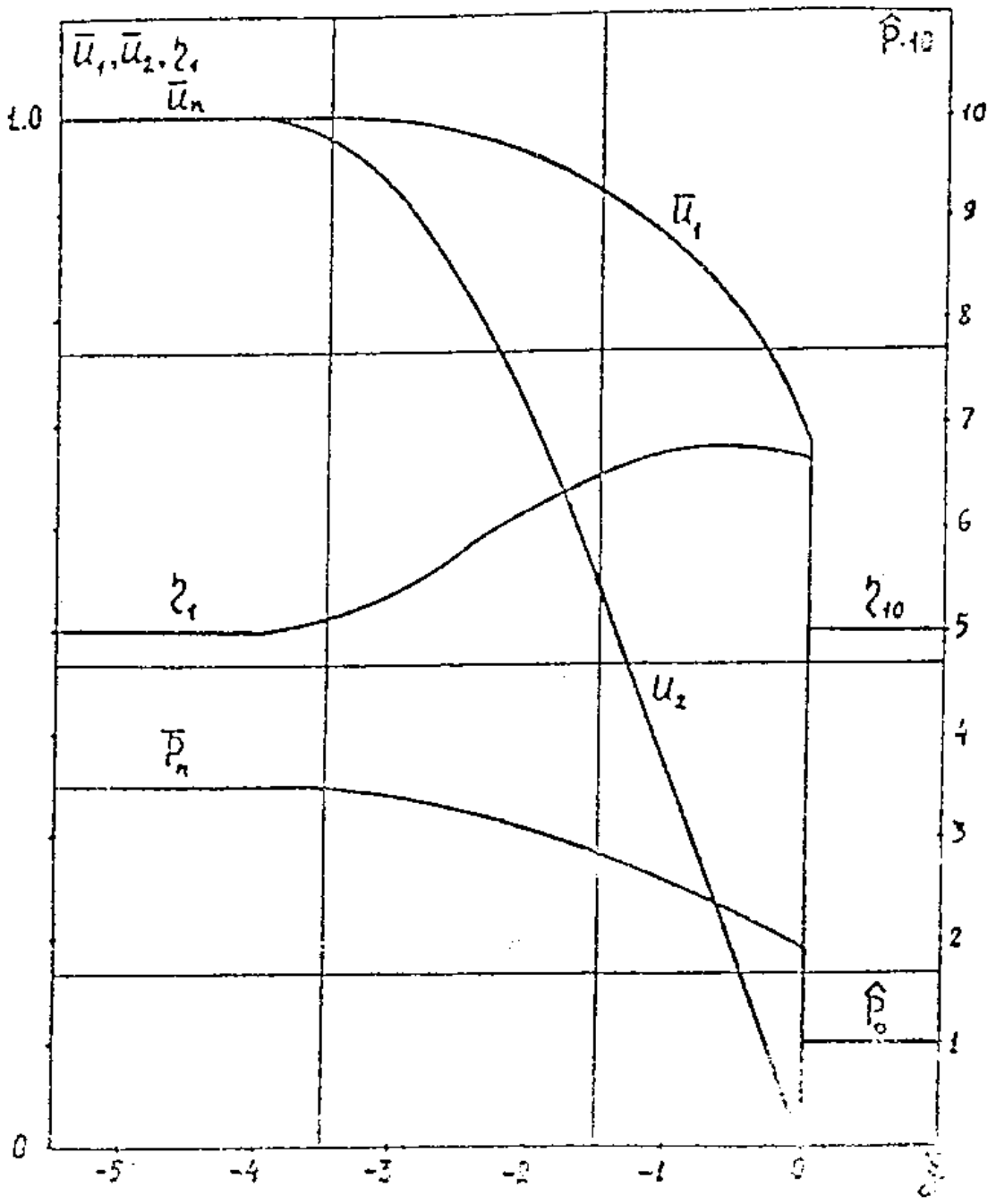

Fig. 2.10.

Fourth type of shock-wave structure front in a mixture of two isothermal gases

= 0.609; = 0.I; = I;

= 0.09II; = 0.09; = I.

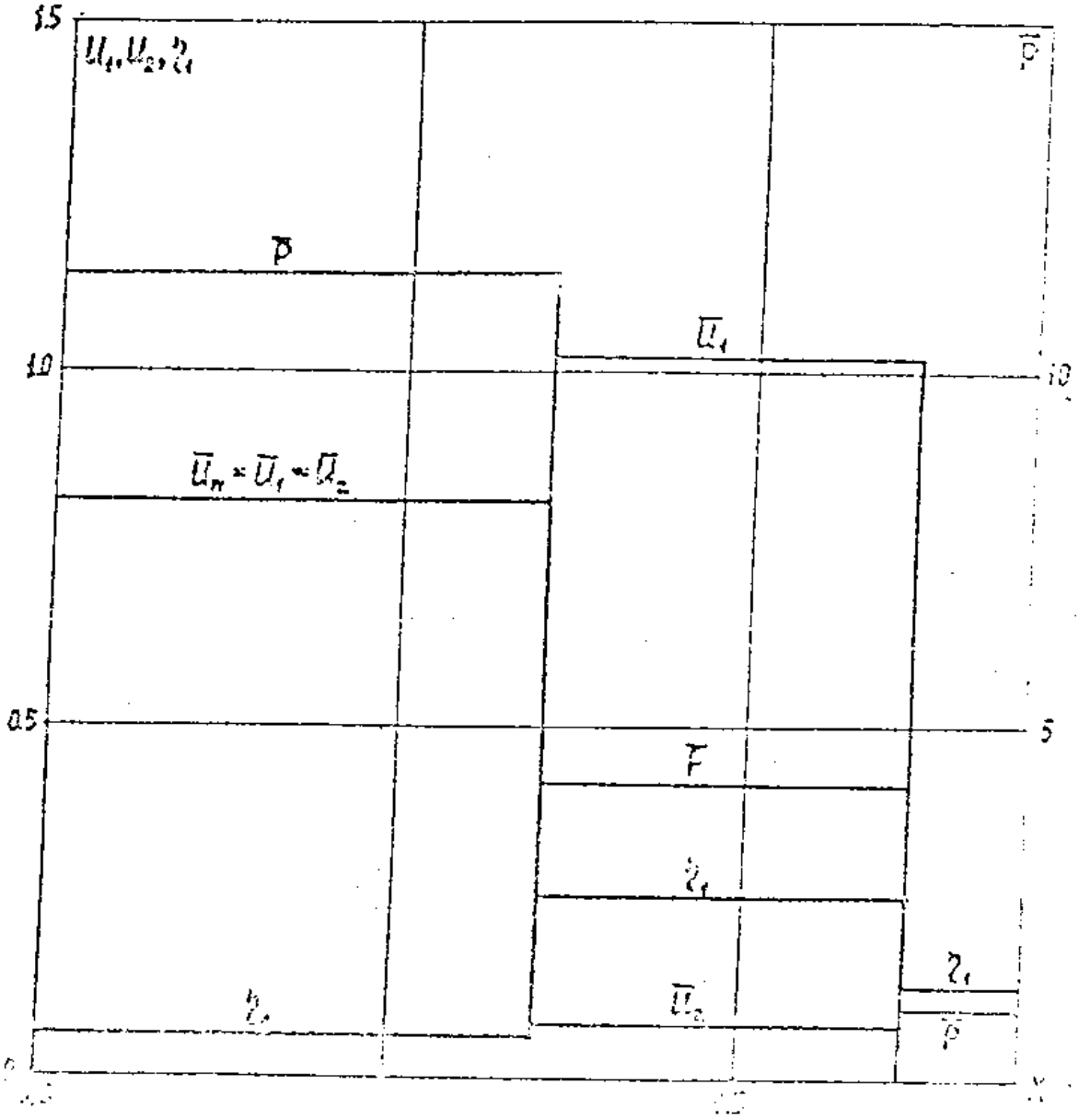

Fig. 2.11.

Solution of the problem of a piston moving at a constant velocity into a mixture of two polytropic gases. $t = 1$.

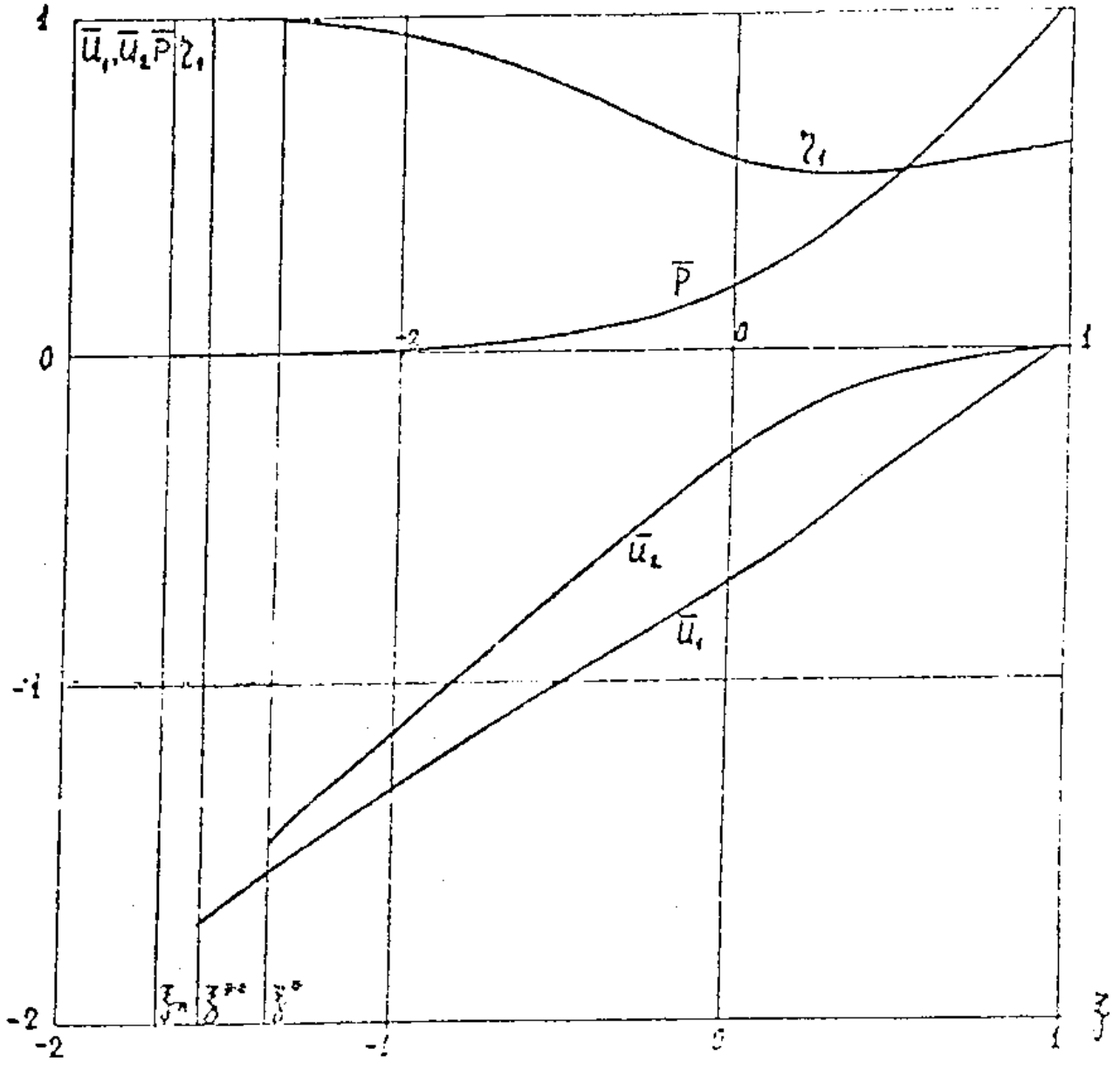

Fig. 2.12.

Solution of the problem of a piston moving at a constant velocity out of a mixture of two polytropic gases. Complete separation of components in a rarefaction wave.

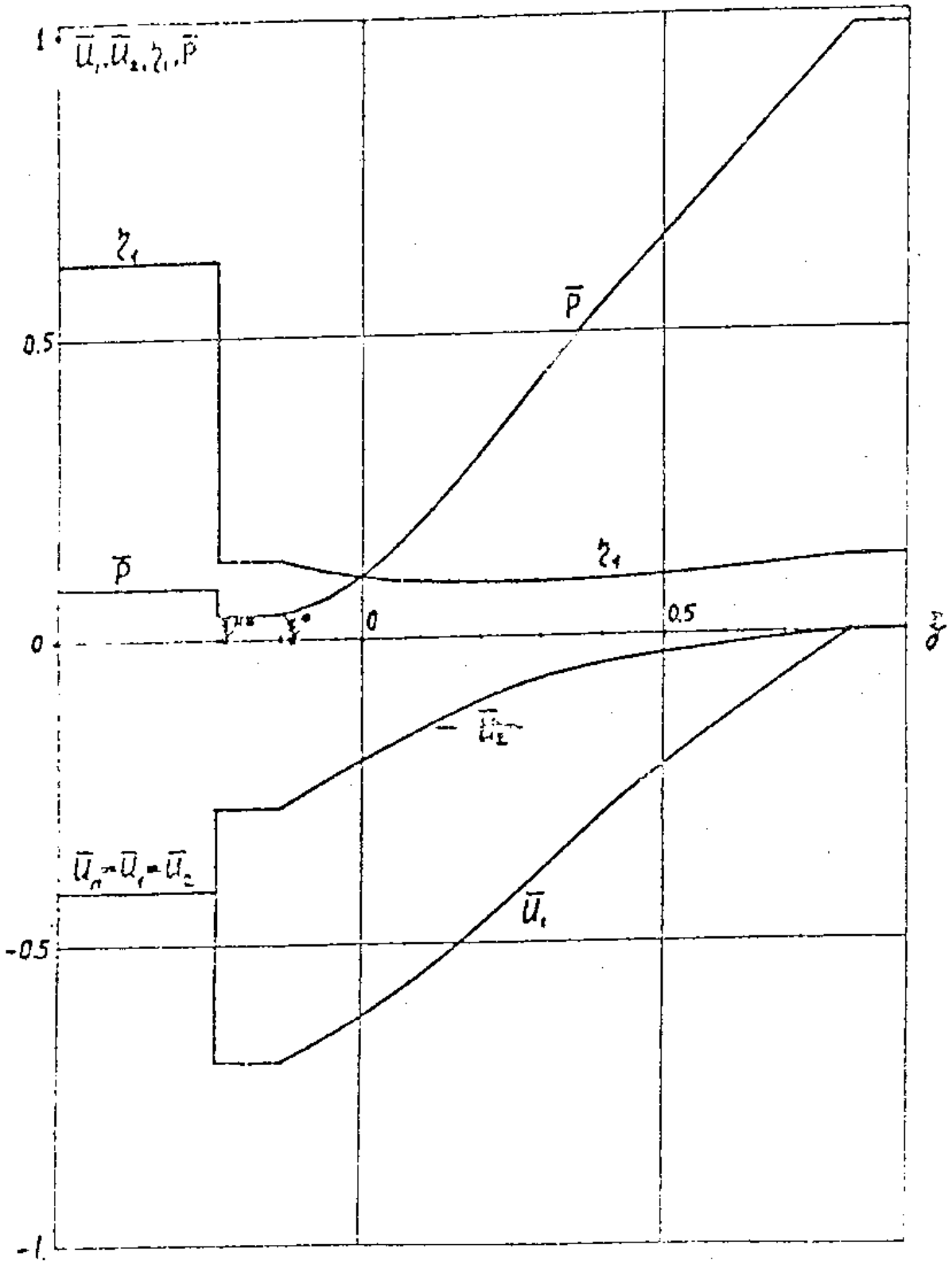

Fig. 2.13.

Solution of the problem of a piston moving at a constant velocity out of a mixture of two polytropic gases. Partial separation of components in a rarefaction wave.

The problem of an advancing piston with complete separation in the RW for a heterogeneous mixture of two polytropic gases has been solved [7]. The solutions of the models of a multicomponent and heterogeneous medium have been demonstrated to be qualitatively and quantitatively similar to this class of problem over a wide range of controlling parameters (see Figs. 2.14 and 2.15)

The problem of dissemination of RW and SW in a mixture of two condensed substances taking into account the associated-mass effect has been solved [8]. The equation of state of the components was used in the form

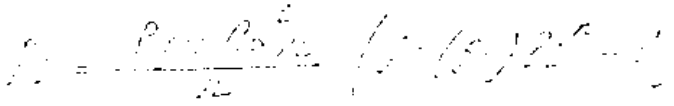

The extent of a strong effect on the i component from the j was taken as

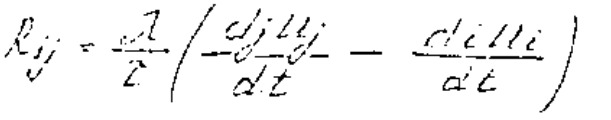

The flow arising during SW propagation has the following qualitative nature.

Strong explosions move through the mixture in the initial state. The parameters of both components jump in each of these. The explosions move at different velocities and diverge with time in space. It is characteristic of the first strong explosion that the velocity of the light component behind its front is greater than the piston velocity. The velocity of the light component decreases for the second strong explosion although the pressure in the mixture increases in this explosion (see Fig. 2.16).

One of three situations is possible for RW dissemination in a mixture of two solids.

1) At a certain point ζ^*, the mass concentration of the heavy component reverts to zero whereas the velocity of the light component has still not reached that of the piston and the pressure of the mixture is not at the null value. Thus, the velocity of the light component reaches either the piston velocity (see Fig. 2.17)